Unclassified

Security Classification of this page

REPORT DOCUMENTATION PAGE

1a Report Security Classification Unclassified	1b Restrictive Markings
2a Security Classification Authority	3 Distribution Availability of Report
2b Declassification/Downgrading Schedule	Approved for public release; distribution is unlimited.
4 Performing Organization Report Number(s)	5 Monitoring Organization Report Number(s)
6a Name of Performing Organization: Naval Postgraduate School	6b Office Symbol (*If Applicable*) 39
6c Address (*city, state, and ZIP code*): Monterey, CA 93943-5000	7a Name of Monitoring Organization: Naval Postgraduate School
8a Name of Funding/Sponsoring Organization	8b Office Symbol (*If Applicable*)
8c Address (*city, state, and ZIP code*)	7b Address (*city, state, and ZIP code*): Monterey, CA 93943-5000
	9 Procurement Instrument Identification Number
	10 Source of Funding Numbers

Program Element Number	Project No	Task No	Work Unit Accession No

11 Title (*Include Security Classification*) DESIGN AND CONTROL OF A SPACE BASED TWO LINK MANIPULATOR WITH LYAPUNOV BASED CONTROL LAWS

12 Personal Author(s) Dennis R. Sorensen

13a Type of Report	13b Time Covered		14 Date of Report (*year, month,day*)	15 Page Count
	From	To		
Engineer's Thesis			September 1992	128

16 Supplementary Notation The views expressed in this thesis are those of the author and do not reflect the official policy or position of the Department of Defense or the U.S. Government.

17 Cosati Codes			18 Subject Terms (*continue on reverse if necessary and identify by block number*)
Field	Group	Subgroup	Non-Linear Control System Design, Robotics, Satellite Attitude Control

19 Abstract (*continue on reverse if necessary and identify by block number*)

The Flexible Spacecraft Simulator (FSS) at the Naval Postgraduate School was modified by replacing the flexible appendage with a two link robotic manipulator. This experimental setup was designed to simulate motion of a spacecraft about the pitch axis. The spacecraft consists of a main body, a two link manipulator, and momentum wheel with actuator to control the pitch attitude of the spacecraft. Position information from the main body and manipulators were obtained from Rotary Variable Displacement Transducers (RVDT's). The equations of motion were developed assuming that the main body and manipulator were rigid bodies. The resulting coupled, nonlinear, time variant equations of motion were used to analyze the dynamics and kinematics of the body, manipulator as well as the interaction between the two. Three different control strategies were developed using Lyapunov's Second or Direct Method. With the first controller, simple linear feedback of position and velocity information with constant gains was used to position the manipulator and stabilize the main body. A fifth order polynomial was used to generate a reference trajectory for the second controller. This trajectory was used in conjunction with a tracking Lyapunov controller to position and stabilize the system. In the third controller, a near-minimum-time technique was used to generate a reference trajectory. This reference trajectory was employed to design a tracking controller similar to that used in the polynomial reference controller.

20 Distribution/Availability of Abstract	21 Abstract Security Classification
[X] unclassified/unlimited [ ] same as report [ ] DTIC users	Unclassified

22a Name of Responsible Individual	22b Telephone (*Include Area code*)	22c Office Symbol
Brij N. Agrawal	(408) 646-3338	AA/Ag

DD FORM 1473, 84 MAR 83 APR edition may be used until exhausted

All other editions are obsolete

security classification of this page Unclassified

Approved for public release; distribution is unlimited.

DESIGN AND CONTROL OF A SPACE BASED TWO LINK MANIPULATOR WITH LYAPUNOV BASED CONTROL LAWS

by

Dennis R. Sorensen
Lieutenant Commander, United States Navy
B.S., Iowa State University, 1981
M.S. Astronautical Engineering, Naval Postgraduate School, 1991

Submitted in partial fulfillment
of the requirements for the degree of

ENGINEER OF AERONAUTICS AND ASTRONAUTICS

from the

NAVAL POSTGRADUATE SCHOOL
September 1992

ABSTRACT

The Flexible Spacecraft Simulator (FSS) at the Naval Postgraduate School was modified by replacing the flexible appendage with a two link robotic manipulator. This experimental setup was designed to simulate motion of a spacecraft about the pitch axis. The spacecraft consists of a main body, a two link manipulator, and momentum wheel actuator to control the pitch attitude of the spacecraft. Position information from the main body and manipulators was obtained from Rotary Variable Displacement Transducers (RVDT). The equations of motion were developed assuming that the main body and manipulator were rigid bodies. The resulting coupled, nonlinear, time invariant equations of motion were used to analyze the dynamics and kinematics of the main body and manipulator as well as the interaction between the main body and manipulator.

Three different control strategies were developed using Lyapunov's Second or Direct Method. With the first controller, simple linear feedback of position and velocity information with constant gains was used to position the manipulator and stabilize the main body. A fifth order polynomial was used to generate a reference trajectory for the second controller. This trajectory was used in conjunction with a tracking controller to position and stabilize the system. In the third controller, a near-minimum-time technique was used to generate a reference trajectory. This reference trajectory was employed using a tracking controller similar to that used in the polynomial reference controller.

ACKNOWLEDGMENTS

Many people have contributed to the success of this project but the most notable among these people was Mr. Rafford Bailey. Mr. Bailey was the laboratory manager for the Spacecraft Robotics Simulator and was primarily responsible for the design, manufacture, and assembly of the manipulator. Mr. Pat Hickey and Mr. John Moulton of the Department Of Aeronautics were instrumental in the manufacture of manipulator components in a timely and expeditious manner. Air Force Captain Gary Yale and Dr. Hyochoong Bang provided invaluable assistance with many of the theoretical and analytical aspects for the design and analysis of the control system. Professor John L. Junkins, the George J. Eppright Chair Professor at Texas A & M University and visiting Co-Chair of the Space Systems Academic Group at the Naval Postgraduate School presented a firm foundation for the non-linear control theory and Lyapunov stability theory that formed the theoretical basis for the control law design. Finally, to Professor Brij N. Agrawal, who provided the funding, spacecraft attitude, dynamics and control expertise, and was responsible for the overall coordination and success of this project.

TABLE OF CONTENTS

LIST OF TABLES

LIST OF FIGURES

I. INTRODUCTION

During the past few years there has been a significant increase in the use of robotics. Applications range from performing routine tasks in manufacturing to deep sea and interplanetary space exploration. The interplanetary and extraterrestrial environment has become the focus of research for future industrial development and scientific exploration. With the hazards of this environment and cost of manned space flight, researchers will become increasingly dependent upon robotics for assembly, service, and repair of equipment in space as well as the exploration of space itself. Due to the requirements for terrestrial and space applications, there has been a significant increase in theoretical and experimental research in the areas of robotic dynamics and control.

Space based robotic applications differ from terrestrial applications in one important area. For the space based applications, no support is provided to stabilize the manipulator. A space based manipulator, when repositioned, imparts moments and forces on the spacecraft. In addition, there is no friction to dissipate energy that is added to the system. To counteract these forces and moments, an attitude control system normally consisting of thrusters in combination with a momentum wheel is used to stabilize the spacecraft. Control system problems are exasperated as the mass of the load that is being positioned becomes larger in relation to the mass of the spacecraft. It is this interaction between spacecraft and the motion of a manipulator that warrants further research.

The primary objective for any control system is to remain stable over a wide range of operating conditions while still providing adequate levels of performance. It is desired to meet this objective in the face of hardware

characteristics, changing loads as well as unmodeled disturbances and system dynamics. These requirements and restrictions present the control system design engineer with significant challenges.

Before the system can be analyzed, the equations of motions must be determined. The equations of motion for a robotic system can easily be developed through Lagrange's equations and are in the form of a set of second order differential equations. These equations are coupled and nonlinear with trigonometric and higher order terms. Attempts to simplify these equations result in equations of motion that are valid over a limited range of motion or for specific boundary conditions. The current trend in trajectory control requires highly nonlinear maneuvers that are valid over a wide range of applications and operating conditions. These requirements dictate that the full, nonlinear equations be used to describe the motion of the system. With the introduction of the nonlinear equations of motion, many traditional tools in control theory used to analyze linear, time-invariant systems are not available or are meaningless.

Recently, research by Junkins [Ref. 1] and Bang [Ref. 2] has revived interest in using Lyapunov's second method for a flexible structure control system design. This technique is very attractive because it can be applied to nonlinear, time invariant, systems with guaranteed stability for a wide range of conditions. An important feature of Lyapunov's second method is the freedom to select the Lyapunov function and the corresponding feedback control law. The Lyapunov function can be selected based on physical insight and the control law can be selected to ensure that the system is stable. The Lyapunov function must be positive definite and is normally related to the system energy for a large class of mechanical natural systems. The control law can be selected such that the

Lyapunov function or system energy will always decrease to zero or some equilibrium point.

The purpose of this thesis is to apply a general methodology for finding Lyapunov stable control laws for stabilizing the spacecraft main body while controlling a two link manipulator attached to that spacecraft. A complete description of the experimental setup is discussed in Chapter II. Topics include the physical characteristics of the manipulator, main body, actuators, sensors, test, simulation, and data collection equipment. In Chapter III, the coordinate systems and the equations of motion are developed. Three different control strategies were developed using Lyapunov's Second or Direct Method. With the first controller, simple linear feedback of position and velocity information with constant gains was used to position the manipulator while stabilizing the main body. A fifth order polynomial was used to generate a reference trajectory for the second controller. This trajectory was used in conjunction with a tracking controller to position and stabilize the system. In the third controller, a near-minimum-time technique was used to generate a reference trajectory. This reference trajectory was employed with a tracking controller similar to that used in the polynomial reference controller. Simulation results are presented in Chapter IV. Chapter V includes a summary of the conclusions as well as topics for future research.

II. EXPERIMENTAL SETUP

A. SPACE ROBOTICS SIMULATOR DESCRIPTION

The Spacecraft Robotics Simulator (SRS) is a modification to the Flexible Spacecraft Simulator (FSS) used for previous work by Hailey [Ref. 3], and Watkins [Ref. 4]. The FSS was modified by removing the flexible appendage and replacing this appendage with a two link manipulator. The SRS consists of a central main body with a two link robotic manipulator. Pitch axis control of the main body is provided by a single momentum wheel driven by an electric servo-motor. The central body was constrained to rotational motion only by an I-beam mounted over the over the granite table. The main body and manipulator were supported by air bearings that float upon a thin cushion of air on an optical quality granite surface. Each of the two links were positioned via geared DC servo-motors. A Rotary Variable Displacement Transducer (RVDT) was used to obtain position information at each joint for position feedback. This setup was designed to simulate a zero-gravity environment in two dimensions. The SRS is depicted in Figure 2.1.

B. EXPERIMENT DESCRIPTION

The SRS is composed of the following major components:

- Spacecraft Main Body
- Two Link Robotic Manipulator
- RVDT Position Sensors
- Granite Table
- Electrical Power Supplies
- AC-100
- VAX 3100 Series Computer

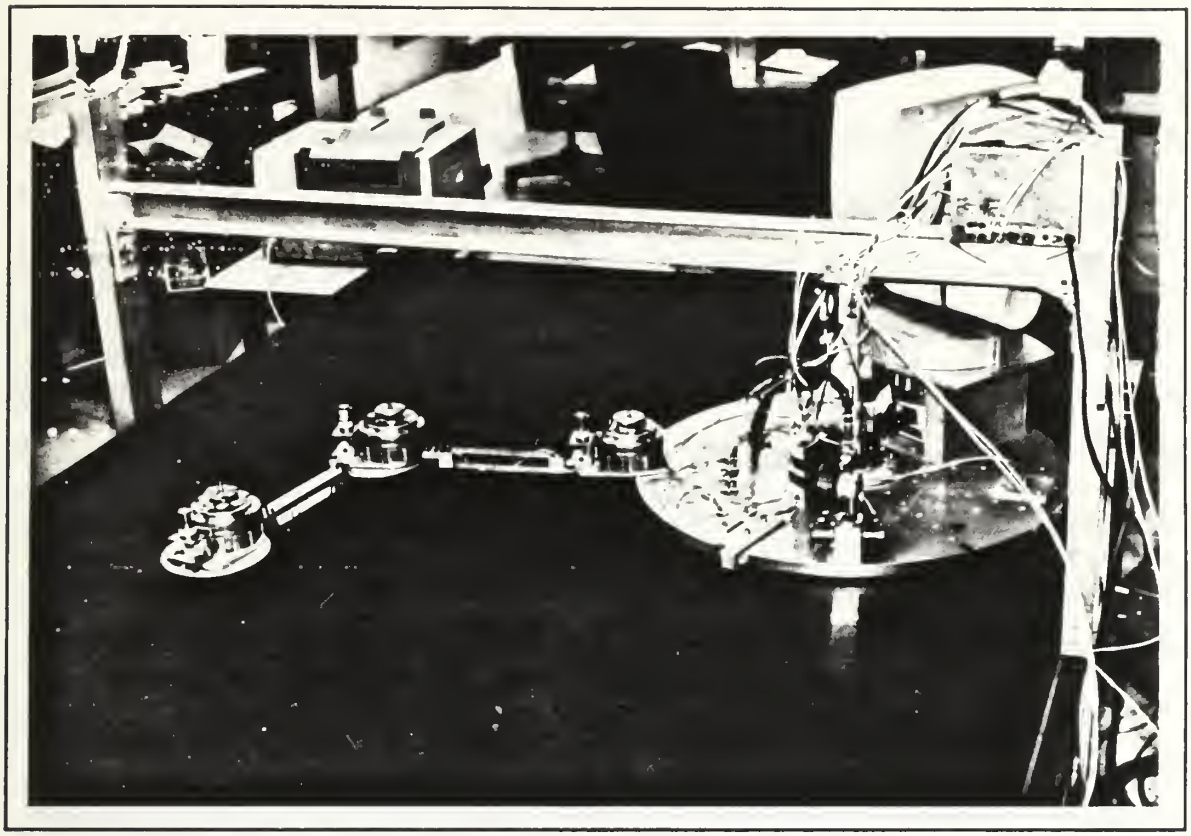

Figure 2.1 Spacecraft Robotics Simulator

1. Spacecraft Main Body

The spacecraft main body consists of a rigid, 7/8 inch thick, 30 inch diameter, aluminum disk. The main body is designed to simulate the two dimensional planar motion of a spacecraft about its pitch axis. The main body is supported by three air bearings spaced at 120 degree intervals. Each of the bearings is capable of supporting a load of 60 pounds. A fourth air bearing supported by an overhead I-beam constrains the spacecraft main body to rotational motion only. The air bearings are designed to float the spacecraft main body on a thin film of air supplied by an external air source. A RVDT, model R30D, was connected to the rotor of the air bearing by a bellow-type device.

The RVDT was manufactured by Schaevitz Sensing Systems was used to measure angular displacements of the spacecraft main body.

Attached to the spacecraft main body was a 10.7 kilogram steel momentum wheel and servo motor. The momentum wheel was designed to apply a torque to the main body by increasing or decreasing the angular velocity of the momentum wheel. The motion of the spacecraft about its pitch axis was controlled by the torque generated by this momentum wheel. The servo motor, model JR16M4CH/F9T used to drive the momentum wheel was manufactured by PMI industries. Characteristics of this motor are presented in Table 2.1.

TABLE 2.1 Momentum Wheel Actuator Characteristics

Characteristic	**Units**	
Manufacturer		PMI Motion Technologies
Model Number		JR16M4CH-1
Rated Speed	rev per minute	3000
Rated Power	horse power	1.4
Rated Torque	inch-pound	31.85
Rated Current	amps	7.79
Rated Voltage	volts	168
Outside Diameter	inches	7.4
Height	inches	4.5
Weight	pounds	17.5

An integral analog tachometer, model ARS-C121-1A, manufactured by Watson Industries, Inc. was mounted on the servo-motor to measure angular velocity.

A more detailed description of the motor, momentum wheel, and spacecraft main body can be found in [Ref. 3], and [Ref. 4].

2. Two Link Manipulator

Attached to the main body was a two link manipulator. Components for the manipulator were designed and built by the Aeronautics and Astronautics Department at the Naval Postgraduate School. All components for the arm were manufactured from 7075 and 6061 series aluminum. All components were connected with SAE grade 8 medium carbon chrome alloy cap screws. A picture of the manipulator can be found in Figure 2.2.

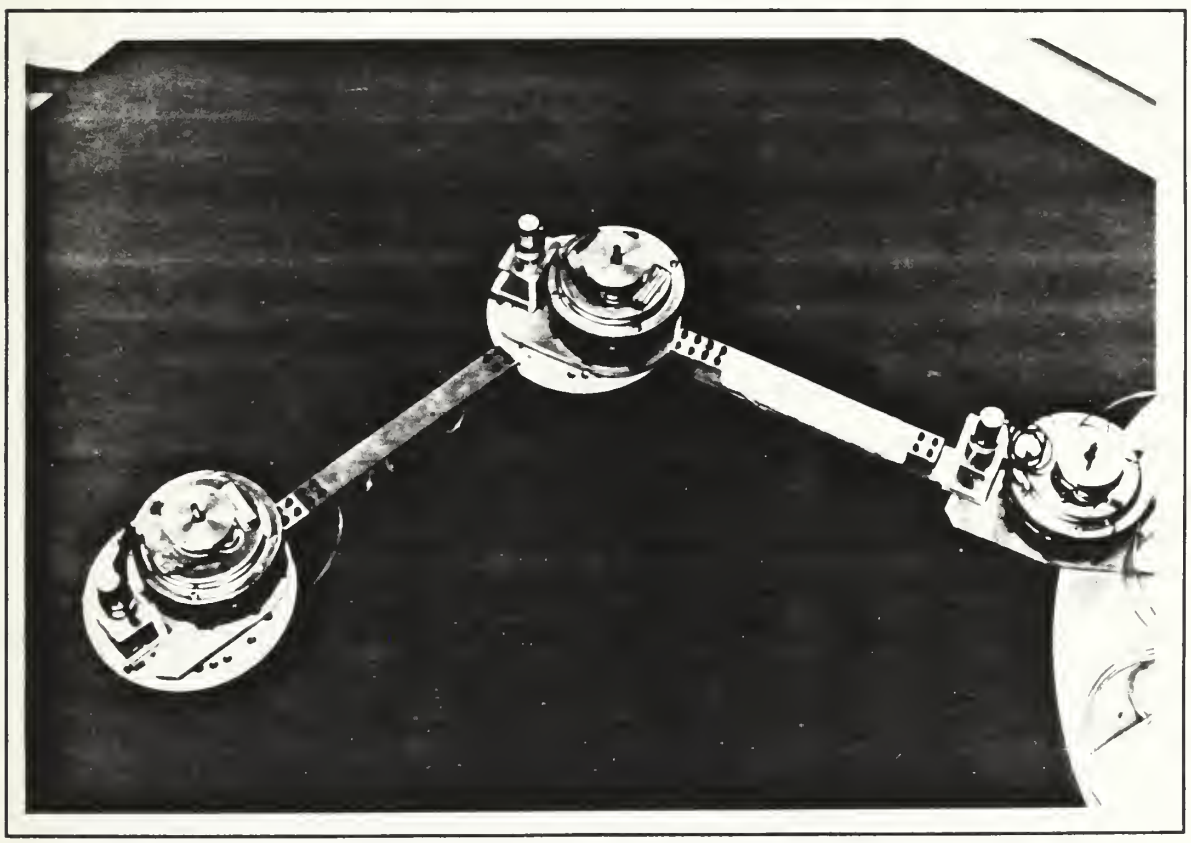

Figure 2.2 Two Link Manipulator

The links of the manipulator were positioned by two geared, servo-disk motors manufactured by PMI. A third motor, identical to the first two actuators and was mounted on the tip of link two for the purpose of orienting a simulated tool or pointing some type of antenna. Characteristics for the link actuators are presented in Table 2.2. At each joint, a RVDT, model R30D, manufactured by Schaevitz was used to measure relative angular displacement.

TABLE 2.2 Link Actuator Characteristics

Characteristic	**Units**	
Manufacturer		PMI Motion Technologies
Model Number		9FGHD
Rated Speed	rev per minute	22
Rated Torque	inch-pound	80
Rated Current	amps	5.6
Rated Voltage	volts	12
Outside Diameter	inches	4.75
Height	inches	3
Weight	pounds	3.2

The power supplies used to drive the actuators of the manipulators were manufactured by Kepco Inc. of Flushing, New York. The Kepco series BOP Bipolar Power Supplies were designed to be fast, programmable, fully dissipative, linear amplifiers. The BOP power supply is an all solid-state design, featuring integrated circuit operational amplifiers in the control circuit section and silicon power transistors mounted on special fan-cooled heat sinks in the complementary

power stage. Characteristics for the Kepco model BOP 20-10 power supply are presented in Table 2.3.

TABLE 2.3 Kepco Power Supply Characteristics

Output Power	watts	200
Max. Input Current	amps	5.5
Max. Input Power	watts	540
DC. Output Range	volts	$\pm$ 20
	amps	$\pm$ 10
Closed Loop Gain	volts/volt	2
	amps/volt	1
Bandwidth	kilohertz	18 (voltage mode)
	kilohertz	6 (current mode)
Rise Time	microseconds	20 (voltage mode)
	microseconds	60 (current mode)
Recovery Step Load	microseconds	80 (voltage mode)
	microseconds	20 (current mode)

The BOP can be operated in either the voltage or current mode through two bipolar control channels. These modes are manually selectable through the front control panel or through remote signals. Each of the principal control channels is protected by bipolar limit circuits. All control and limit channels are connected to the output stage via an "Exclusive-Or" gate so that only one channel is in control of the BOP output at any one time. The BOP output can be programmed over its full output range by a $\pm$10 volt signal applied to either one of the inputs to the

voltage or current channel. The limit control channels can be remotely controlled by a 0 to +10 volt signal applied to there respective inputs.

3. Granite Table

The entire mechanical assemblage, including the main body and manipulator were supported by air bearings that float on a thin cushion of air on a granite table with dimensions of 8 feet by 6 feet by 10.5 inches thick. The surface of the table was highly polished to optical quality grade A (0.001 inch peak to valley). The smooth surface allows the air bearings to float freely over the surface of the granite table to minimize the effects of friction on the motion of the main body and manipulator. The granite table was carefully leveled to eliminate gravity induced accelerations. The mass of the table provided an extremely stable platform upon which to conduct the experiments.

4. AC - 100

The AC-100 is a microprocessor based, programmable, real time control system manufactured by Integrated Systems International, Inc. of San Jose, California. The AC-100 was designed to automate the development of real-time systems by combining graphical modeling tools with a real-time controller. In addition to modeling and controlling, the AC-100 was also capable of data collection and storage. The AC-100 consists of the following major components: Intel 80386 Application Processor, Intel 80386 Multibus II Input / Output Processor, Intel 80386 Communication Processor, Intel 80387 Coprocessor, Weitek 3167 Coprocessor, Analog To Digital and Digital To Analog Digital Data Translation DT2402 Input/ Output Board, Two - INX-04 Encoder and Digital To Analog Servo Boards, Ethernet Interface Module, and Cabinet Enclosure and Power Supply

The software tools used with the AC-100 include a Design Package and a Run-Time Package. The Design Package included $Matrix_X$, System Build, and Auto Code. These tools are used for analysis, design, and code generation respectively. The Run-Time Software Package provides the Graphical User Interface (GUI) cross compiler, device drivers, data acquisition, and Ethernet interface required to run software code generated by Auto Code on the AC-100.

5. VAX 3100 Series Computer

The VAX 3100 Series Model 30 workstation was configured with 8 megabytes of main memory, a 19 inch (diagonal) color monitor, two 104 megabyte Winchester hard disks and a mouse. The VAX workstation is capable of 2.8 Million Instructions Per Second (MIPS).

C. SYSTEM INTEGRATION

The AC-100 is integrated with a VAX 3100 Series computer via the Ethernet interface. In this system, the VAX 3100 computer was used to analyze and design the control system. Auto Code was then used to convert the final control system design into fully compiled and linked "C" computer code. This code was then down linked to the AC-100 via the Ethernet interface. The control system, in the form of C - code software can then be used to control the servo-amplifiers which in turn were used to drive the actuators of the manipulator in real time. Manual control of the system is still provided through the VAX computer acting through the Ethernet interface. A block diagram of the integration of the control system for the two link manipulator and spacecraft main body are presented in Figure 2.3. Mass and inertia characteristics are summarized in Table 2.4

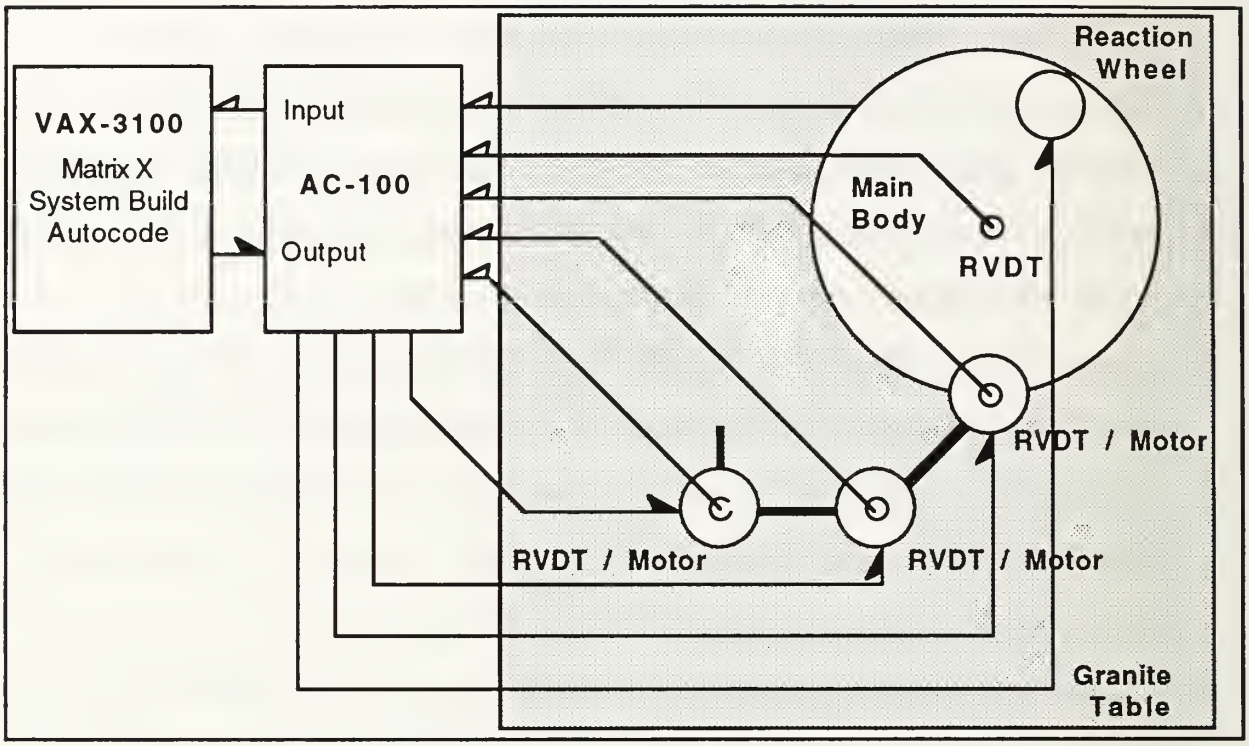

Figure 2.3 Control System Integration

TABLE 2.4 Mass And Inertia Characteristics

Body	Characteristic	Units	Value
Arm 1	Mass	kg	2.09
	Inertia (1)	kg-m^2	0.3102
	Inertia (2)	kg-m^2	0.032
	Center Of Mass(3)	cm	36.45
Arm 2	Mass	kg	2.47
	Inertia (1)	kg-m^2	0.3542
	Inertia (2)	kg-m^2	0.054
	Center Of Mass(3)	cm	34.90
Main Body	Mass	kg	52.73
	Inertia (1)	kg-m^2	0.3542
Momentum Wheel	Mass	kg	10.67
	Inertia (1)	kg-m^2	0.0912
	Center Of Mass	cm	20

Notes: (1) Moment Of Inertia About Arm Axis Of Rotation.
(2) Moment Of Inertia About Center Of Mass.
(3) Center Of Mass Location With Respect To Axis Of Rotation.

III. ANALYTICAL MODEL

The Spacecraft Robotics Simulator (SRS) consists of a central main body to which is attached a two link robotic manipulator. The motion of the main body is constrained to move in a plane resulting in a system with three degrees of freedom. This planar motion constraint greatly simplifies the problems associated with the derivation of the equation of motion and control system design yet still retains the most critical analytical elements. The manipulator and main body were modeled as rigid structures. Lagrange's equation was used to derive the equations of motion. This section will first describe how the equations of motion were derived and then how the control system was developed.

A. COORDINATE SYSTEMS

Before the spacecraft attitude and manipulator can be controlled the dynamics of the system must be carefully defined and understood. The first step in this process, is to determine the equations of motion for the system.

In this model, the main body is constrained to rotational motion only. Four different coordinate systems were used for this analysis. The $\vec{N}_1, \vec{N}_2, \vec{N}_3$ axis for this problem was fixed in inertial space coincident with the axis of rotation of the main body. The coordinate system, $\vec{x}_1, \vec{y}_1, \vec{z}_1$, is fixed in the main body with the $\vec{x}_1$ axis pointing toward the attachment point for link 1. The $\vec{x}_1, \vec{y}_1, \vec{z}_1$ coordinate system is obtained by rotating about the $\vec{N}_3$ axis of the inertial coordinate, by an angle of θ_1 . In a similar way, the coordinate systems, $\vec{x}_2, \vec{y}_2, \vec{z}_2$, is fixed at the axis of rotation of link 1 and points toward the attachment point for link 2. The $\vec{x}_2, \vec{y}_2, \vec{z}_2$ coordinate system can be obtain by rotating about the $\vec{N}_3$ axis of the

inertial coordinate system by an angle of θ_2. The coordinate system, $\vec{x}_3$, $\vec{y}_3$, $\vec{z}_3$, is fixed in the body of link 2 with the $\vec{x}_3$ axis pointing toward the end point of link 2. This coordinate system is obtained by rotating by an angle, θ_3 about the $\vec{N}_3$ axis of the inertial system. Coordinate systems are presented in Figure 3.1.

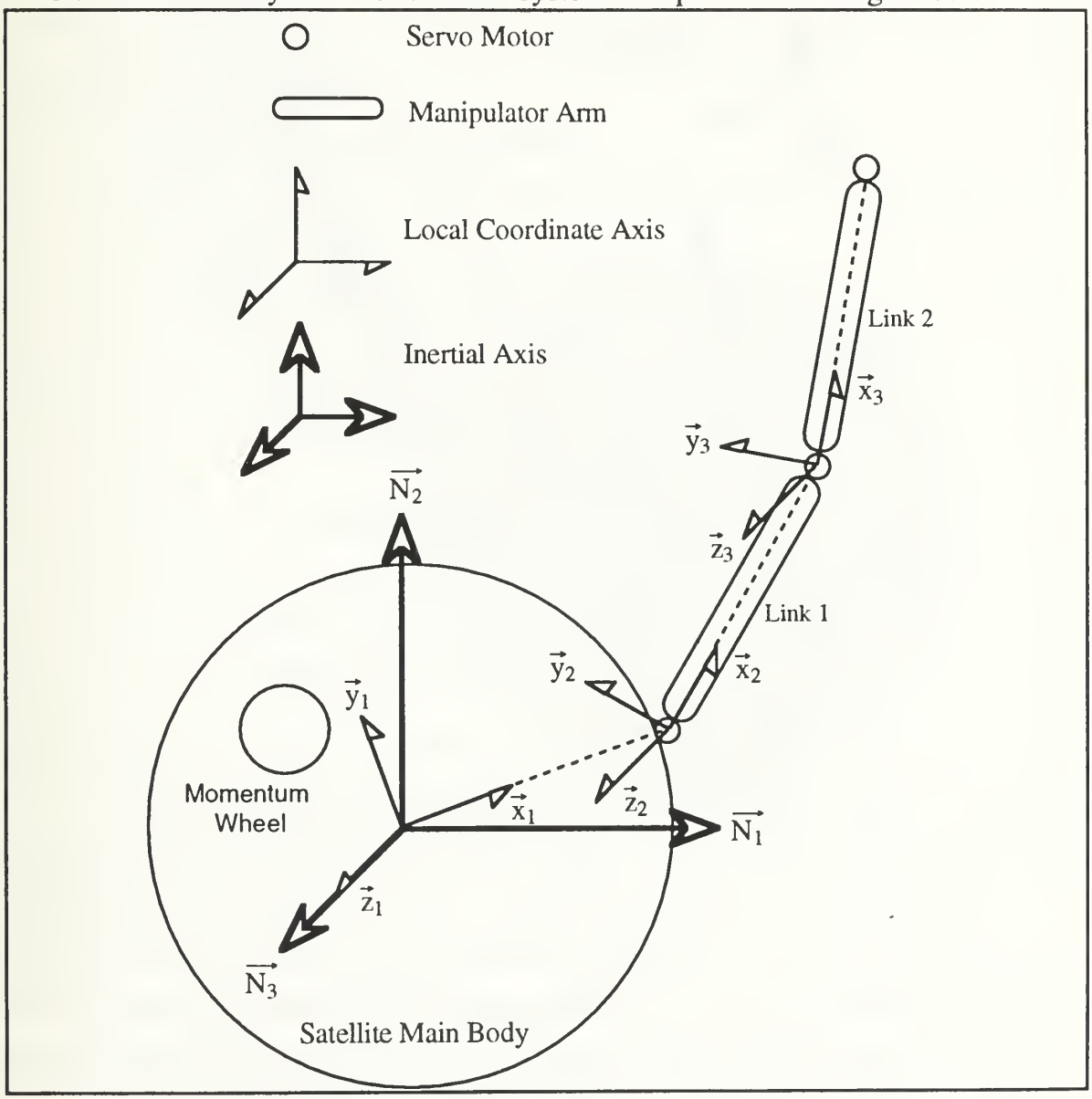

Figure 3.1 Inertial And Local Coordinate Systems

All angles, θ_1, θ_2, and θ_3, as well as vectors $\vec{r}_1$, $\vec{r}_2$, and $\vec{r}_3$ are defined in terms of inertial coordinates where these quantities are defined in Figure 3.1

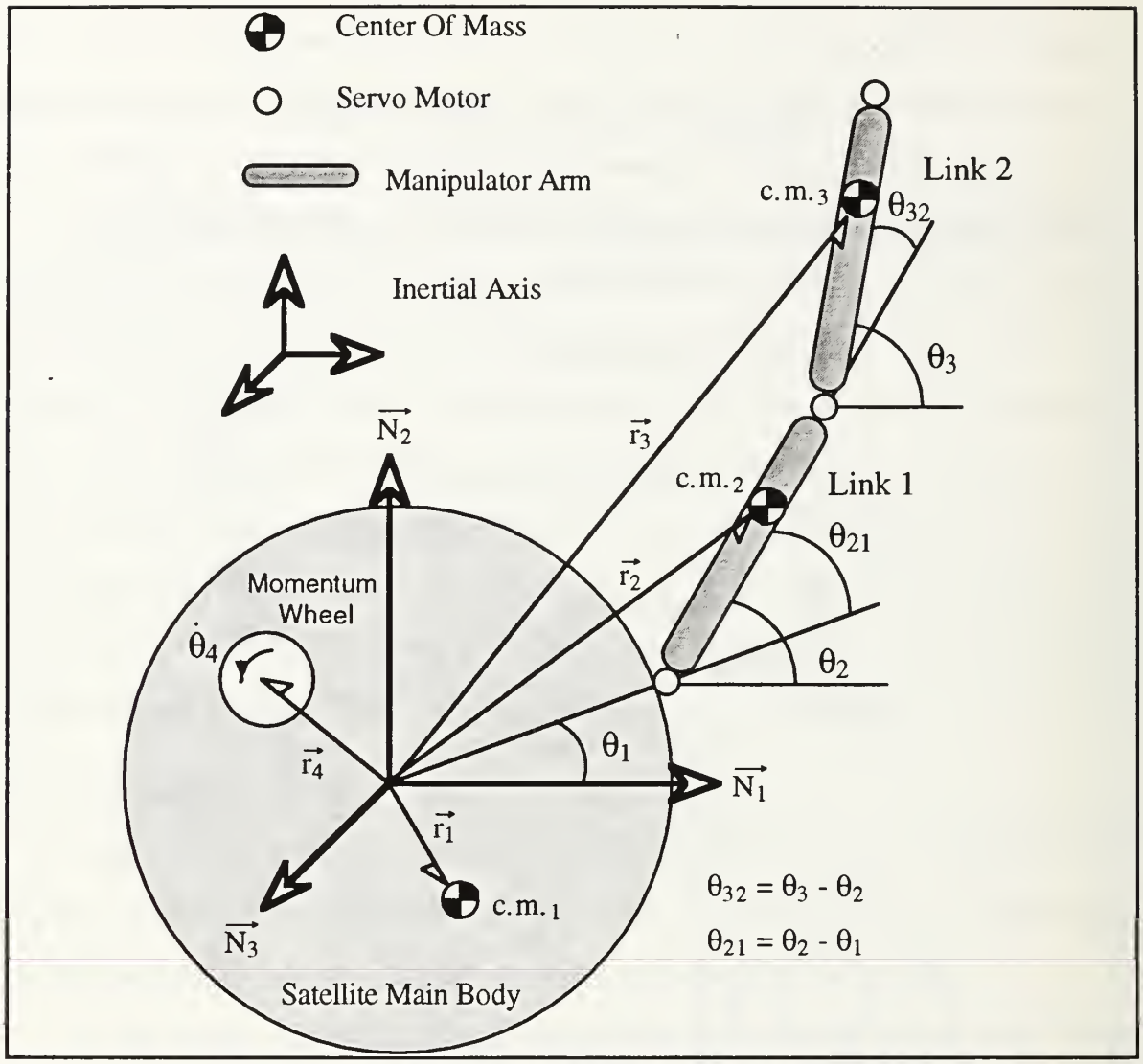

Figure 3.2 Inertial Angles And Vectors

The vectors $\vec{r}_1$, $\vec{r}_2$, and $\vec{r}_3$ describe the location of the center of mass of each of the manipulators in terms of inertial coordinates. The angles θ_{21}, θ_{31}, and θ_{32} represent relative displacements of the joints and can be derived from the inertial coordinates θ_1, θ_2, and θ_3 in such a way that $\theta_{21} = \theta_2 - \theta_1$, $\theta_{31} = \theta_3 - \theta_1$, and $\theta_{32} = \theta_3 - \theta_2$.

B. EQUATIONS OF MOTION

A momentum wheel was used to apply a control torque to the main body. The motion of the momentum wheel is de-coupled from the motion of the main body. It is assumed that the momentum wheel is only an actuator that is used to control the motion of the main body and counteract torques generated by the movement of the manipulator.

1. Lagrange's Equations Of Motion

Lagrange's equation for n-dimensional dynamic systems are stated as

$$\frac{d}{dt}\left(\frac{\partial L}{\partial \dot{q}_i}\right) - \frac{\partial L}{\partial q_i} = Q_i \text{, where } i = 1, 2, 3, ..., n \qquad (3.1)$$

$L = T - V$

V - Potential Energy

T - Kinetic Energy

q_i - i^{th} Generalized Coordinate

$\dot{q}_i$ - i^{th} Generalized Velocity

Q_i - i^{th} Applied Non conservative Force

For this particular problem, the system requires three degrees of freedom to describe its governing equations of motion. The generalized coordinates and velocities are chosen to be in terms of inertial coordinates as presented below.

$$q = \{\theta_1, \theta_2, \theta_3\}^T \equiv \{q_1, q_2, q_3\}^T \qquad (3.2)$$

$$q = \{\dot{\theta}_1, \dot{\theta}_2, \dot{\theta}_3\}^T \equiv \{\dot{q}_1, \dot{q}_2, \dot{q}_3\}^T \qquad (3.3)$$

2. Kinetic Energy

The first step is to determine the total kinetic energy of the system. The total kinetic energy of the system is given by

$$T=\sum_{i=1}^{3} T_i \tag{3.4}$$

$$T_i = \frac{1}{2} I_i \dot{\theta}_i^{\,2} + \frac{1}{2} m_i \left(\dot{\vec{r}}_i \cdot \dot{\vec{r}}_i\right) \tag{3.5}$$

I_i - i^{th} Mass Moment Of Inertia About Center Of Mass

m_i - i^{th} Mass

$$\dot{\vec{r}}_i \cdot \dot{\vec{r}}_i = \sum_{i=1}^{3} \sum_{j=1}^{3} l_i^2 \, l_j^2 \dot{\theta}_i \, \dot{\theta}_j \left(\vec{y}_i \cdot \vec{y}_j\right) \tag{3.6}$$

A more detailed algebraic procedure can be found in Appendix B.

3. Equation Of Motion

Lagrange's equations can be applied to equation (3.4) and the terms can be arranged in matrix form so that the final form can be written as (3.9).

$$M(\theta)\,\ddot{\theta} + G(\theta, \dot{\theta}) = Q \tag{3.9}$$

where

$$M(\theta) = \begin{bmatrix} m_{11} & m_{12} & m_{13} \\ m_{21} & m_{22} & m_{23} \\ m_{31} & m_{32} & m_{33} \end{bmatrix} \tag{3.10}$$

and

$$m_{11} = I_1 + L_1^2 \left[m_1 + m_2 + m_3\right] + m_4 L_4^2 \tag{3.11}$$

$$m_{22} = I_{c.m_2} + L_2^2 \left[m_2 \left(\frac{L_{c.m_2}}{L_2} \right)^2 + m_3 \right] \tag{3.12}$$

$$m_{33} = I_{c.m.3} + L_{c.m.3}^{\,2} \, m_3 \tag{3.13}$$

$$m_{12} = m_{21} = L_1 L_2 \cos(\theta_{21}) \left[m_2 \left(\frac{L_{c.m_2}}{L_2} \right) + m_3 \right] \tag{3.14}$$

$$m_{13} = m_{31} = L_1 L_{c.m_3} \cos(\theta_{31}) \, m_3 \tag{3.15}$$

$$m_{23} = m_{32} = L_2 L_{c.m_3} \cos(\theta_{32})\ m_3 \tag{3.16}$$

$$G(\theta,\dot{\theta}) = \begin{bmatrix} G(1) \\ G(2) \\ G(3) \end{bmatrix} \tag{3.17}$$

$$G(1) = [\,(m_2 L_1 L_{c.m.2}) + (m_3 L_1 L_2)\,] \sin(\theta_{21})\,\dot{\theta}_2^2 + (m_3 L_1 L_{c.m.3}) \sin(\theta_{31})\,\dot{\theta}_3^2 \tag{3.18}$$

$$G(2) = -[\,(m_2 L_1 L_{c.m.2}) + (m_3 L_1 L_2)\,] \sin(\theta_{21})\,\dot{\theta}_1^2 + (m_3 L_2 L_{c.m.3}) \sin(\theta_{31})\,\dot{\theta}_3^2 \tag{3.19}$$

$$G(3) = -(m_3 L_1 L_{c.m.3}) \sin(\theta_{21})\,\dot{\theta}_1^2 - (m_3 L_2 L_{c.m.3}) \sin(\theta_{32})\,\dot{\theta}_2^2 \tag{3.20}$$

4. Applied Torques

D' Alembert's principle for virtual work expression was used to determine the expressions for Q for the equations of motion. As written, Q is a vector containing the torques applied by the actuators at each joint in terms of inertial coordinates. At this point it will be beneficial to rewrite the Q vector in terms of local coordinates. The virtual work applied to the system is given by the following equation.

$$\delta W = \sum_{i=1}^{3} Q_i \delta\theta_i \equiv \sum_{i=1}^{3} \delta W_i \tag{3.21}$$

The elements of Q are in terms of torques applied to inertial coordinates. Since each actuator applies a local torque, it was beneficial to rearrange (3.21) and write Q in terms of the local torques applied by the individual actuators. The virtual

work described in equation (3.21) can be described in terms of these local torques as follows.

$$\delta W_1 = u_1 \delta\theta_1 - u_2 \delta\theta_1 \tag{3.22}$$

$$\delta W_2 = u_2 \delta\theta_2 - u_3 \delta\theta_2 \tag{3.23}$$

$$\delta W_3 = u_3 \delta\theta_2 \tag{3.24}$$

In matrix format Q can be written in terms of a control influence matrix B and the local torque vector, $\underline{u}$ as written in (3.25).

$$Q = B\,u = [Q_1, Q_2, Q_3]^T \tag{3.25}$$

$$Q_1 = u_1 - u_2 \tag{3.26}$$

$$Q_2 = u_2 - u_3 \tag{3.27}$$

$$Q_3 = u_3 \tag{3.28}$$

where

$$B = \begin{bmatrix} 1 & -1 & 0 \\ 0 & 1 & -1 \\ 0 & 0 & 1 \end{bmatrix} \qquad \underline{u} = \begin{bmatrix} u_1 \\ u_2 \\ u_3 \end{bmatrix}$$

C. LYAPUNOV STABLE CONTROLLER DESIGN

This design for a stable non-linear controller is based upon Lyapunov's Stability Theory. This theory is also known as Lyapunov's Second or Direct method. This theory is covered in greater detail in [Refs. 1, 2, 14, and 15]. To review the Lyapunov Stability Theory, a system without any external forces or torques is assumed. This system is assumed to have a single equilibrium state. For this system, a positive definite function is assumed to be an exact integral of the

system under some idealization. This function is termed a Lyapunov function and is selected to satisfy the requirements that it is zero at the desired equilibrium and positive everywhere else. This function may be represented by the system total energy or the Hamiltonian of the system for most of the time invariant mechanical systems. If this system is perturbed from its equilibrium state, the energy state is increased to some positive energy level. Depending upon the nature of the Lyapunov function, one of the following conclusions can be drawn.

- If the system dynamics dictate that the initial energy of the system does not increase with time, then the system is stable.
- If the energy of the system monotonically decreases with time for all initial conditions, and eventually goes to zero, then the system is asymptotically stable.
- If the energy increases for any initial condition, then the system is unstable.
- If the energy measure neither increases, nor decreases as a function of time then no conclusion can be drawn.

Despite the power of this theory, there is no unified process to find candidate Lyapunov functions that globally satisfy stability requirements. A more complete description of the Lyapunov stable controller design for flexible structures can be found in [Refs. 1 and 2].

1. Lyapunov Stable Controller With Linear Feedback

For this application, a simple non-linear controller with linear feedback of position and velocity information is the primary objective. The candidate Lyapunov function for this application is of the form

$$U = E + f\left(\delta\theta_1, \delta\theta_2, \delta\theta_3\right) \tag{3.29}$$

where E is defined as the "work energy" of the Lyapunov function and "f" is a positive function of $\delta\theta_1$, $\delta\theta_2$, and $\delta\theta_3$. Note that "f" is a pseudo potential energy that renders the Lyapunov function positive definite with respect to the new equilibrium point. In addition, $\delta\theta_i = \theta_i - \theta_{i_f}$, where θ_{i_f} is a constant that describe the final joint angle.

$$\left(\theta_1, \theta_2, \theta_3, \dot{\theta}_1, \dot{\theta}_2, \dot{\theta}_3\right) f = \left(\theta_1 f, \theta_2 f, \theta_3 f, 0, 0, 0\right) \tag{3.30}$$

The Lyapunov function in (3.30), can be differentiated to obtain

$$\dot{U} = \dot{E} + \sum_{i=1}^{3} \frac{\partial f}{\partial(\delta\theta_i)} \delta\dot{\theta}_i \tag{3.31}$$

The "work energy rate", $\dot{E}$, of (3.31) can be directly obtained from (3.22) through (3.24) and the "pseudo energy rate" of the system is defined in (3.33).

$$\dot{E} = (u_1 - u_2)\, \delta\dot{\theta}_1 + (u_2 - u_3)\, \delta\dot{\theta}_2 + u_3\, \delta\dot{\theta}_3 \tag{3.32}$$

$$\text{"Pseudo Energy Rate"} \equiv \sum_{i=1}^{3} \frac{\partial f}{\partial(\delta\theta_i)} \delta\dot{\theta}_i \tag{3.33}$$

Equations (3.32) and (3.33) can be substituted into (3.31) to form equation (3.34) which can be further simplified to equation (3.35).

$$\begin{aligned} \dot{U} = {} & (u_1 - u_2)\, \delta\dot{\theta}_1 + (u_2 - u_3)\, \delta\dot{\theta}_2 + u_3\, \delta\dot{\theta}_3 \\ & + \sum_{i=1}^{3} \frac{\partial f}{\partial(\delta\theta_i)} \delta\dot{\theta}_i \end{aligned} \tag{3.34}$$

$$\begin{aligned} \dot{U} = {} & \delta\dot{\theta}_1 \left(u_1 - u_2 + \frac{\partial f}{\partial(\delta\theta_1)}\right) + \delta\dot{\theta}_2 \left(u_2 - u_3 + \frac{\partial f}{\partial(\delta\theta_3)}\right) \\ & + \delta\dot{\theta}_3 \left(u_3 + \frac{\partial f}{\partial(\delta\theta_3)}\right) \end{aligned} \tag{3.35}$$

Based on (3.35), it is evident that a function can be selected such that $\dot{U} \leq 0$, which is the stability condition in the Lyapunov sense. Therefore, the control laws are chosen to satisfy the following relations

$$u_1 - u_2 + \frac{\partial f}{\partial(\delta\theta_1)} = -g_{1_v}\,\delta\dot{\theta}_1 \tag{3.36}$$

$$u_2 - u_3 + \frac{\partial f}{\partial(\delta\theta_2)} = -g_{2_v}\,\delta\dot{\theta}_2 \tag{3.37}$$

$$u_3 + \frac{\partial f}{\partial(\delta\theta_3)} = -g_{3_v}\,\delta\dot{\theta}_3 \tag{3.38}$$

where,

$$g_{1_v} > 0,\ g_{2_v} > 0,\ g_{3_v} > 0,\ g_{1_p} > 0,\ g_{2_p} > 0, \text{ and } g_{3_p} > 0$$

for

$$f > 0$$

In addition,

$$\dot{U} = -\left(g_{1_v}\,\delta\dot{\theta}_1^{\,2} + g_{2_v}\,\delta\dot{\theta}_2^{\,2} + g_{3_v}\,\delta\dot{\theta}_3^{\,2} \right) \tag{3.40}$$

By selecting an appropriate function for "f" equation, the stabilizing control laws (u_1, u_2, u_3) satisfying the $\dot{U} \le 0$ requirement can be built. For this case, assume that "f" is defined as follows

$$f = \frac{1}{2}\left(g_{1_p}\delta\theta_1^2 + g_{2_p}\delta\theta_2^2 + g_{3_p}\delta\theta_3^2\right) \tag{3.41}$$

where

$$g_{1_p} > 0,\ g_{2_p} > 0,\ g_{3_p} > 0$$

For a controller using pure linear feedback, (3.36-3.38) can be simplified as described below.

$$u_3 = -\,g_{3_p}\,\delta\theta_3 - g_{3_v}\,\delta\dot{\theta}_3 \tag{3.42}$$

$$u_2 = u_3 - g_{2_p}\,\delta\theta_2 - g_{2_v}\,\delta\dot{\theta}_2 \tag{3.43}$$

$$u_1 = u_2 - g_{1_p}\,\delta\theta_1 - g_{1_v}\,\delta\dot{\theta}_1 \tag{3.44}$$

$$\delta\theta_i = \theta_i - \theta_{i_f}, \text{ for } i = 1, 2, 3 \tag{3.45}$$

$$\delta\dot{\theta}_i = \dot{\theta}_i - \dot{\theta}_{i_f} \tag{3.46}$$

where

$$\dot{\theta}_{i_f} = 0 \text{ for } i = 1, 2, 3$$

2. Lyapunov Stable Tracking Controller

In a similar way, the Lyapunov stable tracking controller can also be derived. Lyapunov stability is not proven here but is discussed in more detail in [Ref. 1]. In this application, a function generator was used to generate a reference trajectory for the controller to follow. With this type of controller, a fifth order polynomial was used to generate a desired tip trajectory with a two link closed loop inverse kinematic solution in one case. In another case a "near-minimum-time" torque shaping scheme was utilized to generate a reference trajectory. Both these trajectory generators will be discussed in more detail in following sections. The control torques required for this reference tracking controller are presented next.

$$\delta u_3 = - g_{3_p} \delta\theta_3 - g_{3_v} \delta\dot{\theta}_3 \tag{3.47}$$

$$\delta u_2 = \delta u_3 - g_{2_p} \delta\theta_2 - g_{2_v} \delta\dot{\theta}_2 \tag{3.48}$$

$$\delta u_1 = \delta u_2 - g_{1_p} \delta\theta_1 - g_{1_v} \delta\dot{\theta}_1 \tag{3.49}$$

where

$$\delta\theta_i = \theta_i - \theta_{i_{ref}} \tag{3.50}$$

$$\delta\dot{\theta}_i = \dot{\theta}_i - \dot{\theta}_{i_{ref}} \tag{3.51}$$

$$\delta u_i = u_i - u_{i_{ref}} \tag{3.52}$$

The control laws presented above can be rigorously proven to satisfy the Lyapunov Stability condition if $\delta\theta_j$ and $\delta\dot{\theta}_j$ are very small.

D. REFERENCE TRAJECTORY GENERATION

For the tracking controller developed previously while discussing the Lyapunov stable tracking controller requires some reference trajectories. Here trajectory refers to a time history of position, velocity, and acceleration for each degree of freedom. The primary consideration for generating a trajectory lies in the fact that the trajectory must first of all be smooth and second it must be easily calculated. In this thesis, two different techniques will be used to generate the required trajectory information to stabilize and control the system.

The first trajectory that will be discussed involves using a fifth order polynomial to describe the path of the tip of the link three of the manipulator. In the second trajectory, a near-minimum-time maneuver using input torque shaping will be used to generate the desired trajectory.

1. Polynomial Reference Trajectory

For the tracking controller discussed in the previous section, it is usually difficult if not impossible to obtain the open-loop solutions for the theoretical reference system of differential equations. For practical considerations it is often advantageous to design the control system that will follow an easy to calculate path. For robotic applications, a polynomial of order 3 or higher is often used to specify the position of the end of the manipulator. For this application, imagine a two link manipulator attached to the spacecraft main body as depicted in Figure 3.3. In this case, the maneuver attempts to position link two from an initial angle of 20 degrees to a final position of 40 degrees and link three is maneuvered from 40 to 60 degrees. For a two link manipulator, there exists a closed loop solution

to the inverse kinematic problem that can be quickly and easily computed. The closed loop solution is described in more detail in appendix B. For this manipulator, given the beginning and final coordinates of the manipulator, the vector $\vec{r}$ is used to specify the position of the end point of link two as a function of time. This vector is presented in Figure 3.3.

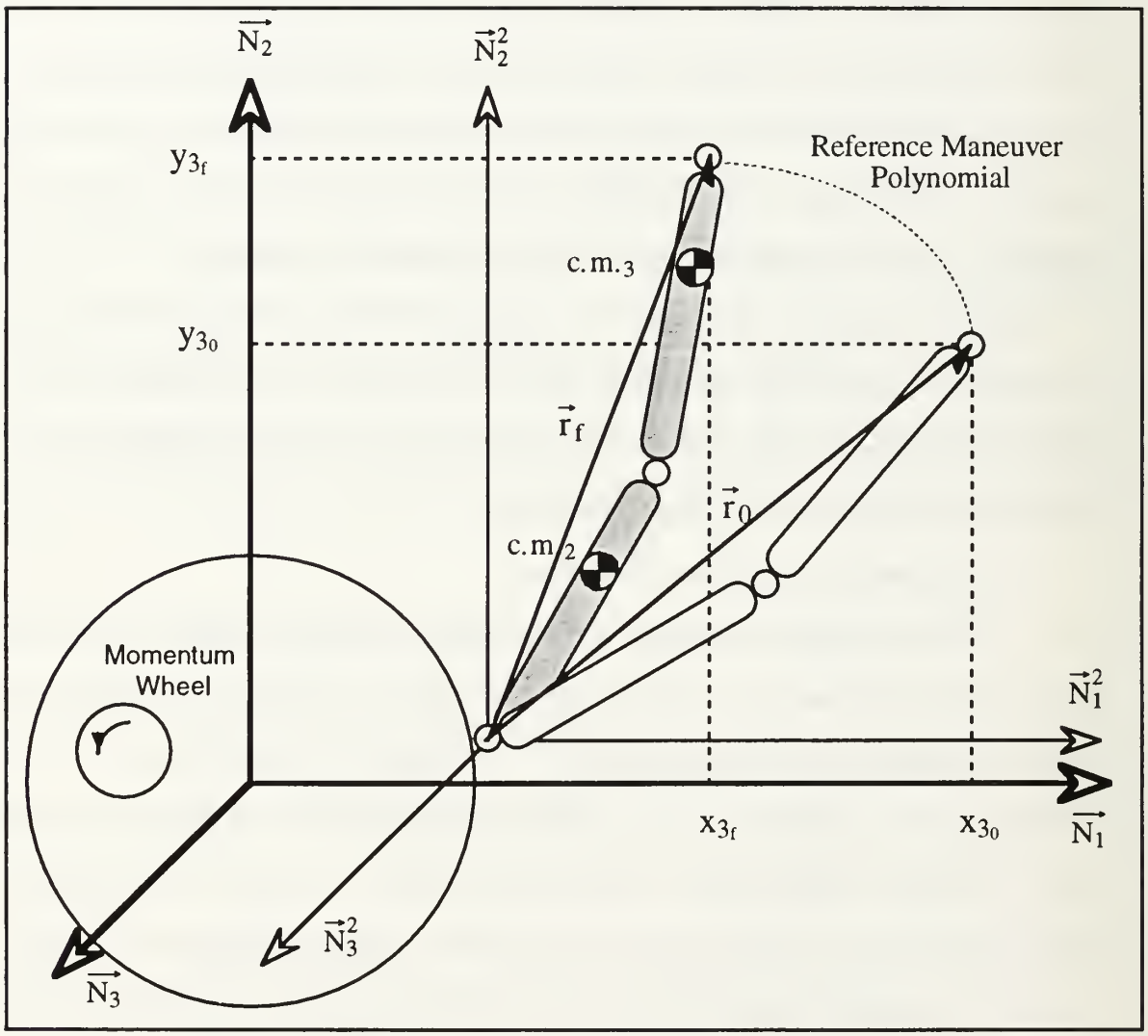

Figure 3.3 Polynomial Reference Maneuver

$$\vec{r}(t) = \vec{r}(t_0) + f(t)\left[\vec{r}(t_f) - \vec{r}(t_0)\right] \tag{3.53}$$

To simplify the calculations, t can be written as a function of normalized time, τ, given the start time t_0 and finish time t_f. Note that for $t_0 < t < t_f$, then $0 < \tau < 1$.

$$\tau = \frac{t - t_0}{t_f - t_0} \tag{3.54}$$

A fifth order polynomial was used for this application. This allowed the user to specify the beginning and final velocities and accelerations as well as the beginning and final positions of the tip. The polynomial for this controller was of the form

$$f(\tau) = c_1 + c_2\tau + c_3\tau^2 + c_4\tau^3 + c_5\tau^4 + c_6\tau^5 \tag{3.55}$$

and was subject to the following boundary conditions.

$$f(0) = 0, \dot{f}(0) = 0, \ddot{f}(0) = 0$$

$$f(1) = 1, \dot{f}(1) = 0, \ddot{f}(1) = 0$$

The resulting expression for $f(\tau)$ is obtained as

$$f(\tau) = 10\tau^3 - 15\tau^4 + 6\tau^5 \tag{3.56}$$

Equation (3.56) can be differentiated with respect to time. These expressions were utilized to calculate velocities and accelerations and are presented in equations (3.57) and (3.58).

$$\dot{f}(\tau) = 30\tau^2 - 60\tau^3 + 30\tau^4 \tag{3.57}$$

$$\ddot{f}(\tau) = 60\tau - 180\tau^2 + 120\tau^3 \tag{3.58}$$

Equation (3.53) can also be differential with respect to time to give the velocity and acceleration of the tip of link three purely as a function of time.

Vector Position:

$$\vec{r}(\tau) = \vec{r}(t_0) + f(\tau)\left[\vec{r}(t_f) - \vec{r}(t_0)\right] \tag{3.59}$$

Vector Velocity:

$$\dot{\vec{r}}(\tau) = \dot{f}(\tau)\left[\frac{\vec{r}(t_f) - \vec{r}(t_0)}{t_f - t_0}\right] \tag{3.60}$$

Vector Acceleration:

$$\ddot{\vec{r}}(\tau) = \ddot{f}(\tau)\left[\frac{\vec{r}(t_f) - \vec{r}(t_0)}{(t_f - t_0)^2}\right] \tag{3.61}$$

With the position of the tip known as a function of time, the angles θ_{21} and θ_{32} can be solved for directly as can θ_2 and θ_3 via the two link closed loop solution of the inverse kinematics problem. At this point θ_1, $\dot{\theta}_1$, and $\ddot{\theta}_1$ are all assumed to be comparatively small. The Jacobian can be used to define the relationship between the velocity and angular velocity as well as the tip acceleration and angular acceleration as described in the following equations.

$$\dot{\vec{r}} = H\left\{\dot{\theta}\right\} \tag{3.62}$$

where H is the Jacobian corresponding to the given configuration.

$$H = \begin{bmatrix} -l_2 \sin(\theta_2), & -l_3 \sin(\theta_3) \\ l_2 \cos(\theta_2), & l_3 \cos(\theta_3) \end{bmatrix} \tag{3.63}$$

$$\ddot{\vec{r}} = H\left\{\ddot{\theta}\right\} + \dot{H}\left\{\dot{\theta}\right\} \tag{3.64}$$

$$\dot{H} = \begin{bmatrix} -l_2 \cos(\theta_2), & -l_3 \cos(\theta_3) \\ -l_2 \sin(\theta_2), & -l_3 \sin(\theta_3) \end{bmatrix} \tag{3.65}$$

With the above equations, the position (angular and cartesian), velocity (angular and cartesian), and acceleration (angular and cartesian), can all be determined as functions of time. With this information, and the physical

characteristics of the system, the reference torques can also be determined using equation presented below.

$$u_{ref} = B^{-1}\left[M(\theta)\ddot{\theta} + G(\theta,\dot{\theta})\right] \tag{3.66}$$

2. Minimum-Time-Maneuver

For an ideal case, of a single degree of freedom system, the minimum time required to perform a particular maneuver is achieved by applying the maximum available torque for one-half of the time required to complete the maneuver followed by the remaining half with the maximum negative torque. This results in a controller where the torque is always operated at its maximum value and gives rise to a torque shaping function, position, velocity, and accelerations profiles as presented in Figure 3.4. This type of controller is sometimes referred to as a bang-bang controller.

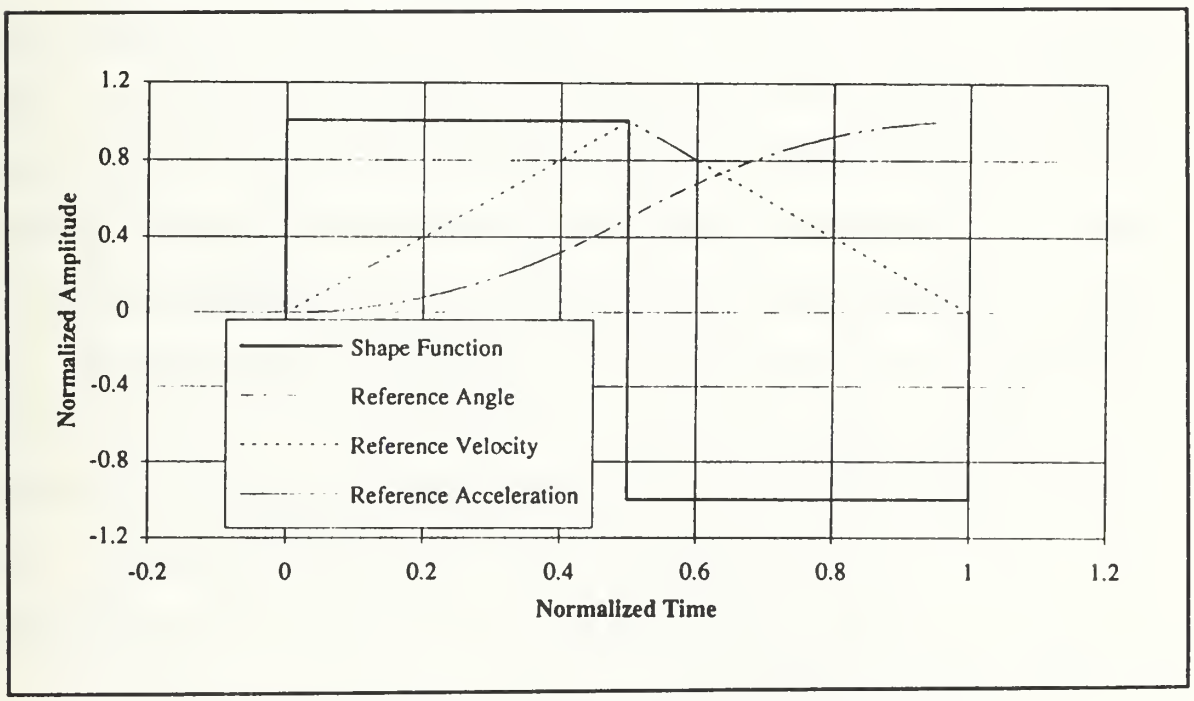

Figure 3.4 Bang-Bang Minimum Time References

For an application with a single degree of freedom, the relationship between the angular acceleration and the applied torque is given by equation (3.67) with the applied torques given by equation (3.68).

$$I\ddot{\theta} = u \tag{3.67}$$

$$u = \begin{cases} u_{max}, \text{ for } 0 \le t \le \frac{t_f}{2} \\ -u_{max}, \text{ for } \frac{t_f}{2} \le t \le t_f \\ 0, \text{ for } t_f \le t \end{cases} \tag{3.68}$$

Bang-Bang control theory for minimum time maneuvers is discussed in more detail in [Refs. 1 and 2].

3. Near-Minimum-Time Rigid Body Maneuver

A more general case of the bang-bang, minimum time controller is the near-minimum-time controller. The bang-bang controller does maneuver the manipulator from the initial to final positions in the minimum amount of time. The primary drawback of the bang-bang controller is the rapid rise of the torque trajectory. This results in a rapid acceleration followed by a rapid deceleration which will require actuators with instantaneous switching capacity which is not practical and a robust structural design for the manipulators themselves. By introducing an input shape function, the instantaneous rise in the torque trajectory can be reduced, resulting in slightly smaller accelerations which will in turn require smaller actuators and reduced structural requirements. For comaparison, the input shaping function for $\alpha = 0.1$ and $\alpha = 0.25$ are presented in Figures 3.5 and 3.6 respectively.

The differential equations used to describe the minimum time maneuver above can be modified so that they are of the form.

$$I\ddot{\theta}_{ref} = u_{ref} = u_{max}\, f(\Delta t, t_f, t) \tag{3.70}$$

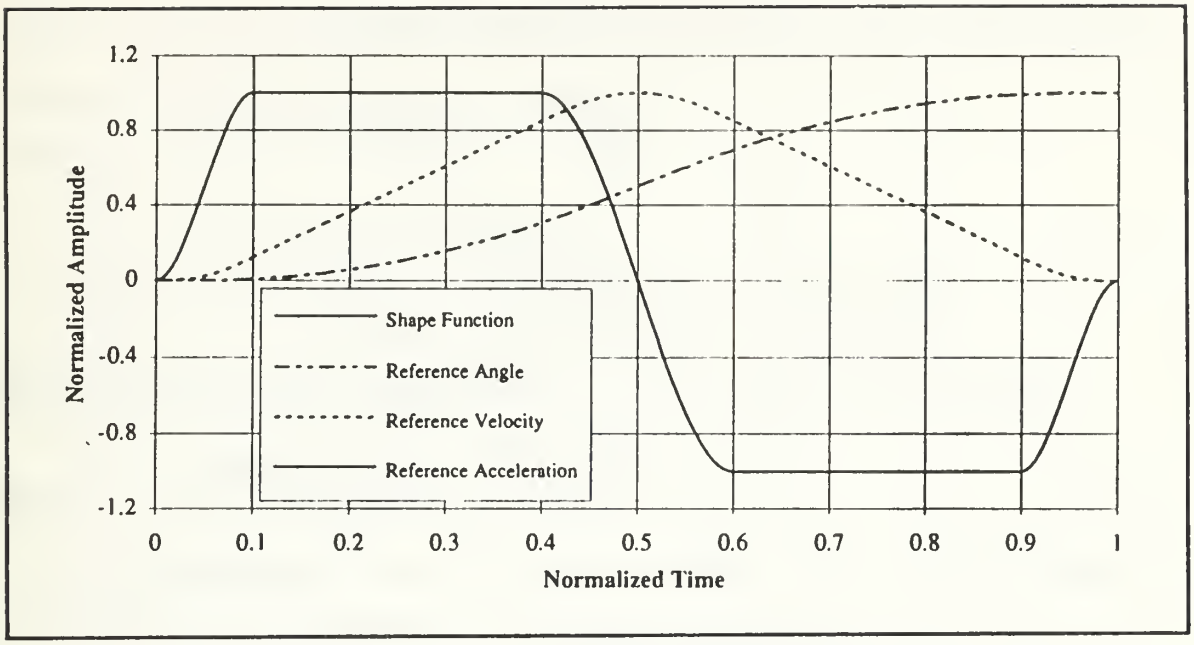

Figure 3.5 Normalized Input Shaping Funciton With $\alpha = 0.1$

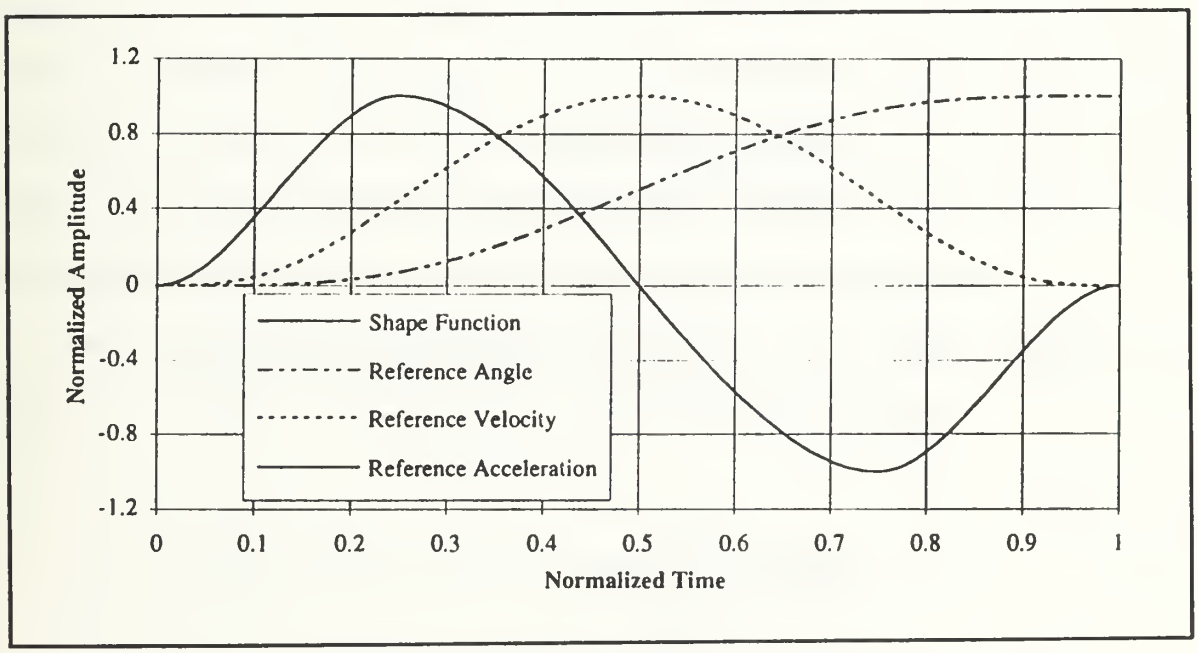

Figure 3.6 Normalized Input Shaping Funciton With $\alpha = 0.25$

Where the input shaping function is suggested in the form.

$$f(\Delta t, t_f, t) = \begin{cases} = \left(\frac{t}{\Delta t}\right)^2 \left[3 - 2\left(\frac{t}{\Delta t}\right)\right] \text{ for } 0 \le t < \Delta t \\ = 1 \text{ for } \Delta t \le t < t_1 \\ = 1 - 2\left\{\left(\frac{t - t_1}{2\Delta t}\right)^2 \left[3 - 2\left(\frac{t - t_1}{2\Delta t}\right)\right]\right\} \text{ for } t_1 \le t < t_2 \\ = -1 \text{ for } t_2 \le t < t_3 \\ = -1 + \left\{\left(\frac{t - t_3}{\Delta t}\right)^2 \left[3 - 2\left(\frac{t - t_3}{\Delta t}\right)\right]\right\} \text{ for } t_3 \le t < t_f \end{cases} \quad (3.69)$$

where

t_f = Maneuver Time

$t_1 = t_s - \Delta t$

$t_2 = t_s + \Delta t$

$t_3 = t_f - \Delta t$

$\Delta t = \alpha t_f$ = Rise Time

$t_s = \beta t_f$ = Switching Time, where $\beta = 0.5$

To determine a relationship between the angular acceleration and the maximum available torque we begin with the non-linear equations of motion

$$M(\theta)\ddot{\theta} + G(\theta, \dot{\theta}) = B\,\underline{u} \quad (3.70)$$

where

$M(\theta)$ - Mass Matrix

$G(\theta, \dot{\theta})$ - Coriolis Acceleration Terms

$\underline{u}$ - Local Torques

Equation (3.70) is linearized by eliminating all non-linear cosine, sine, and higher order terms. These linearization process results in the following equation for an i^{th} link.

$$I\,\ddot{\theta}_{ref} = u_{ref} = u_{max}\, f(\Delta t, t_f, t) \tag{3.71}$$

I - Moment Of Inertia About Axis Of Rotation

Equation (3.71) can be reorganized into the form of the following equation.

$$\ddot{\theta}_{ref} = \frac{u_{max}\, f(\Delta t, t_f, t)}{I} \tag{3.72}$$

In this equation, u_{max} is a design parameter that is determined by the characteristics of the actuator used to drive the manipulators. For this application, all the actuators are the same geared motor. $f(\Delta t, t_f, t)$ can be modified by varying the α variable. I, the linearized mass moment of inertia, is determined by the mass characteristics of the system and does not vary with time or changing geometry. Given a maximum torque u_{max}, and an input shaping function with suitable boundary conditions, the reference position and velocities can be determined by integrating the following equations piece wise of the time interval determined by the maximum torque.

$$\dot{\theta}_{ref}(t) = \dot{\theta}_0 + \frac{u_{max}}{I} \int_{t_0}^{t} f(\Delta t, t_f, \tau)\, d\tau \tag{3.73}$$

$$\theta_{ref}(t) = \theta_0 + \dot{\theta}_0\,(t-t_0) + \frac{u_{max}}{I} \int_{t_0}^{t} \int_{t_0}^{\tau_1} f(\Delta t, t_f, \tau_2)\, d\tau_2\, d\tau_1 \tag{3.74}$$

where

$$t_0 = 0 \qquad \theta(0) = \theta_0 \qquad \dot{\theta}(0) = 0$$

$$t = t_f \qquad \theta(t_f) = \theta_f \qquad \dot{\theta}(t_f) = 0$$

are the boundary conditions at the start and completion of the maneuver. The resulting reference equations are presented in Appendix B.

The near-minimum-time to complete the maneuver can be obtained by setting $t = t_f$ in the equation presented below and obtained from Appendix B.

$$\theta_f = \frac{u_{max}}{I}\left\{\left[\frac{1}{4} - \frac{1}{2}\alpha + \frac{1}{10}\alpha^2\right] t_f^2\right\} \tag{3.75}$$

By doing this, a relationship between the time to complete the maneuver and the maximum torque available can be determined for an i^{th} link.

$$t_i = \sqrt{\frac{I_i(\theta_{f_i} - \theta_{0_i})}{u_{max_i}\left(\frac{1}{4} - \frac{1}{2}\alpha + \frac{1}{10}\alpha^2\right)}} \tag{3.76}$$

$$u_{max_i} = \frac{I_i(\theta_{f_i} - \theta_{0_i})}{t_{f_i}^2\left(\frac{1}{4} - \frac{1}{2}\alpha + \frac{1}{10}\alpha^2\right)} \tag{3.77}$$

For this application, the time derived with the above equations represents the near-minimum-time required to perform the maneuver for only one joint.

E. ANALYTICAL MODEL SUMMARY

This research project analyzes how a two link manipulator can be controlled from a spacecraft main body while minimizing the effect of manipulator motion upon the main body In general one can calculate the interaction force between the links and main body by using the Newtonian approach with free body diagrams. Based on this analysis, the more smoothly that the maneuver is performed, the smaller the interactive force will be. Two basic type of controllers were developed. In the first controller, linear feedback of position and velocity

information from the joints was used to control the endpoint position. In the second type of controller, position and velocity information are used in conjunction with a reference trajectory to control endpoint position.

For this type of controller, two different schemes were used to generate the reference trajectory. In the first, a fifth order polynomial in conjunction with the two link closed loop solution for the manipulator inverse kinematics and the Jacobian were used to generate the reference trajectory. In the second, a near-minimum-time torque shaping technique was used to determine the reference trajectory. All components, including the manipulator and main body, are modeled as rigid bodies.

IV. RESULTS AND DISCUSSION

Analytical results from the simulation are presented in this section. Three different techniques were used to control and stabilize the position of the manipulator. Results from the linear feedback controller with constant gains, polynomial reference tracking controller and near-minimum-time reference tracking controllers are presented sequentially.

A. REFERENCE MANEUVER

The three most import criteria with respect to this research are the end tip final position, joint torques, and the effect of manipulator motion on the attitude of the main body. Final position for the endpoint of the manipulator is critical for performing assembly tasks. Joint torques are important to verify if the servo-actuators can perform the desired maneuvers. The effect of the manipulator motion upon the main body is critical due to the excitation of flexible structures on the spacecraft or the effect upon antenna pointing accuracy to maintain a communications link.

To be able to effectively compare the performance of the three different controllers, a standard reference maneuver was developed. For this maneuver, the desired rotation of the main body was zero. Link 1 was programmed to move from an inertial angle of 20 degrees to 40 degrees. Link 2 was programmed to move from an initial inertial angle of 40 degrees to a final position of 60 degrees. This reference maneuver is depicted in Figure 4.1

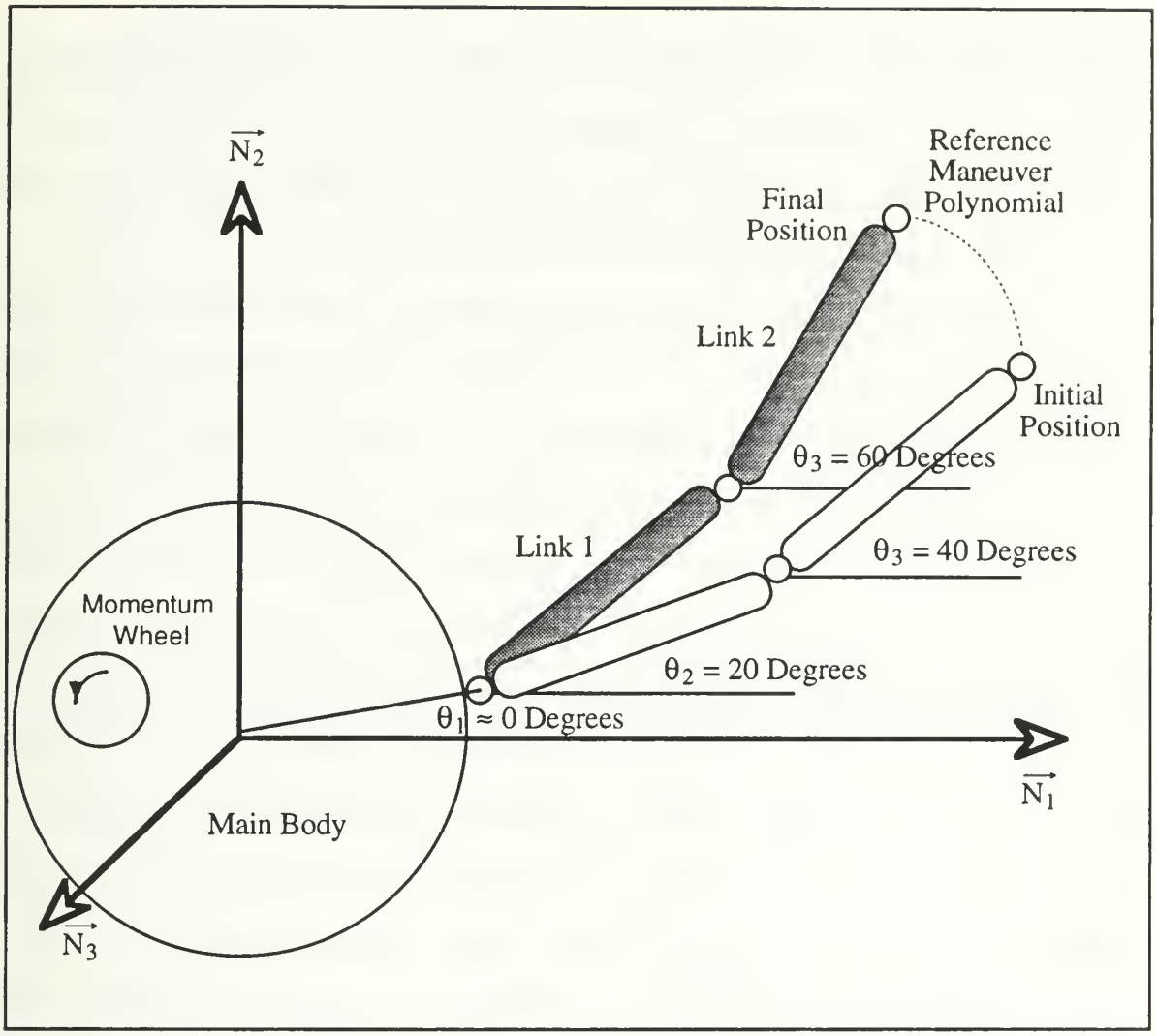

Figure 4.1 Reference Maneuver

B. LINEAR CONSTANT GAIN FEEDBACK CONTROLLER

The theory behind the linear constant gain feedback, controller is described in more detail in Chapter III and [Ref. 1,15]. Position gains of 1 ($G_P = 1$)and velocity gains of 5 ($G_V = 5$) were used for these plots. Small gain ($G_P = 0.1$ and $G_V = 0.2$) plots are presented in Appendix D for comparison.

The linear feedback controller was the simplest controller conceptually and the easiest to implement. This controller provided stable control over a wide

range of gains and for a wide variety of maneuvers. No knowledge of the system mass or inertia characteristics was required for this controller. Only the position and velocity gains, and beginning and final arm positions were required to calculate the required control torques to perform the maneuver.

The joint time history for this case is presented in Figure 4.2 and the joint velocity time history is presented in Figure 4.3. Performance of this control system was directly related to gain selection. The system was relatively sensitive to small changes in the position and velocity gains. This resulted in changes to the maneuver time and control system damping. The system was stable for all gains and maneuvers evaluated and it could be proven by Lyapunov stability theory that the system was globally stable. Even with system stability not really in question, there was no way to systematically select position and velocity gains to optimize maneuver time or torques to achieve desired performance measures.

The magnitude of the gains directly impacted the performance of the manipulator and the stability of the main body. Larger gains generated larger control torques and reduced the time required to perform the maneuver. The damping of the system could also be varied with the gain selection. The effect of this movement on the main body was small but still resulted in a displacement of nearly 2 degrees. Although this is apparently a small displacement, 2 degrees may still cause degradation in communication with the satellite due to antenna pointing errors.

Time history plots for torques and momentum wheel speed are presented in Figures 4.4 and 4.5 respectively. The response of this system to the controller was characterized by a very rapid increase in torque immediately after initiation of

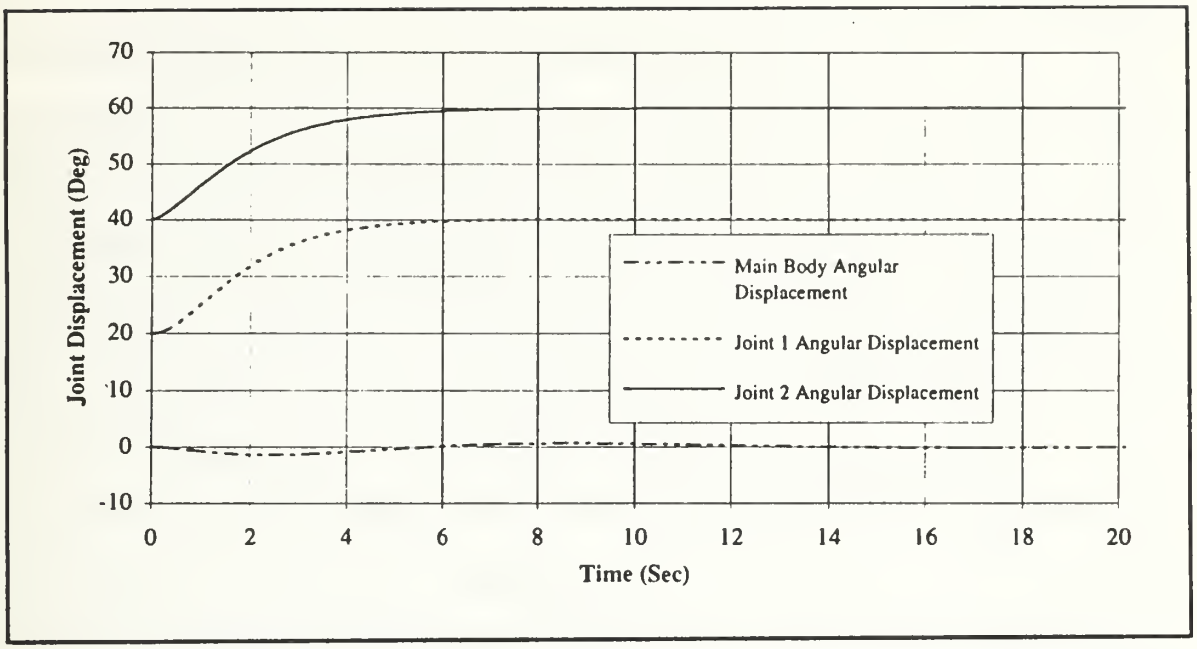

Figure 4.2 Linear Constant Gain Feedback Joint Position Time History With G_p=1 and G_v=5

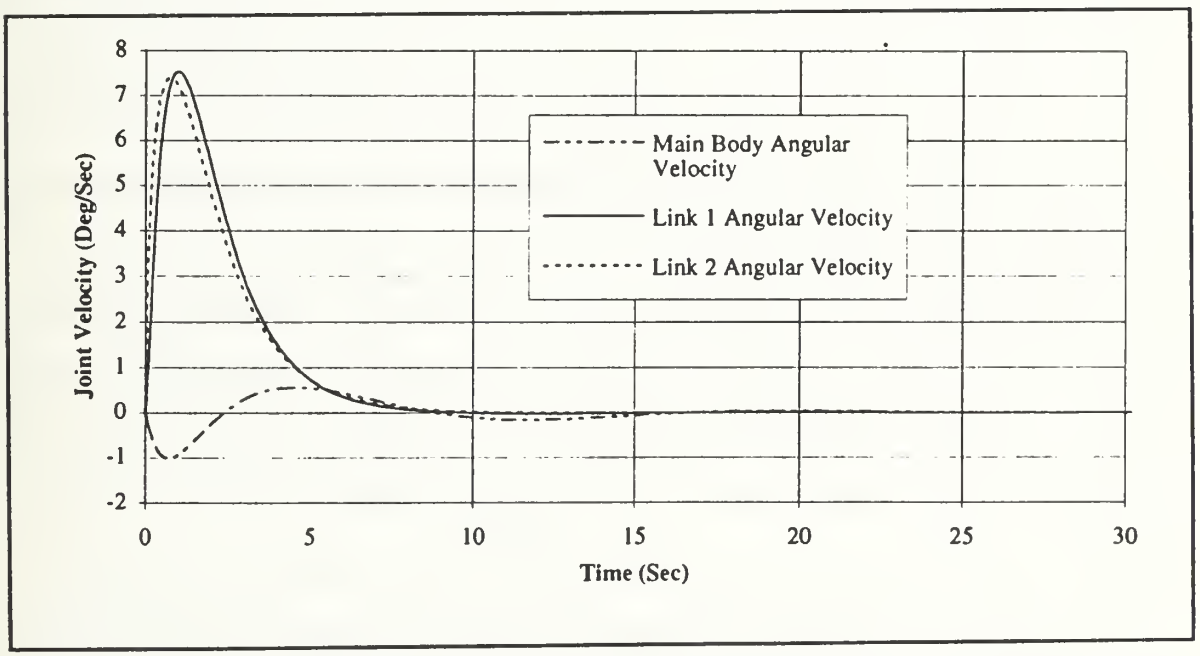

Figure 4.3 Linear Constant Gain Feedback Joint Velocity Time History With G_p=1 and G_v=5

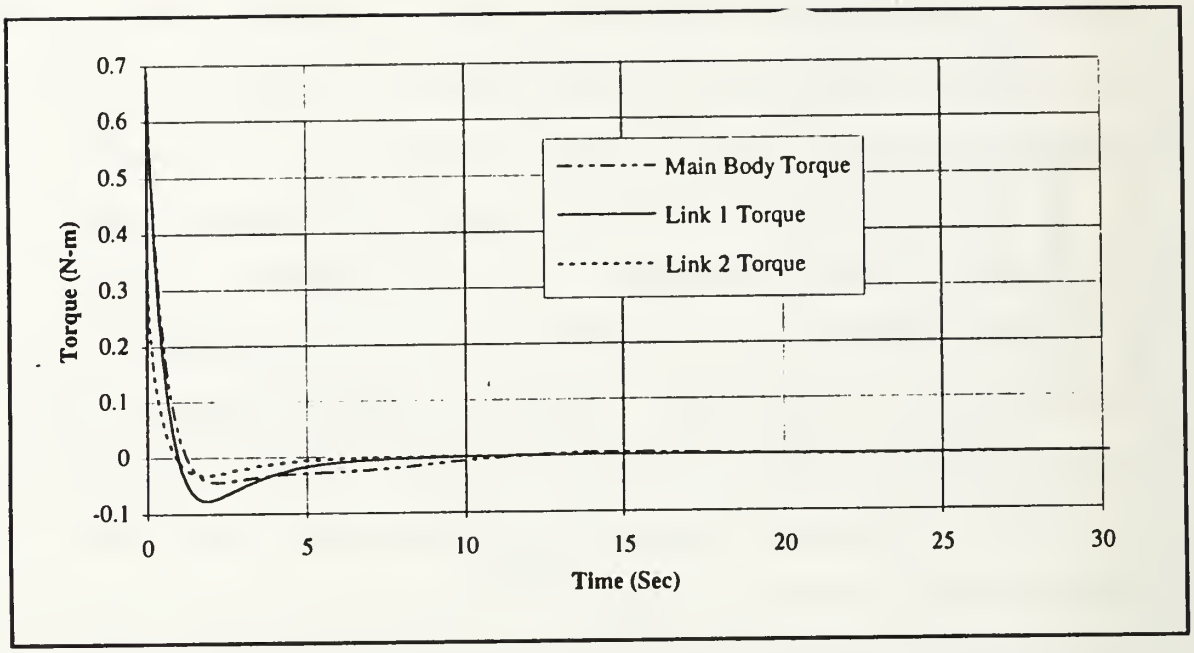

Figure 4.4 Linear Constant Gain Feedback Torque Time History With G_p=1 and G_v=5

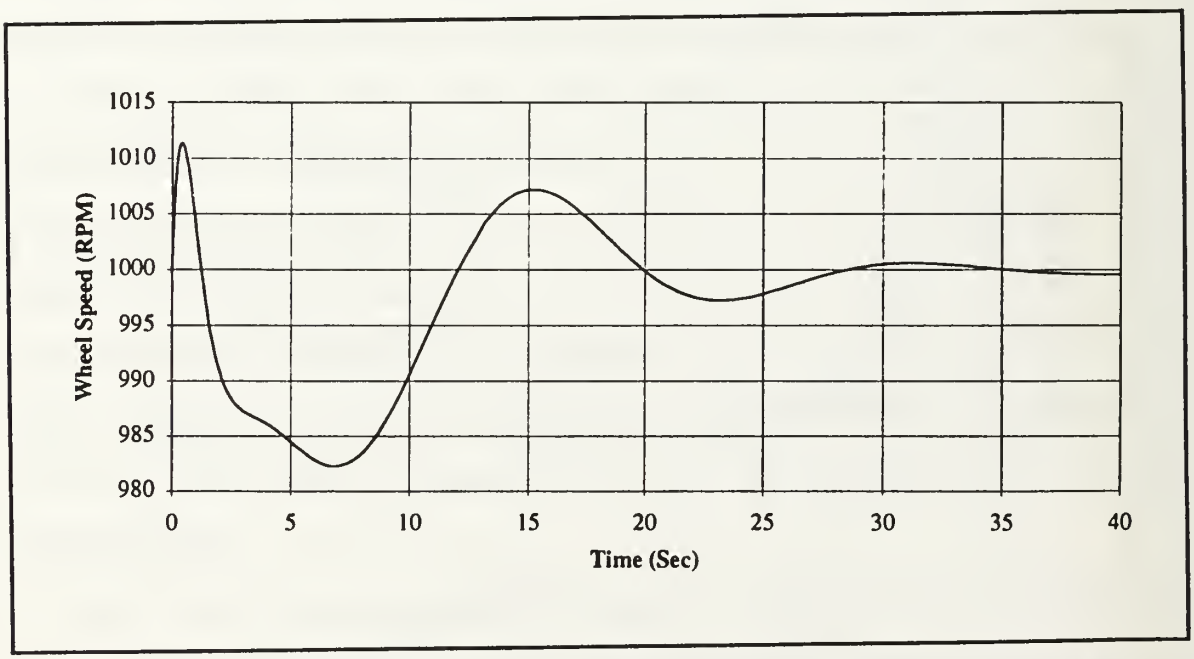

Figure 4.5 Linear Constant Gain Feedback Momentum Wheel Speed Time History With G_p=1 and G_v=5

the maneuver followed by a rapid decrease after a few seconds. This response was similar to an impulse input that became more pronounced with increased commanded motion or with increased gains. Large gains are desirable to achieve acceptable levels of performance but must be balanced against actuator characteristics , magnitude of the maneuver, and structural considerations.. A large and sudden increase in commanded torque could saturate the actuator or excite flexible appendages attached to the spacecraft.

The large initial torques, depicted in Figures 4.4 and 4.5, correspond to rapid changes in the speed of the momentum wheel. Large speed changes are required during the initial portion of the maneuver to generate large toques to counteract the forces generated by the manipulator. Based on previous experience with the FSS and analysis of electrical power requirements of the actuator and power supply, it is reasonable that the actuator will be able to compensate for the torques generated by the movement of the manipulator.

C. POLYNOMIAL REFERENCE TRACKING CONTROLLER

To rectify the problems encountered with the simple linear constant gain feedback controller a reference tracking controller was implemented. In the previous case, there was a large initial error for which the system was attempting to correct. In this controller, a smooth, fifth order polynomial was used to generate a reference trajectory so that the correction could be evenly partitioned over a specified maneuver time. With this information, reference torques, angular position, velocity, and acceleration were obtained as a smooth function of time. As a result the initial "jump" generated by the linear feedback controller was eliminated and the manipulator was able to track a smooth path from initial to

final conditions. A variation of the Lyapunov stable control law used in the previous controller was used with this reference trajectory controller.

With this controller, the time required to perform the maneuver could be specified but was subject to the characteristics of the actuators and the task being performed. Two maneuver times were analyzed. In the first case, the time to perform the maneuver was fixed at 2.5 seconds. This time was selected to determine joint torques, velocities, and momentum wheel speeds while operating near the torque limit of the actuators. In the second case, a time of 5 seconds used to determine the effect of maneuver time on the actuators. These plots for the 5 second maneuver time are included in Appendix D to demonstrate the effect of maneuver time upon joint torques and velocities.

Position and velocity time history of the manipulator for a maneuver time of 2.5 seconds are presented in Figure 4.6. and 4.7 respectively. Torque and momentum wheel speed plots for a maneuver time of 2.5 seconds are presented in Figures 4.8 and 4.9 respectively.

Movement of the manipulator did not cause measurable disturbance to the main body. Manipulator torques were smoothly applied, and the control system was able to counter these torques effectively and in a timely manner, negating motion by the main body. The stability of the main body during manipulator motion is desirable since it will reduce pointing errors for unstablized imaging devices or high gain antenna communications systems.

The polynomial reference controller demonstrated stable operation over a wide variety of operating conditions and feedback gains. The magnitude of the gains had little or no effect upon the maneuver time since this characteristic was specified in the reference maneuver. Commanded torques closely tracked the

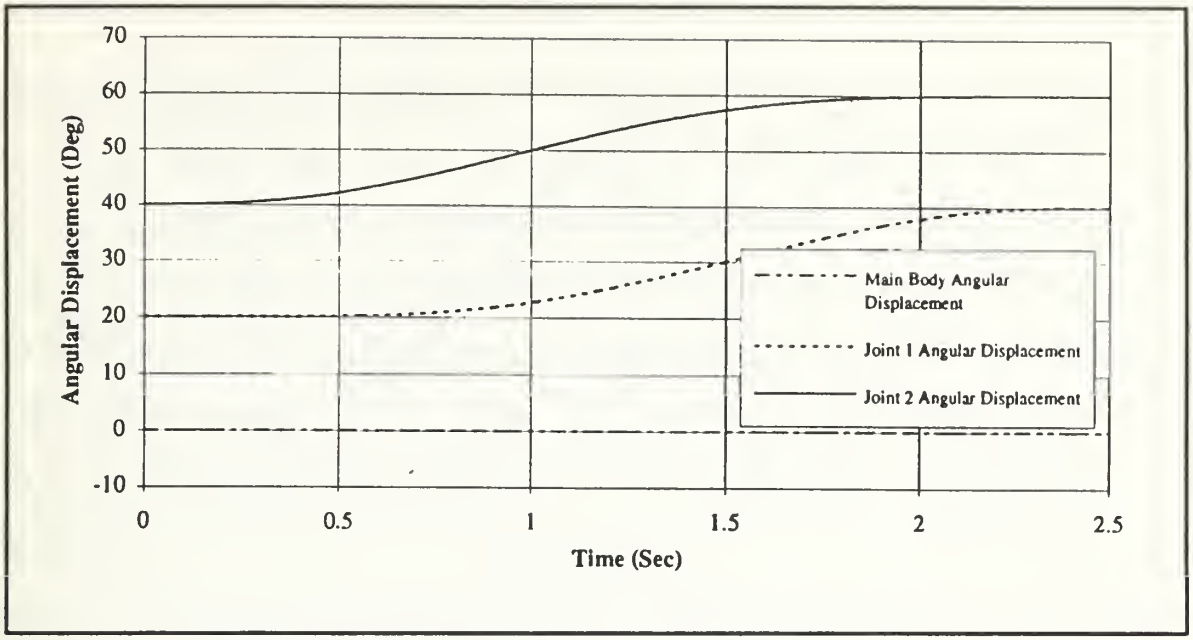

Figure 4.6 Polynomial Reference Tracking Controller Joint Position Time History With G_P=1, G_V=5 And Maneuver Time Of 2.5 Seconds

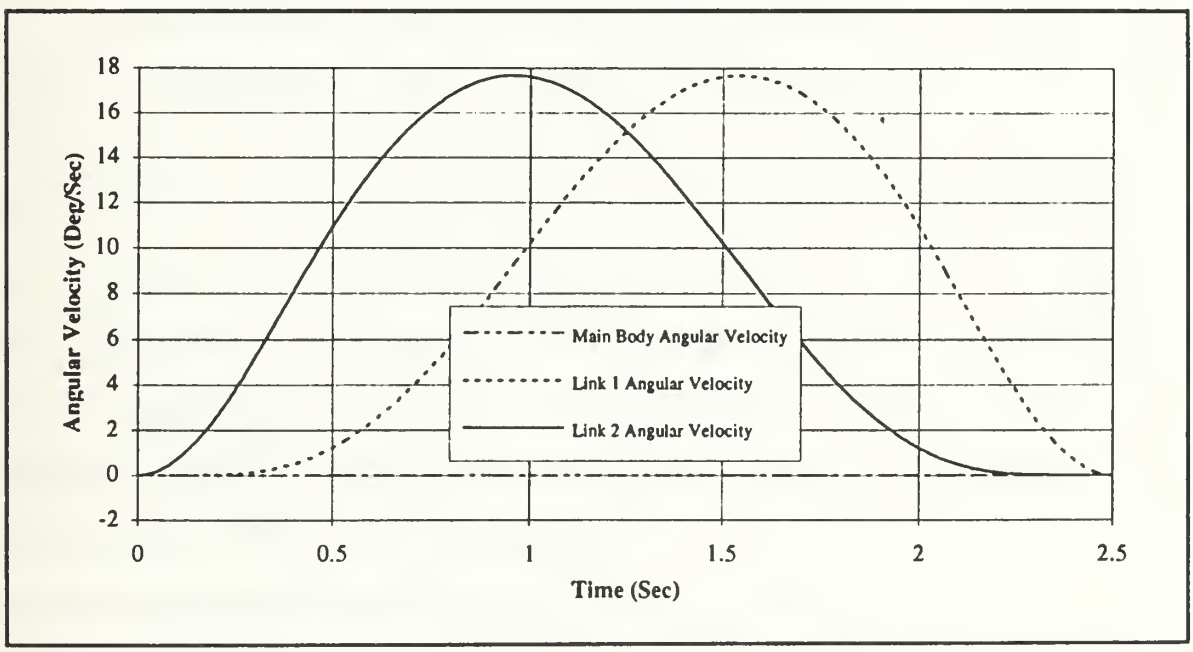

Figure 4.7 Polynomial Reference Tracking Controller Joint Velocity Time History With G_P=1, G_V=5 And Maneuver Time Of 2.5 Seconds

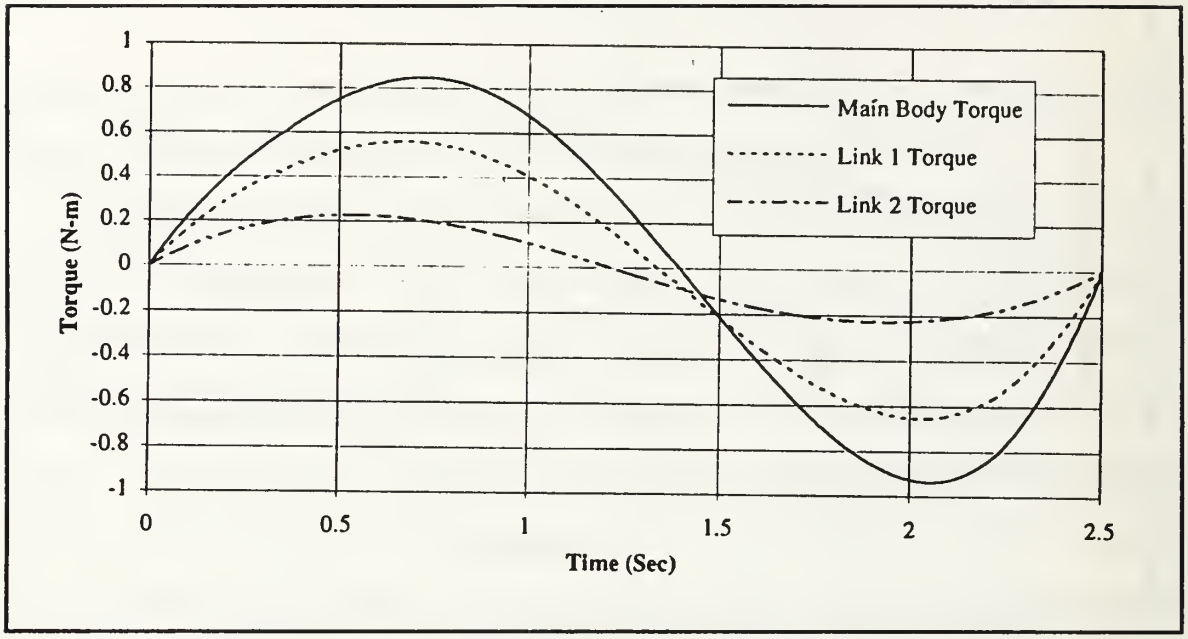

Figure 4.8 Polynomial Reference Tracking Controller Torque Time History With G_P=1, G_V=5 And Maneuver Time Of 2.5 Seconds

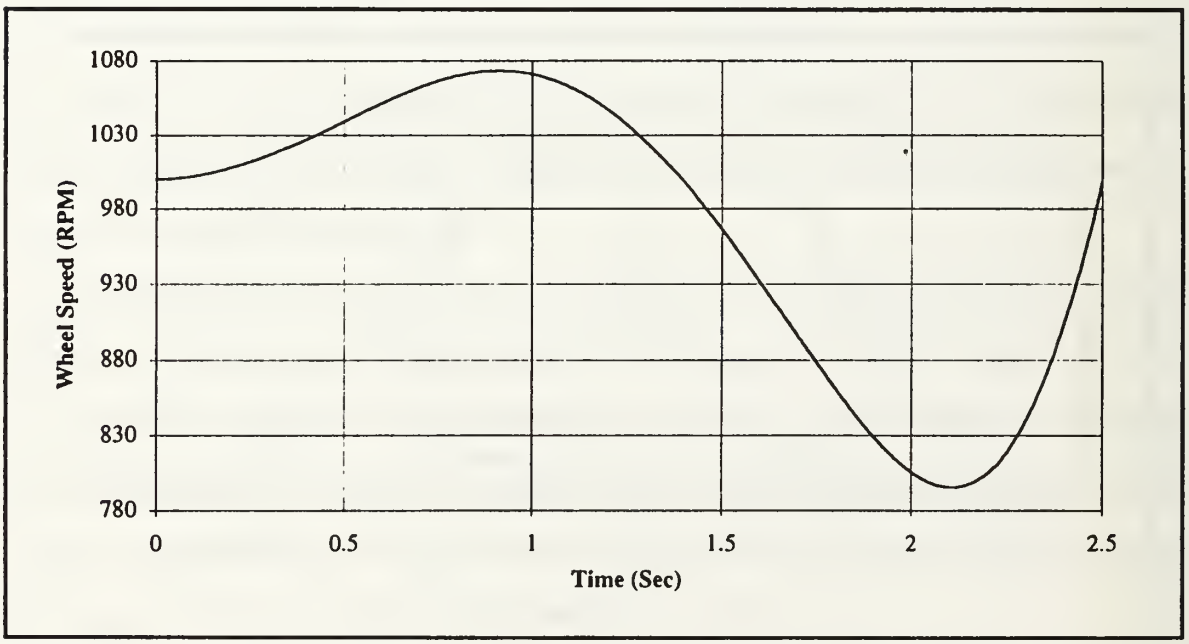

Figure 4.9 Polynomial Reference Tracking Controller Momentum Wheel Speed Time History With G_P=1, G_V=5 And Maneuver Time Of 2.5 Seconds

reference torques with no discernible difference between the reference and commanded torques. The polynomial reference tracking controller provided smooth position control commands for all maneuvers. With the tracking controller, there were no discontinuities or sudden changes in torque commands. The performance was independent of the magnitude of the commanded maneuver with no effect of gain selection being noted. Maneuver time could be specified but was subject to actuator and structural characteristics. Feedback errors remained small throughout the maneuver as the controller smoothly tracked the reference. This resulted in smoothly changing torque commands with smooth and predictable motion of the manipulator.

D. NEAR-MINIMUM-TIME REFERENCE TRACKING CONTROLLER

The theory behind the near-minimum-time tracking controller is described in Chapter III and [Ref. 1, 2]. Two cases for this controller were selected. In the first case, α was set equal to 0.25. The shape function generated by this reference are sinusoidal in shape. In the second case, an α of 0.1 was used. As α approaches zero, the input torque shape approached that of a square wave with a period of the maneuver time. This shape more closely approximated the minimum time bang-bang controller. A maneuver times of 2.5 seconds was used so that the polynomial reference and the near-minimum-time control system performance characteristics could be compared. Similar plots with a maneuver time of 5 seconds can be found in Appendix D.

The general performance of the near-minimum-time reference tracking controller provided some of the advantages and disadvantages of the two previous control systems. Since this was a tracking controller and the feedback

errors were generally small, the commanded torques were generally smooth with only minor disturbances to the main body.

Near minimum-time reference position and velocity time history of the manipulator for a maneuver time of 2.5 seconds with $\alpha = 0.25$ are presented in Figure 4.10. and 4.11 respectively. Momentum wheel speed plots for a maneuver time of 2.5 seconds with $\alpha = 0.25$ are presented in Figures 4.12 and 4.13 respectively. Near minimum-time reference position and velocity time history of the manipulator for a maneuver time of 2.5 seconds with $\alpha = 0.1$ are presented in Figure 4.14. and 4.15 respectively. Momentum wheel speed plots for a maneuver time of 2.5 seconds with $\alpha = 0.1$ are presented in Figures 4.16 and 4.17 respectively.

With $\alpha = 0.25$ the input torque shaping closely resembles that of the polynomial reference trajectory tracking controller. As with the polynomial reference trajectory, the manipulator links moved smoothly from the initial to the final conditions. Note that for this controller, there is only a very small angular displacement of the main body.

Joint velocities for the manipulator links follow a smooth path, beginning and ending with zero velocities. With this controller, note that unlike the previous controller, there is no phase difference between the movement of the manipulator links. Both links move with the same velocity at the same time. The main body also displays a very small angular velocity.

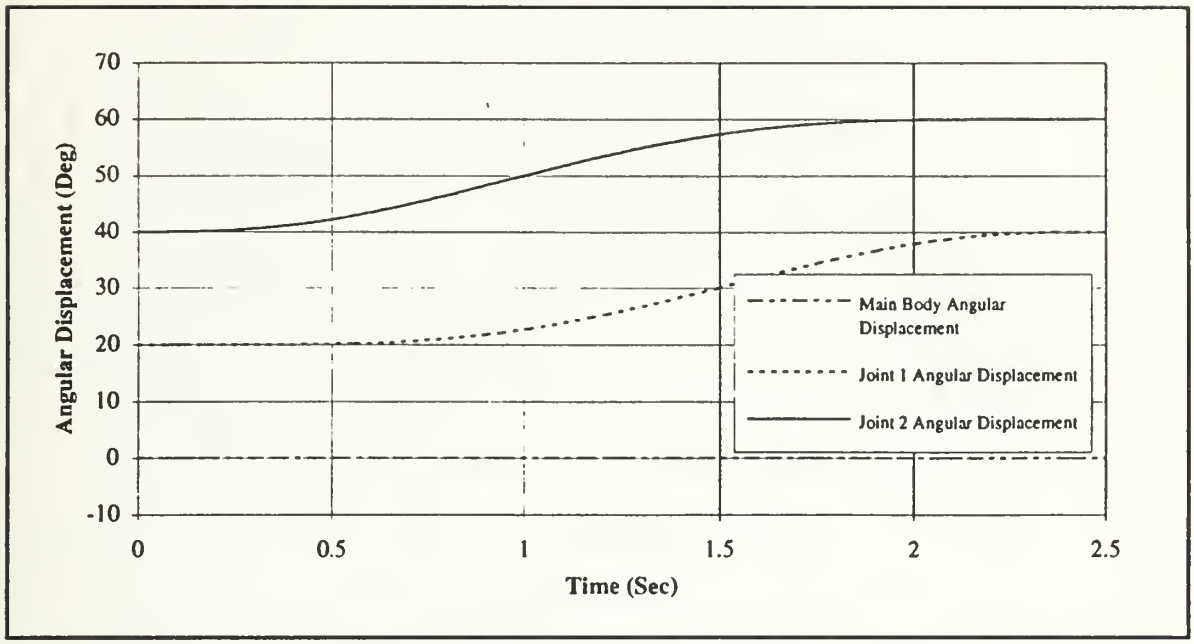

Figure 4.10 Near-Minimum Time Tracking Controller Joint Position Time History With G_P=1 and G_V=5, Maneuver Time Of 2.5 Seconds , And α = 0.25

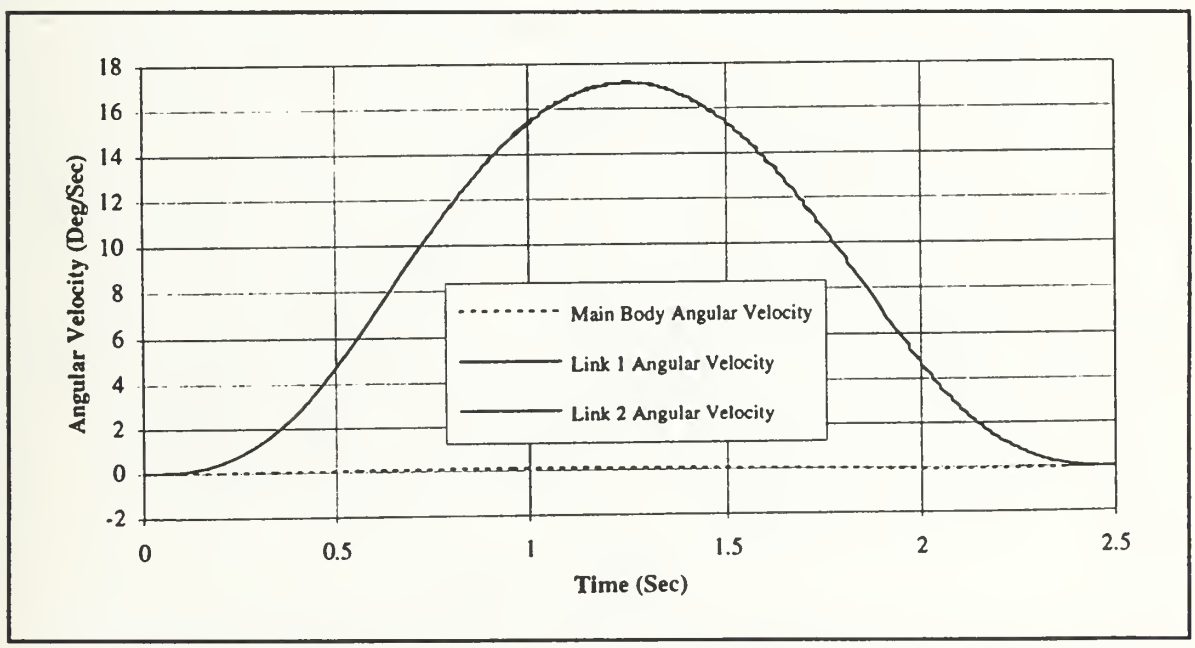

Figure 4.11 Near-Minimum Time Tracking Controller Joint Velocity Time History With G_P=1 and G_V=5, Maneuver Time Of 2.5 Seconds , And α = 0.25.

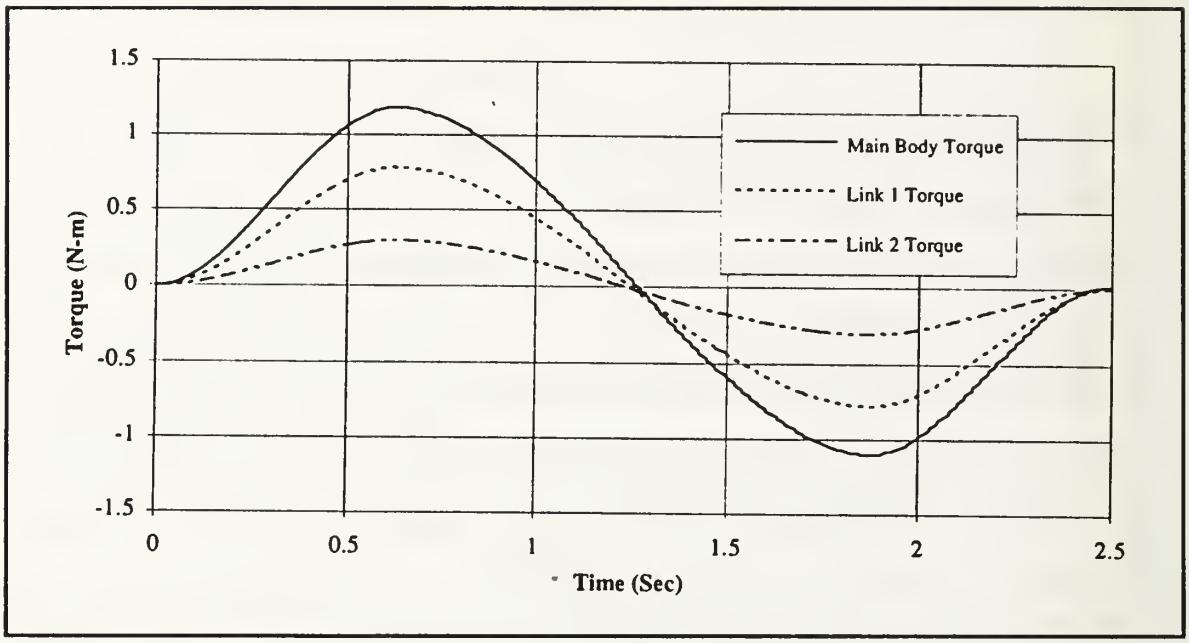

Figure 4.12 Near-Minimum Time Tracking Controller Torque Time History With G_P=1 and G_V=5, Maneuver Time Of 2.5 Seconds , And α = 0.25

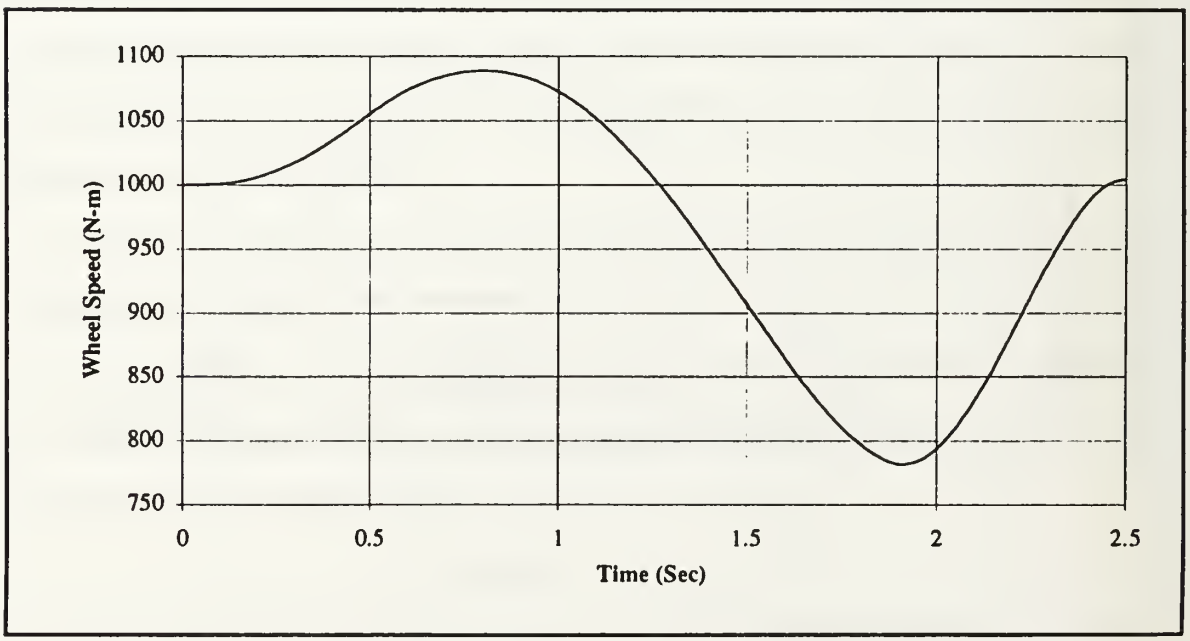

Figure 4.13 Near-Minimum Time Tracking Controller Wheel Speed Time History With G_P=1 and G_V=5, Maneuver Time Of 2.5 Seconds , And α = 0.25

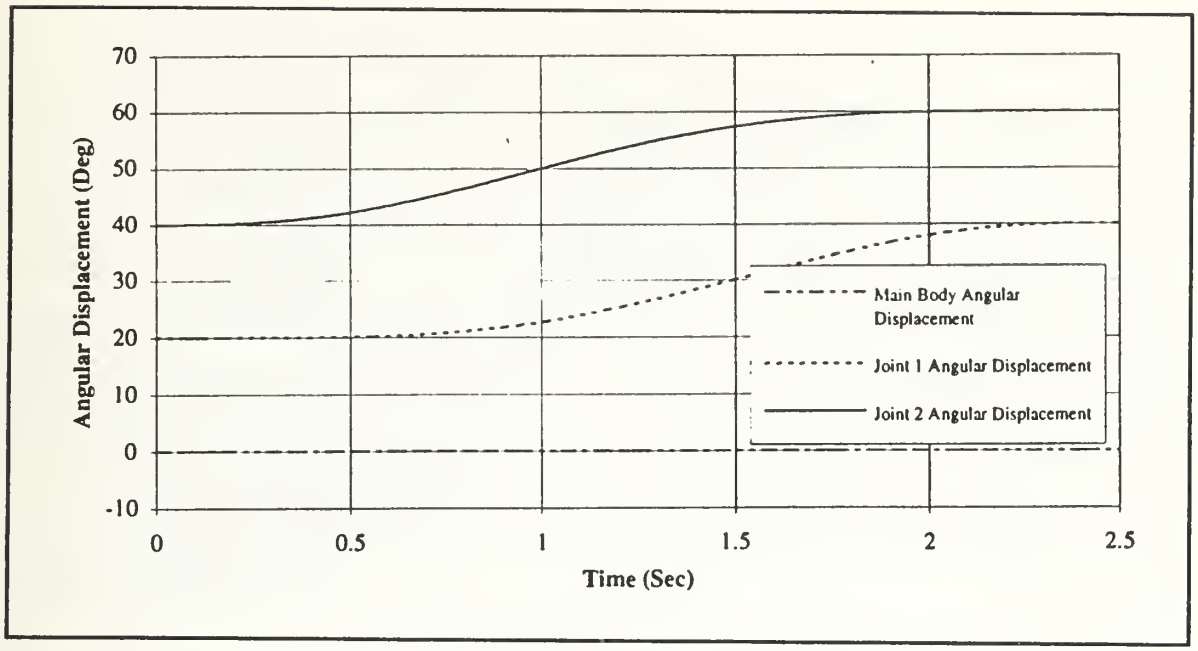

Figure 4.14 Near-Minimum Time Tracking Controller Joint Position Time History With G_P=1 and G_V=5, Maneuver Time Of 2.5 Seconds , And $\alpha = 0.1$

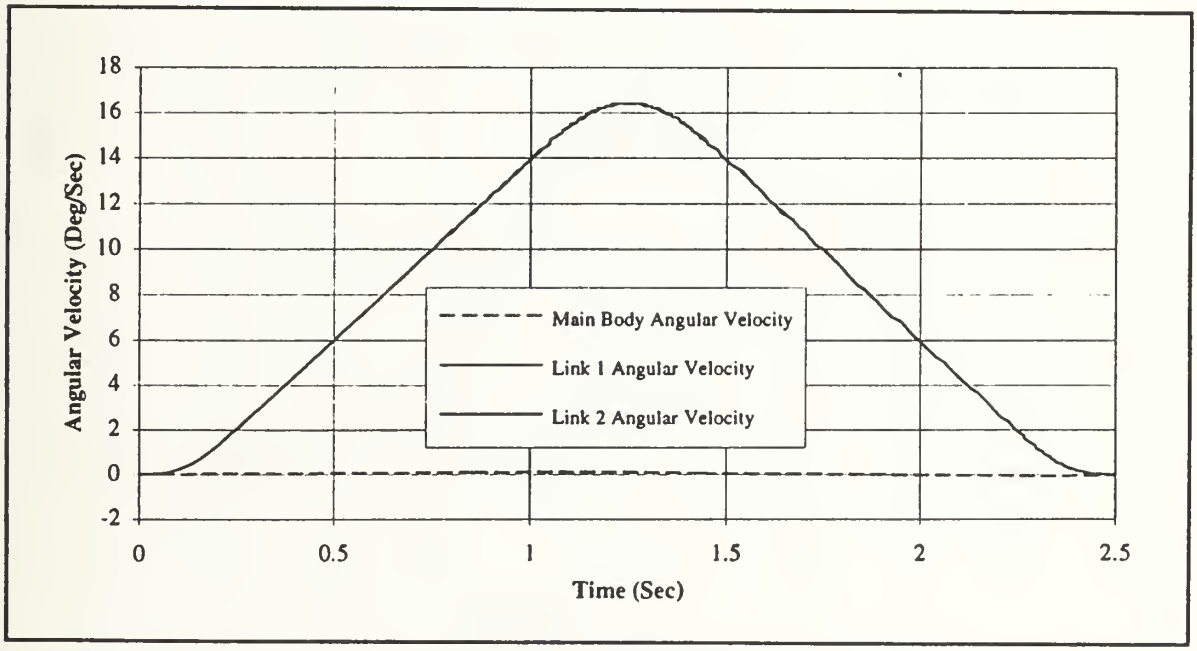

Figure 4.15 Near-Minimum Time Tracking Controller Joint Velocity Time History With G_P=1 and G_V=5, Maneuver Time Of 2.5 Seconds , And $\alpha = 0.1$

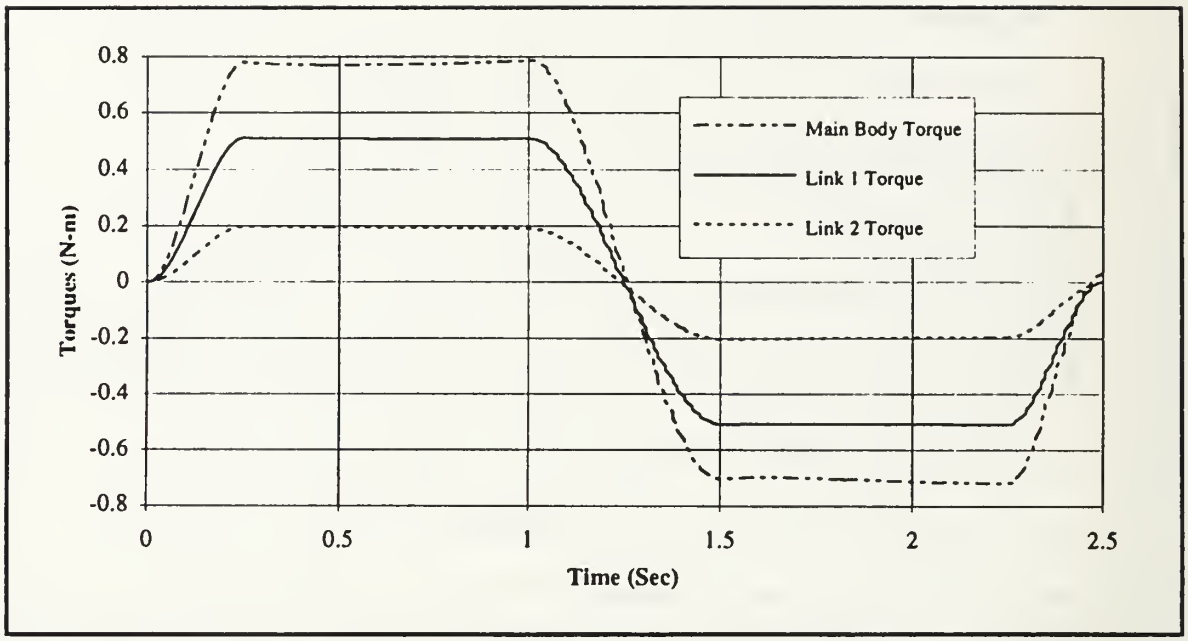

Figure 4.16 Near-Minimum Time Tracking Controller Torque Time History With G_P=1 and G_V=5, Maneuver Time Of 2.5 Seconds , And α = 0.1

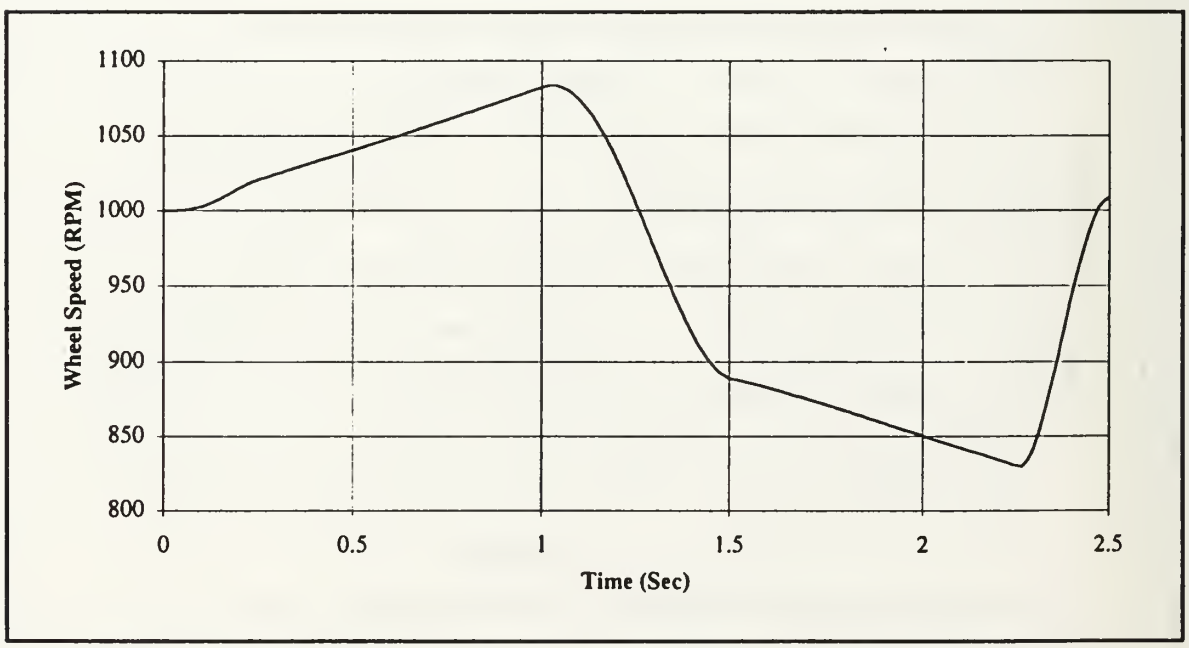

Figure 4.17 Near-Minimum Time Tracking Controller Wheel Speed Time History With G_P=1 and G_V=5, Maneuver Time Of 2.5 Seconds , And α = 0.1

As α goes toward zero, the shape of the input torque reference becomes more square. The square corners of the torque input are difficult for the controller to track and required larger gains. This characteristic is best noted in the previous depicted plots with $\alpha = 0.1$. Note that rapid changes in the wheel speed are required. Even with large gains, the main body was still disturbed by motions. The jerky motion of the manipulator disturbed the main body and resulted in small but detectable position changes. As in the previous controllers, any disturbance to the main body can degrade communications links or cause pointing errors for optical imaging devices.

V. CONCLUSIONS

Three different control systems were simulated and analyzed. All three controllers were stable and were able to position the manipulator in a timely and effective manner. The most significant difference between the controllers turned out to be how effective the control system was stabilizing the main body while positioning the manipulator.

The linear feedback controller was the simplest controller conceptually and the easiest to implement. This controller provided stable control over a wide range of gains and for a wide variety of maneuvers. Large gains were required to achieve acceptable levels of performance. Large gains corresponded to large torques and large displacements of the main body. Position and velocity gains had to be selected to balance control torques, system performance, and motion of the main body. As the control system was implemented, it was not possible to achieve all of these objectives for the given reference maneuver.

The polynomial reference trajectory for robotic applications represents a classic approach for generating a reference trajectory to position and control a two link manipulator. This approach also offers the advantage that the reference trajectory can be pre-calculated off line prior to the maneuver. These pre-calculated values for the reference trajectory can be used in conjunction with the controller to minimize real time computational requirements.

The polynomial reference tracking controller provided smooth position control commands for all maneuvers. With the tracking controller, there were no discontinuities or sudden changes in torque commands. The performance was independent of the magnitude of the commanded maneuver and only slightly

affected by gain selection. Maneuver time could be specified but was subject to actuator and structural characteristics. Feedback errors remained small throughout the maneuver as the controller smoothly tracked the reference. This resulted in smoothly changing torque commands with smooth and predictable motion of the manipulator. The polynomial reference tracking controller was the most effective controller implemented with respect to accurate and timely positioning of the manipulator, and stabilization of the main spacecraft body.

The general performance of the near-minimum-time reference tracking controller provided some of the advantages and some of the disadvantages of the two previous control systems. Since this was a tracking controller and the feedback errors were generally small, the commanded torques were generally smooth with only minor disturbances to the main body.

The near-minimum-time for the reference maneuver was determined by the maximum torque capability of each actuator and the magnitude of the maneuver. The maximum of the three times calculated for each of the three joints was specified as the maneuver time. For each maneuver, one joint would then become the limiting case for the selected maneuver based on these requirements. Two of the three remaining actuators therefore would operate at less than the maximum toque capability in order to complete the maneuver at the same time as the other links completed the maneuver.

Large gains were required to force the controller to closely track the reference input as the input torque shape approached the minimum maneuver time. Even with larger gains, the controller was not able to completely negate the torques generated by the manipulator and some small rotations of the main body were observed.

Two different control laws were evaluated. In the first, constant gains with linear feedback was utilized. This controller proved to be the easiest to implement but did not effectively stabilize the main body during movements by the manipulator. The second control law entailed using a tracking controller with constant gains. The reference tracking controller represents a traditional and successful way of positioning the manipulator. With the reference tracking controller two different references were used. In the first a polynomial was used to generate a reference trajectory. This technique proved to be only slightly more complex than the linear feedback controller with constant gains, was dependent upon mass and inertia characteristics of the manipulator and was the most effective at positioning the manipulator while minimizing the motion of the main body. In the second, a near-minimum-time technique was employed to generate a reference trajectory. This reference was more complex, but provided the capability to position the manipulator in near-minimum-time. This technique provided greater flexibility in shaping the input torque reference but was not as successful as the polynomial reference tracking controller in stabilizing the main body. In the end, the polynomial reference tracking controller provided the best performance of the three controllers simulated.

A. SUBJECTS FOR FUTURE RESEARCH

Lyapunov theory represents only one methodology for nonlinear control system design. Many other methodologies including neural networks, adaptive controllers, sliding controllers, and robust controllers among others provide additional areas for research.

With the addition of the vision server to the Spacecraft Robotics Simulation Lab, the capability to track a target as well as the endpoint of the manipulator will

become available. This provides the capabilty to perform end point tracking tasks. Once this is successful with a stationary target, the same can be repeated with a moving target.

The design of the manipulators allows for the replacement of the rigid manipulator arm design with a flexible arm design. Control system design for accurately and quickly positioning the flexible manipulator provides another area for future research.

The minimum time to complete the maneuver was the longest of the three joint maneuver times and was based on the maximum torque capabilities of the actuator and the magnitude of the maneuver. With the near-minimum-time reference tracking controller, the switching time for the maneuver was specified to be one half of the maneuver time. This methodology resulted in only one of the three actuators working at maximum torque. By parameterizing the near-minimum-time equations in another way, it may be possible to optimize the solution in terms of a variable switching time and variable maneuver time for each of the actuators. This may allow optimization of the torques or time required to perform the maneuver, maneuver time or torque requirements.

APPENDIX A

TABLE A.1 Servo Motor Characteristics

Characteristic	Units	Manipulator Actuator	Momentum Wheel Actuator
Model Number		9FGHD	JR16M4CH-1
Gear Reduction Ratio		147.51 : 1	1:1.0
Rated Speed	rev per minute	17	3000
Rated Torque	inch-pound	80	31.85
Rated Current	amps	5.6	7.79
Rated Voltage	volts	12	168
Peak Torque	inch-pound	119	341.43
Peak Current	amps	62	79.3
Peak Voltage	volts	13.2	7.67
Outside Diameter	inches	4.75	7.4
Height	inches	3.1	4.5
Weight	pounds	3.2	17.5
Torque Constant	oz-in/amp	3.23	69.01
Back EMF Constant	volts/krpm	2.39	51
Terminal Resistance	ohms	0.95	1.4
Average Friction Torque	oz-in	2.5	11
Viscous Damping Constant	oz-in/krpm	0.3	7.84
Moment Of Inertia	oz-in/sec^2	0.0052	0.084

APPENDIX B

A. SYSTEM KINETIC ENERGY

1. Body 1 Kinetic Energy

$$T_1 = \frac{1}{2} I_1 \dot{\theta}_1^2 \tag{B.1}$$

2. Body 2 Kinetic Energy

$$\begin{aligned} T_2 = {} & \frac{1}{2} I_{c.m.2} \dot{\theta}_2^2 + \frac{1}{2} m_2 L_1^2 \dot{\theta}_2^2 \\ & + m_2 L_1 L_{c.m.2} \dot{\theta}_1 \dot{\theta}_2 \cos(\theta_{21}) \\ & + \frac{1}{2} m_2 L_{c.m.2}^2 \dot{\theta}_2^2 \end{aligned} \tag{B.2}$$

3. Body 3 Kinetic Energy

$$\begin{aligned} T_3 = {} & \frac{1}{2} I_{c.m.3} \dot{\theta}_3^2 + \frac{1}{2} m_3 \left[L_1^2 \dot{\theta}_1^2 + L_2^2 \dot{\theta}_2^2 + L_{c.m.3}^2 \dot{\theta}_3^2 \right] \\ & + m_3 L_1 L_2 \dot{\theta}_1 \dot{\theta}_2 \cos(\theta_{21}) + m_3 L_3 L_{c.m.3} \dot{\theta}_1 \dot{\theta}_3 \cos(\theta_{31}) \\ & + m_3 L_2 L_{c.m.3} \dot{\theta}_2 \dot{\theta}_3 \cos(\theta_{32}) \end{aligned} \tag{B.3}$$

4. Total Kinetic Energy

$$T = \sum_{i=1}^{3} T_i \tag{B.4}$$

B. EQUATIONS OF MOTION

1. Mass Matrix

The mass matrix is a function of the mass and inertia characteristics of the system as well as the geometry of the system. The mass matrix is defined in equation (B.5) where the elements of the mass matrix are described as follows in equations (B.6) through (B.11).

$$M(\theta) = \begin{bmatrix} m_{11} & m_{12} & m_{13} \\ m_{21} & m_{22} & m_{23} \\ m_{31} & m_{32} & m_{33} \end{bmatrix} \tag{B.5}$$

where

$$m_{11} = I_1 + L_1^2 [m_1 + m_2 + m_3] + m_4 L_4^2 \tag{B.6}$$

$$m_{22} = I_{c.m_2} + L_2^2 \left[m_2 \left(\frac{L_{cm_2}}{L_2} \right)^2 + m_3 \right] \tag{B.7}$$

$$m_{33} = I_{c.m_3} + L_{cm_3}{}^2 m_3 \tag{B.8}$$

$$m_{12} = m_{21} = L_1 L_2 \cos(\theta_{21}) \left[m_2 \left(\frac{L_{cm_2}}{L_2} \right) + m_3 \right] \tag{B.9}$$

$$m_{13} = m_{31} = L_1 L_{cm_3} \cos(\theta_{31}) m_3 \tag{B.10}$$

$$m_{23} = m_{32} = L_2 L_{cm_3} \cos(\theta_{32}) m_3 \tag{B.11}$$

2. Coriolis And Centrifugal Acceleration Terms:

$$G(\theta,\dot{\theta}) = \begin{bmatrix} G(1) \\ G(2) \\ G(3) \end{bmatrix} \tag{B.12}$$

$$G(1) = [(m_2 L_1 L_{c.m.2}) + (m_3 L_1 L_2)] \sin(\theta_{21}) \dot{\theta}_2^2 + (m_3 L_1 L_{c.m.3}) \sin(\theta_{31}) \dot{\theta}_3^2 \tag{B.13}$$

$$G(2) = -[(m_2 L_1 L_{c.m.2}) + (m_3 L_1 L_2)] \sin(\theta_{21}) \dot{\theta}_1^2 + (m_3 L_2 L_{c.m.3}) \sin(\theta_{31}) \dot{\theta}_3^2 \tag{B.14}$$

$$G(3) = -(m_3 L_1 L_{c.m.3}) \sin(\theta_{21}) \dot{\theta}_1^2 - (m_3 L_2 L_{c.m.3}) \sin(\theta_{32}) \dot{\theta}_2^2 \tag{B.15}$$

C. POLYNOMIAL REFERENCE TRAJECTORY

1. Vector Polynomial Describing Tip Position:

$$\vec{r} = \vec{r}(t_0) + f(t)\left[\vec{r}(t_f) - \vec{r}(t_0)\right] \tag{B.16}$$

$$\tau = \frac{t - t_0}{t_f - t_0} \qquad ,0 < t < t_f, 0 < \tau < 1$$

$$f(\tau) = c_1 + c_2\tau + c_3\tau^2 + c_4\tau^3 + c_5\tau^4 + c_6\tau^5 \tag{B.17}$$

2. Boundary Conditions And Polynomials

$$f(0) = 0, \dot{f}(0) = 0, \ddot{f}(0) = 0$$
$$f(1) = 1, \dot{f}(1) = 0, \ddot{f}(1) = 0$$

$$f(\tau) = 10\tau^3 - 15\tau^4 + 6\tau^5 \tag{B.18}$$

$$\dot{f}(\tau) = 30\tau^2 - 60\tau^3 + 30\tau^4 \tag{B.19}$$

$$\ddot{f}(\tau) = 60\tau - 180\tau^2 + 120\tau^3 \tag{B.20}$$

3. Vector Position

$$\vec{r}(\tau) = \vec{r}(t_0) + f(\tau)\left[\vec{r}(t_f) - \vec{r}(t_0)\right] \tag{B.21}$$

4. Vector Velocity

$$\dot{\vec{r}}(\tau) = \dot{f}(\tau)\left\{\frac{\vec{r}(t_f) - \vec{r}(t_0)}{t_f - t_0}\right\} \tag{B.22}$$

5. Vector Acceleration

$$\ddot{\vec{r}}(\tau) = \ddot{f}(\tau)\left\{\frac{\vec{r}(t_f) - \vec{r}(t_0)}{(t_f - t_0)^2}\right\} \tag{B.23}$$

D. TWO LINK INVERSE KINEMATICS

Law Of Sines & Cosines:

$$x_2^2 + y_2^2 = l_1^2 + l_2^2 + 2\, l_1\, l_2 \cos(\theta_2 - \theta_1) \tag{B.24}$$

$$\theta_{21} = \theta_2 - \theta_1 \tag{B.25}$$

$$\cos(\theta_{21}) = \frac{x_2^2 + y_2^2 - l_1^2 - l_2^2}{2\, l_1\, l_2} \tag{B.26}$$

$$\sin(\theta_{21}) = \pm\sqrt{1 - \cos(\theta_{21})^2} \tag{B.27}$$

$$\theta_{21} = \text{atan2}\left(\frac{\sin(\theta_{21})}{\cos(\theta_{21})}\right) \tag{B.28}$$

Velocity Vector:

$$\dot{\vec{r}} = [H]\{\dot{\theta}\} \tag{B.29}$$

$$H = \begin{bmatrix} -l_2 \sin(\theta_2), & -l_3 \sin(\theta_3) \\ l_2 \cos(\theta_2), & l_3 \cos(\theta_3) \end{bmatrix} \tag{B.30}$$

Acceleration Vector:

$$\ddot{\vec{r}} = [H]\{\ddot{\theta}\} + [\dot{H}]\{\dot{\theta}\} \tag{B.31}$$

$$\dot{H} = \begin{bmatrix} -l_2 \cos(\theta_2), & -l_3 \cos(\theta_3) \\ -l_2 \sin(\theta_2), & -l_3 \sin(\theta_3) \end{bmatrix} \tag{B.32}$$

E. NEAR MINIMUM TIME RIGID BODY MANEUVER

1. Near-Minimum-Time Maneuver

$$I\,\ddot{\theta}_{ref} = u_{ref} = u_{max}\, f(\Delta t, t_f, t) \tag{B.33}$$

I - Moment Of Inertia About Axis Of Rotation

t_f - Maneuver Time

$t_1 = t_s - \Delta t$

$t_2 = t_s + \Delta t$

$t_3 = t_f - \Delta t$

$\Delta t = \alpha\, t_f$ = Rise Time

$t_s = \beta\, t_f$ = Switching Time, where $\beta = 0.5$

2. Torque Shaping Function

$$f(\Delta t, t_f, t) = \begin{cases} = \left(\frac{t}{\Delta t}\right)^2 \left[3 - 2\left(\frac{t}{\Delta t}\right)\right] \text{ for } 0 \le t < \Delta t \\ = 1 \text{ for } \Delta t \le t < t_1 \\ = 1 - 2\left\{\left(\frac{t - t_1}{2\Delta t}\right)^2 \left[3 - 2\left(\frac{t - t_1}{2\Delta t}\right)\right]\right\} \text{ for } t_1 \le t < t_2 \\ = -1 \text{ for } t_2 \le t < t_3 \\ = -1 + \left\{\left(\frac{t - t_3}{\Delta t}\right)^2 \left[3 - 2\left(\frac{t - t_3}{\Delta t}\right)\right]\right\} \text{ for } t_3 \le t < t_f \end{cases} \tag{B.34}$$

$$\dot{\theta}_{ref}(t) = \dot{\theta}_0 + \frac{u_{max}}{I} \int_{t_0}^{t} f(\Delta t, t_f, \tau)\, d\tau \tag{B.35}$$

$$\theta_{ref}(t) = \theta_0 + \dot{\theta}_0 (t-t_0) + \frac{u_{max}}{I} \int_{t_0}^{t} \int_{t_0}^{\tau_1} f(\Delta t, t_f, \tau_2)\, d\tau_2\, d\tau_1 \qquad \text{(B.36)}$$

3. Boundary Conditions

$$t_0 = 0; \qquad \theta(0) = \theta_0 \qquad \dot{\theta}(0) = 0$$

$$t = t_f; \qquad \theta(t_f) = \theta_f \qquad \dot{\theta}(t_f) = 0$$

Solution for the piece wise integration of equations (B.35) and (B.36) for the given time interval provides us with refeence angular displacements and angular velocity.

4. Reference Angular Displacements And Velocities

$0 \le t \le \Delta t$

$$\theta_{ref} = \frac{u_{max}}{I} \Delta t^2 \left[\frac{1}{4} \left(\frac{t}{\Delta t} \right)^4 + \frac{1}{10} \left(\frac{t}{\Delta t} \right)^5 \right] \qquad \text{(B.37)}$$

$$\dot{\theta}_{ref} = \frac{u_{max}}{I} \left[\left(\frac{t}{\Delta t} \right)^3 - \frac{1}{2} \left(\frac{t}{\Delta t} \right)^4 \right] \qquad \text{(B.38)}$$

$\Delta t \le t \le t_1$

$$\theta_{ref} = \frac{u_{max}}{I} \left[\frac{1}{2} t^2 - \frac{1}{2} t\, \Delta t + \frac{3}{20} (\Delta t)^5 \right] \qquad \text{(B.39)}$$

$$\dot{\theta}_{ref} = \frac{u_{max}}{I} \left(t - \frac{1}{2} \Delta t \right) \qquad \text{(B.40)}$$

$t_1 \leq t \leq t_2$

$$\theta_{ref} = \frac{u_{max}}{I} \left\{ \begin{array}{c} \left[\frac{23}{20}\alpha^2 - \frac{3}{4}\alpha + \frac{1}{8}\right] t_f^2 + \\ (2\Delta t)^2 \left[\frac{1}{2}\left(\frac{t - t_1}{2\Delta t}\right)^2 - \frac{1}{2}\left(\frac{t - t_1}{2\Delta t}\right)^4 + \frac{1}{5}\left(\frac{t - t_1}{2\Delta t}\right)^5\right] + \\ \left(\frac{1}{2} t_f - \frac{3}{2}\Delta t\right)(t - t_1) \end{array} \right\} \qquad \text{(B.41)}$$

$$\dot{\theta}_{ref} = \frac{u_{max}}{I} \left\{ t_1 - \frac{1}{2}\Delta t + 2\Delta t \left[\left(\frac{t - t_1}{2\Delta t}\right) - 2\left(\frac{t - t_1}{2\Delta t}\right)^3 + \left(\frac{t - t_1}{2\Delta t}\right)^4\right]\right\} \qquad \text{(B.42)}$$

$t_2 \leq t \leq t_3$

$$\theta_{ref} = \frac{u_{max}}{I} \left\{ \begin{array}{c} \left[-\frac{21}{20}\alpha^2 - \frac{1}{4}\alpha + \frac{1}{8}\right] t_f^2 + \frac{1}{2}(t_f - 3\Delta t)(t - t_2) \ldots \\ -\frac{1}{2}\left(t - \frac{1}{2} t_f - \Delta t\right)^2 \end{array} \right\} \qquad \text{(B.43)}$$

$$\dot{\theta}_{ref} = \frac{u_{max}}{I} \left[-t + t_1 + t_2 - \frac{1}{2}\Delta t\right] \qquad \text{(B.44)}$$

$t_3 \leq t \leq t_f$

$$\theta_{ref} = \frac{u_{max}}{I} \left\{ \begin{array}{c} \left[-\frac{1}{20}\alpha^2 - \frac{1}{2}\alpha + \frac{1}{4}\right] t_f^2 + \frac{1}{2}\Delta t (t - t_3)(\Delta t)^2 \\ \left[-\frac{1}{2}\left(\frac{t - t_3}{\Delta t}\right)^2 + \frac{1}{4}\left(\frac{t - t_3}{\Delta t}\right)^4 - \frac{1}{10}\left(\frac{t - t_3}{\Delta t}\right)^5\right] \end{array} \right\} \qquad \text{(B.45)}$$

$$\dot{\theta}_{ref} = \frac{u_{max}}{I} \left\{-\frac{1}{2}\Delta t + \Delta t \left[-\left(\frac{t - t_3}{\Delta t}\right) + \left(\frac{t - t_3}{\Delta t}\right)^3 + \frac{1}{2}\left(\frac{t - t_3}{2\Delta t}\right)^4\right]\right\} \qquad \text{(B.46)}$$

At time $t = t_f$;

$$\theta_{ref} = \frac{u_{max}}{I} \left\{ \left[\frac{1}{4} - \frac{1}{2}\alpha + \frac{1}{10}\alpha^2 \right] t_f^2 \right\} \tag{B.47}$$

$$\dot{\theta}_{ref} = 0 \tag{B.48}$$

5. Near-Minimum-Time Relationships

$$t_{f_i} = \sqrt{\frac{I_i \left(\theta_{f_i} - \theta_{0_i}\right)}{u_{max_i}\left(\frac{1}{4} - \frac{1}{2}\alpha + \frac{1}{10}\alpha^2\right)}} \tag{B.49}$$

$$u_{max_i} = \frac{I_i \left(\theta_{f_i} - \theta_{0_i}\right)}{t_{f_i}^2 \left(\frac{1}{4} - \frac{1}{2}\alpha + \frac{1}{10}\alpha^2\right)} \tag{B.50}$$

APPENDIX C

A. LINEAR FEEDBACK MATLAB SIMULATION PROGRAM

1. Main Program For Linear Feedback Simulation

```
% Constants
% Lenght of Manipulators
L(1) = 15*2.54/100;
L(2) = 17*2.54/100;
L(3) = 17*2.54/100;
L(4) = 20/100;
% Distance From Axis Of Rotation To Center Of Mass
Lcm(1) = 0/100;
Lcm(2) = 36.45/100;
Lcm(3) = 34.9/100;
% Mass Of Major Components (kg)
m(1) = 54.69;
m(2) = 2.09364;
m(3) = 2.466;
m(4) = 10.667;
% Inertias Of Major Components (kg-m^2)
I(1) = 4.32132;
I(2) = 3.20338e-2;
I(3) = 5.38398e-2;
I(4) = 0.0912;
```

```
% Integrate Equations Of Motion Using Commercial
% Matlab Runge-Kutta 4 Routine
% Boundary Conditions
t0 = 0;
tfinal = 40;
x0 = [0.0; 0.0; 0.0; 0*pi/180; 20*pi/180; 40*pi/180];
tol = 1e-8;
trace=1;
Call "lfbrk" Function And Integrate Equations Of Motion
[t,x,uu] = rku2('lfbrk',t0,tfinal,x0,tol,trace);
% Program To Calculate Motor Torque, Current, and Voltage
TF=1.41e-2;          % N-m
KT=2.28e-2;          % N-m/amp
KD=2.00573e-5;   % N-m/rad/sec
KE=2.28271e-2;   % Volt/rad/sec
RT=0.95;             % ohms
j=length(t)
for i=1:j;
 amp22(i) = (uu(i,2)/148.51 + TF + KD * x(i,2)*148.51 ) / KT;
 volt22(i) = KE * x(i,2) + RT * amp22(i);
 amp33(i) = (uu(i,3)/148.51 + TF + KD * x(i,3)*148.51 ) / KT;
 volt33(i) = KE * x(i,3) + RT * amp33(i);
end
```

```
% Program To Calculate Motor Torque, Current, and Voltage
% For Momentum Wheel
TF=0.0777;          %N-m/amp
KD=5.29131e-4;   % N-m/rad/sec
KE=0.48711;         % Volt/rad/sec
RT=1.4;             % ohms
Iw=0.0912;          % kg-m^2
thd0=104.7;         % rad/sec (= 1000rpm)
for i=1:j;
 tor(i) = uu(i,1);
 thddw(i) = tor(i)/Iw;
 thdw(i) = thddw(i) * t(i) + thd0;
 amp(i) = (tor(i) + TF + KD * thdw(i) ) / KT;
 volt(i) = KE * thdw(i) + RT * amp(i);
 x1(i)=L(1)*cos(x(i,4));
 y1(i)=L(1)*sin(x(i,4));
 x2(i)=x1(i)+L(2)*cos(x(i,5));
 y2(i)=y1(i)+L(2)*sin(x(i,5));
 x3(i)=x2(i)+L(3)*cos(x(i,6));
 y3(i)=y2(i)+L(3)*sin(x(i,6));
end
% Store Data For Plotting Later
data1=[t,x*180/pi,uu];
data2=[t,x1',y1',x2',y2',x3',y3'];
data3=[t,thdw'*30/pi,thddw'*30/pi];
```

```
data4=[t,amp',amp22',amp33',volt',volt22',volt33'];
%  Save Data In Text Format
save lfb9.dat data1 /ascii
save lfb10.dat data2 /ascii
save lfb11.dat data3 /ascii
save lfb12.dat data4 /ascii
```

2. Linear Feedback Equation Of Motion Function

```
% Function Containing Linear Feedback Equations Of Motion
function [xdot,U1] = lfbrk(t,x)
% Constants
% Lenght of Manipulators
L(1) = 15*2.54/100;
L(2) = 17*2.54/100;
L(3) = 17*2.54/100;
L(4) = 20/100;
% Distance From Axis Of Rotation To Center Of Mass
Lcm(1) = 0/100;
Lcm(2) = 36.45/100;
Lcm(3) = 34.9/100;
% Mass Of Major Components (kg)
m(1) = 54.69;
m(2) = 2.09364;
m(3) = 2.466;
m(4) = 10.667;
% Inertias Of Major Components (kg-m^2)
I(1) = 4.32132;
I(2) = 3.20338e-2;
I(3) = 5.38398e-2;
I(4) = 0.0912;
```

```
% Angles
thd(1) = x(1);
thd(2) = x(2);
thd(3) = x(3);
% Convert Input Variables Into Variable Used In This Function
th(1) = x(4);
th(2) = x(5);
th(3) = x(6);
% Final Conditions For Manipulator And Main Body
thf1=0;
thf2=40*pi/180;
thf3=60*pi/180;
thdf1=0;
thdf2=0;
thdf3=0;
% Linear Feedback Control Law
g1p=.1;
g2p=.1;
g3p=.1;
g1v=.2;
g2v=.2;
g3v=.2;
```

```
% Control Torques
U(3)=-g3p*(th(3)-thf3)-g3v*(thd(3)-thdf3);
U(2)=U(3)-g2p*(th(2)-thf2)-g2v*(thd(2)-thdf2);
U(1)=U(2)-g1p*(th(1)-thf1)-g1v*(thd(1)-thdf1);
U1=U';
% Calculate Coeffients For The Equation Of Motion And Integrate
[MM,GM] = mgm(th,thd);
B = [1,-1,0;0,1,-1;0,0,1];
thdd=inv(MM)*(B*U1-GM');
xdot = [thdd;x(1);x(2);x(3)];
```

B. POLYNOMIAL REFERENCE TRACKING CONTROLLER

1. Polynomial Reference Maneuver Tracker Main Program

```
% EOM3.m Program
% Constants
% Lenght of Manipulators
L(1) = 15*2.54/100;
L(2) = 17*2.54/100;
L(3) = 17*2.54/100;
L(4) = 20/100;
% Distance From Axis Of Rotation To Center Of Mass
Lcm(1) = 0/100;
Lcm(2) = 36.45/100;
Lcm(3) = 34.9/100;
% Mass Of Major Components (kg)
m(1) = 54.69;
m(2) = 2.09364;
m(3) = 2.466;
m(4) = 10.667;
% Inertias Of Major Components (kg-m^2)
I(1) = 4.32132;
I(2) = 3.20338e-2;
I(3) = 5.38398e-2;
I(4) = 0.0912;
```

```
% Boundary Conditions And Integration Time
t0 = 0;
tfinal = 10;
x0 = [0.0; 0.0; 0.0; 0*pi/180; 20*pi/180; 40*pi/180];
tol = 1e-8;
trace=1;
% Integrate Equations Of Motion
[t,x,uu] = rku2('eom3rk',t0,tfinal,x0,tol,trace);
j=size(t);
% Calculate Electrical Power Requirement For Manipulator Actuators
% Motor Parameters
TF=1.8e-2          % N-m
KT=2.28e-2         % N-m/amp
KD=2.00573e-5          % N-m/rad/sec
KE=2.28271e-2          % Volt/rad/sec
RT=0.95            % ohms
j=size(t)
for i=1:j;
  amp22(i) = (uu(2,i)/148.51 + TF + KD * x(i,2) ) / KT;
  volt22(i) = KE * x(i,2) + RT * amp22(i);
  amp33(i) = (uu(3,i)/148.51 + TF + KD * x(i,3) ) / KT;
  volt33(i) = KE * x(i,3) + RT * amp33(i);
end
% Program To Calculate Motor Torque, Current, and Voltage
% Momentum Wheel
```

```
% Motor Parameters
TF=0.0777          % N-m
KT=0.48732         % N-m/amp
KD=5.29131e-4              % N-m/rad/sec
KE=0.48711         % Volt/rad/sec
RT=1.4             % ohms
Iw=0.0912          % kg-m^2
thd0=104.7         % rad/sec (= 1000rpm)
j=size(t)
for i=1:j;
 tor(i) = uu(1,i);
 thddw(i) = tor(i)/Iw;
 thdw(i) = thddw(i) * t(i) + thd0;
 amp(i) = (tor(i) + TF + KD * thdw(i) ) / KT;
 volt(i) = KE * thdw(i) + RT * amp(i);
end
```

2. Polynomial Reference Tracking Equations Of Motion Function

```
function [xdot,U1] = eom3rk(t,x)
% Constants
L(1) = 15*2.54/100;
L(2) = 17*2.54/100;
L(3) = 17*2.54/100;
L(4) = 20/100;
Lcm(1) = 0/100;
Lcm(2) = 36.45/100;
Lcm(3) = 34.9/100;
% Mass
m(1) = 54.69;
m(2) = 2.09364;
m(3) = 2.466;
m(4) = 10.667;
% Inertia
I(1) = 4.32132;
I(2) = 3.20338e-2;
I(3) = 5.38398e-2;
I(4) = 0.0912;
% Angles
thd(1) = x(1);
thd(2) = x(2);
thd(3) = x(3);
th(1) = x(4);
```

```
th(2)  = x(5);
th(3)  = x(6);
[MM,GM] = mgm(th,thd);
%  Gains
g1p=1.0;
g2p=1.0;
g3p=1.0;
g1v=5.0;
g2v=5.0;
g3v=5.0;
[Uref,thref,thdref,thddref] = eom3ref(t,L,Lcm,m,I);
dU(3)=-g3p*(th(3)-thref(3))-g3v*(thd(3)-thdref(3));
dU(2)=dU(3)-g2p*(th(2)-thref(2))-g2v*(thd(2)-thdref(2));
dU(1)=dU(2)-g1p*(th(1)-thref(1))-g1v*(thd(1)-thdref(1));
U1=Uref+dU';
U=U1';
B = [1,-1,0;0,1,-1;0,0,1];
thdd=inv(MM)*(B*U'-GM');
xdot = [thdd;x(1);x(2);x(3)];
```

3. Polynomial Reference Trajectory Function

```
function [Uref,thref,thdref,thddref] = eom3ref(t,L,Lcm,m,I);
thref(1)=0;

% Initial And Final Time For Maneuver
t0 = 0;
tf = 10;

% Initial And Final Vector Positons
r3x0 = L(1)*cos(thref(1))+L(2)*cos(20*pi/180)+L(3)*cos(40*pi/180);
r3y0 = L(1)*sin(thref(1))+L(2)*sin(20*pi/180)+L(3)*sin(40*pi/180);
r3xf = L(1)*cos(thref(1))+L(2)*cos(40*pi/180)+L(3)*cos(60*pi/180);
r3yf = L(1)*sin(thref(1))+L(2)*sin(40*pi/180)+L(3)*sin(60*pi/180);

% Calculate Reference Maneuver
tau = ( t - t0) / ( tf - t0 );
r3x = r3x0 + ( r3xf - r3x0 ) * ( 10 * tau^3 - 15 * tau^4 + 6 * tau^5 );
r3y = r3y0 + ( r3yf - r3y0 ) * ( 10 * tau^3 - 15 * tau^4 + 6 * tau^5 );
r3xd = ( r3xf - r3x0 ) / ( tf - t0 )* ( 30 * tau^2 - 60 * tau^3 + 30 * tau^4);
r3yd = ( r3yf - r3y0 ) / ( tf - t0 )*( 30 * tau^2 - 60 * tau^3 + 30 * tau^4);
r3xdd = (r3xf-r3x0)/((tf-t0)^2)*(60*tau-180*tau^2+120*tau^3);
r3ydd = (r3yf-r3y0)/((tf-t0)^2)*(60*tau-180*tau^2+120*tau^3);
```

```
if (t>tf);
  r3x=0;
  r3y=0;
  r3xd=0;
  r3yd=0;
  r3xdd=0;
  r3ydd=0;
 end

% Determine Inverse Kinematics
th23 = kink(r3x-L(1)*cos(thref(1)),r3y-L(1)*sin(thref(1)),L(2),L(3));
thref(2) = th23(1);
thref(3) = th23(2);

% Calculate Joint Velocites Using Jacobean
H = [-L(2)*sin(thref(2)),-L(3)*sin(thref(3));....
     L(2)*cos(thref(2)), L(3)*cos(thref(3))];
thd23 = inv(H) * [ r3xd; r3yd ];
thdref(2) = thd23(1);
thdref(3) = thd23(2);

% Calculate Joint Acceleration Using Jacobean
Hdot=[-L(2)*thdref(2)*cos(thref(2)),-L(3)*thdref(3)*cos(thref(3));....
     -L(2)*thdref(2)*sin(thref(2)),-L(3)*thdref(3)*sin(thref(3))];
```

```
thdd23=inv(H)*([r3xdd;r3ydd]-Hdot*[thdref(2);thdref(3)]);
thddref(2) = thdd23(1);
thddref(3) = thdd23(2);
% Calculate Reference Control Torques
[MM,GM] = mgm(thref,thdref);
B = [1,-1,0;0,1,-1;0,0,1];
Uref  = inv(B) * ( MM * thddref' + GM' );
```

C. NEAR-MINIMUM-TIME RERENCE TRACKING CONTROLLER

1. Main Program

```
% nmt1 program
% Constants
L(1) = 15*2.54/100;
L(2) = 17*2.54/100;
L(3) = 17*2.54/100;
L(4) = 20/100;
Lcm(1) = 0/100;
Lcm(2) = 36.45/100;
Lcm(3) = 34.9/100;
% Mass
m(1) = 54.69;
m(2) = 2.09364;
m(3) = 2.466;
m(4) = 10.667;

% Inertia
I(1) = 4.32132;
I(2) = 3.20338e-2;
I(3) = 5.38398e-2;
I(4) = 0.0912;
% Maximum Torque
umax=0.300;
% Shaping Function Coefficient
```

```
alfa=0.1;
beta=0.5;
t0=0;
MM(1,1) = I(1)+L(1)^2*(m(2)+m(3))+L(4)^2*m(4);
MM(2,2) = I(2) + m(2) * Lcm(2)^2 + m(3) * L(2)^2;
MM(3,3) = I(3) + m(3) * Lcm(3)^2;

%  Initial And Final Manipulator Position
th0=[0*pi/180;20*pi/180;40*pi/180];
thf=[0.01*pi/180;40*pi/180;60*pi/180];

%  Determine Minimum Time To Perform Maneuver
T(1)=sqrt(MM(1,1)*(thf(1)-th0(1))/...
      (umax(1)*(1/4-1/2*alfa+1/10*alfa^2)));
T(2)=sqrt(MM(2,2)*(thf(2)-th0(2))/...
      (umax(1)*(1/4-1/2*alfa+1/10*alfa^2)));
T(3)=sqrt(MM(3,3)*(thf(3)-th0(3))/...
      (umax(1)*(1/4-1/2*alfa+1/10*alfa^2)))
T_max=max(T)
tf=T_max
delt=alfa*tf
tf=T_max
dt=alfa*tf
ts=beta*tf
t1=ts-dt
```

```
t2=ts+dt
t3=tf-dt
echo off;
t0=0;
trace=1;
tol=1e-8;
x0=[0;0;0;0*pi/180;20*pi/180;40*pi/180];

%  Integrate Equations Of Motion
[t,x,uu] = rku2('nmtrk',t0,tf,x0,tol,trace);
```

2. Near-Minimum-Time Equations Function

```
function  [xdot,U] = nmtrk(t,x);

umax(1)=0.300;

% Constants

L(1) = 15*2.54/100;
L(2) = 17*2.54/100;
L(3) = 17*2.54/100;
L(4) = 20/100;

Lcm(1) = 0/100;
Lcm(2) = 36.45/100;
Lcm(3) = 34.9/100;

% Mass

m(1) = 54.69;
m(2) = 2.09364;
m(3) = 2.466;
m(4) = 10.667;

% Inertia
```

```
I(1) = 4.32132;
I(2) = 3.20338e-2;
I(3) = 5.38398e-2;
I(4) = 0.0912;

% Angles

thd(1) = x(1);
thd(2) = x(2);
thd(3) = x(3);

th(1)  = x(4);
th(2)  = x(5);
th(3)  = x(6);

[MM,GM] = mgm(th,thd);

% Gains
g1p=.10;
g2p=.10;
g3p=.10;
g1v=.50;
g2v=.50;
g3v=.50;
```

```
[MM,GM] = mgm(th,thd);

[Uref,thref,thdref,thddref] = nmt_ref(t);

dU(3)=-g3p*(th(3)-thref(3))-g3v*(thd(3)-thdref(3));
dU(2)=dU(3)-g2p*(th(2)-thref(2))-g2v*(thd(2)-thdref(2));
dU(1)=dU(2)-g1p*(th(1)-thref(1))-g1v*(thd(1)-thdref(1));

U1=Uref+dU';
U=U1';
B = [1,-1,0;0,1,-1;0,0,1];
xdot = [ inv(MM) * ( B * U' - GM' ); x(1); x(2); x(3) ];
```

3. Near-Minimum-Time Reference Function

```
% Reference Generator Function
function [Uref,thref,thdref,thddref] = nmt_ref(t);
umax(1)=0.300;
% Constants
L(1) = 15*2.54/100;
L(2) = 17*2.54/100;
L(3) = 17*2.54/100;
L(4) = 20/100;
Lcm(1) = 0/100;
Lcm(2) = 36.45/100;
Lcm(3) = 34.9/100;


% Mass
m(1) = 54.69;
m(2) = 2.09364;
m(3) = 2.466;
m(4) = 10.667;
% Inertia
I(1) = 4.32132;
I(2) = 3.20338e-2;
I(3) = 5.38398e-2;
I(4) = 0.0912;
MM(1,1) = I(1)+L(1)^2*(m(2)+m(3))+L(4)^2*m(4);
```

```
MM(2,2) = I(2) + m(2) * Lcm(2)^2 + m(3) * L(2)^2;
MM(3,3) = I(3) + m(3) * Lcm(3)^2;
th0=[0*pi/180;20*pi/180;40*pi/180];
thf=[0.01*pi/180;40*pi/180;60*pi/180];
alfa=0.1;
T(1)=sqrt(MM(1,1)*(thf(1)-th0(1))/(umax(1)*...
      (1/4-1/2*alfa+1/10*alfa^2)));
T(2)=sqrt(MM(2,2)*(thf(2)-th0(2))/(umax(1)*...
      (1/4-1/2*alfa+1/10*alfa^2)));
T(3)=sqrt(MM(3,3)*(thf(3)-th0(3))/(umax(1)*...
      (1/4-1/2*alfa+1/10*alfa^2)));
T_max=max(T);
tf=T_max;
dt=alfa*T_max;
t1=tf/2-dt;
t2=tf/2+dt;
t3=tf-dt;
umax(3)=MM(3,3)*(thf(3)-th0(3))/...
      (tf^2*(1/4-1/2*alfa+1/10*alfa^2));
umax(2)=MM(2,2)*(thf(2)-th0(2))/...
      (tf^2*(1/4-1/2*alfa+1/10*alfa^2));
umax(1)=MM(1,1)*(thf(1)-th0(1))/(tf^2*(1/4-1/2*alfa+1/10*alfa^2));

% Near Minimum Time Reference Maneuver
```

```
if (t>=0 & t<=dt);
 f=(t/dt)^2*(3-2*(t/dt));
 ff=dt*((t/dt)^3-(1/2)*(t/dt)^4);
 fff=(dt^2)*((1/4)*(t/dt)^4-(1/10)*(t/dt)^5);

elseif (t>dt & t<=t1);
 f = 1;
 ff=(t-(1/2)*dt);
 fff=((1/2)*t^2-(1/2)*t*dt+(3/20)*dt^2);

elseif (t>t1 & t<=t2);
 f  = 1 - 2*(((t-t1)/(2*dt))^2*(3-2*((t-t1)/(2*dt))));
 ff  = -(1/2)*dt+t1+2*dt*(((t-t1)/(2*dt))-2*((t-t1)/(2*dt))^3+...
       ((t-t1)/(2*dt))^4);
 fff = ((23/20)*alfa^2-(3/4)*alfa+(1/8))*tf^2+(2*dt)^2*...
      ((1/2)*((t-t1)/(2*dt))^2-(1/2)*((t-t1)/(2*dt))^4...
      +(1/5)*((t-t1)/(2*dt))^5)+((1/2)*tf-(3/2)*dt)*(t-t1);

elseif (t>t2 & t<=t3);
 f = -1;
 ff=-t+t1+t2-(1/2)*dt+2*dt*(((t2-t1)/(2*dt))-...
    2*((t2-t1)/(2*dt))^3+((t2-t1)/(2*dt))^4);
 fff=(-(21/20)*alfa^2+(1/4)*alfa+1/8)*tf^2+...
     (1/2)*(tf-3*dt)*(t-t2)-(1/2)*(t-(1/2)*tf-dt)^2;
```

```
elseif (t>t3 & t<=tf);
 f = -1+(((t-t3)/(dt))^2*(3-2*((t-t3)/dt)));
 ff=((1/2)*dt+dt*(-(t-t3)/dt+((t-t3)/dt)^3-(1/2)*((t-t3)/dt)^4));
 fff=(-(1/20)*alfa^2-(1/2)*alfa+1/4)*tf^2+(1/2)*dt*(t-t3)+...
    dt^2*(-(1/2)*((t-t3)/dt)^2+(1/4)*((t-t3)/dt)^4-(1/10)*((t-t3)/dt)^5);

elseif (t>tf);
 f=0;
 ff=0;
 fff=0;

end

thref(1)=(umax(1)/MM(1,1))*fff+th0(1);
thref(2)=(umax(2)/MM(2,2))*fff+th0(2);
thref(3)=(umax(3)/MM(3,3))*fff+th0(3);

thdref(1)=(umax(1)/MM(1,1))*ff;
thdref(2)=(umax(2)/MM(2,2))*ff;
thdref(3)=(umax(3)/MM(3,3))*ff;

thddref(1)=umax(1)*f/MM(1,1);
thddref(2)=umax(2)*f/MM(2,2);
thddref(3)=umax(3)*f/MM(3,3);
[MM,GM] = mgm(thdref,thref);
```

```
B = [1,-1,0;0,1,-1;0,0,1];
Uref  = inv(B) * ( MM * thddref' + GM' );
```

D. MISCELLANEOUS FUNCITONS

1. Equation Of Motion Coefficient Funciton

```
function [MM,GM] = mgm(th,thd);


% Constants
L(1) = 15*2.54/100;
L(2) = 17*2.54/100;
L(3) = 17*2.54/100;
L(4) = 20/100;
Lcm(1) = 0/100;
Lcm(2) = 36.45/100;
Lcm(3) = 34.9/100;


% Mass
m(1) = 54.69;
m(2) = 2.09364;
m(3) = 2.466;
m(4) = 10.667;


% Inertia
I(1) = 4.32132;
I(2) = 3.20338e-2;
I(3) = 5.38398e-2;
I(4) = 0.00912;
```

```
% Subroutine To Calculate Mass and "G" Matrix
 th21 = th(2) - th(1);
 th31 = th(3) - th(1);
 th32 = th(3) - th(2);

% 'Mass' Matrix
MM(1,1) = I(1)+L(1)^2*(m(2)+m(3))+L(4)^2*m(4);
MM(1,2) = ((m(2)*L(1)*Lcm(2))+(m(3)*L(1)*L(2)))*cos(th21);
MM(1,3) = m(3)*L(1)*Lcm(3)*cos(th31);

MM(2,1) = MM(1,2);
MM(2,2) = I(2) + m(2) * Lcm(2)^2 + m(3) * L(2)^2;
MM(2,3) = m(3) * L(2) * Lcm(3) * cos(th32);

MM(3,1) = MM(1,3);
MM(3,2) = MM(2,3);
MM(3,3) = I(3) + m(3) * Lcm(3)^2;

% 'G' Matrix

c122 = ((m(2)*L(1)*Lcm(2))+(m(3)*L(1)*L(2)))*sin(th21);
c133 =  m(3)*L(1)*Lcm(3)*sin(th31);

c211 = - ((m(2)*L(1)*Lcm(2))+(m(3)*L(1)*L(2)))*sin(th21);
c233 =    m(3)*L(2)*Lcm(3)*sin(th32);
```

```
c311 = - m(3)*L(1)*Lcm(3)*sin(th31);
c322 = - m(3)*L(2)*Lcm(3)*sin(th32);

c1=[0,0,0;...
   0,c122,0;...
   0,0,c133];

c2=[c211,0,0;...
   0,0,0;...
   0,0,c233];

c3=[c311,0,0;...
   0,c322,0;...
   0,0,0];

GM(1) = thd * c1 * thd';
GM(2) = thd * c2 * thd';
GM(3) = thd * c3 * thd';
```

2. Inverse Kinematics Function

```
function theta=kink(x,y,L1,L2)
% Subroutine To Determine Inverse Kinematic Solution

c12=(x^2+y^2-L1^2-L2^2)/(2*L1*L2);
s12=sqrt(1-c12^2);
theta12=atan2(s12,c12);
minv=inv([L1+L2*c12,-L2*s12;L2*s12,L1+L2*c12]);
c=minv*[x;y];
theta(1)=atan2(c(2),c(1));
theta(2)=theta(1)+theta12;
```

APPENDIX D

A. LINEAR CONSTANT GAIN FEEDBACK CONTROLLER

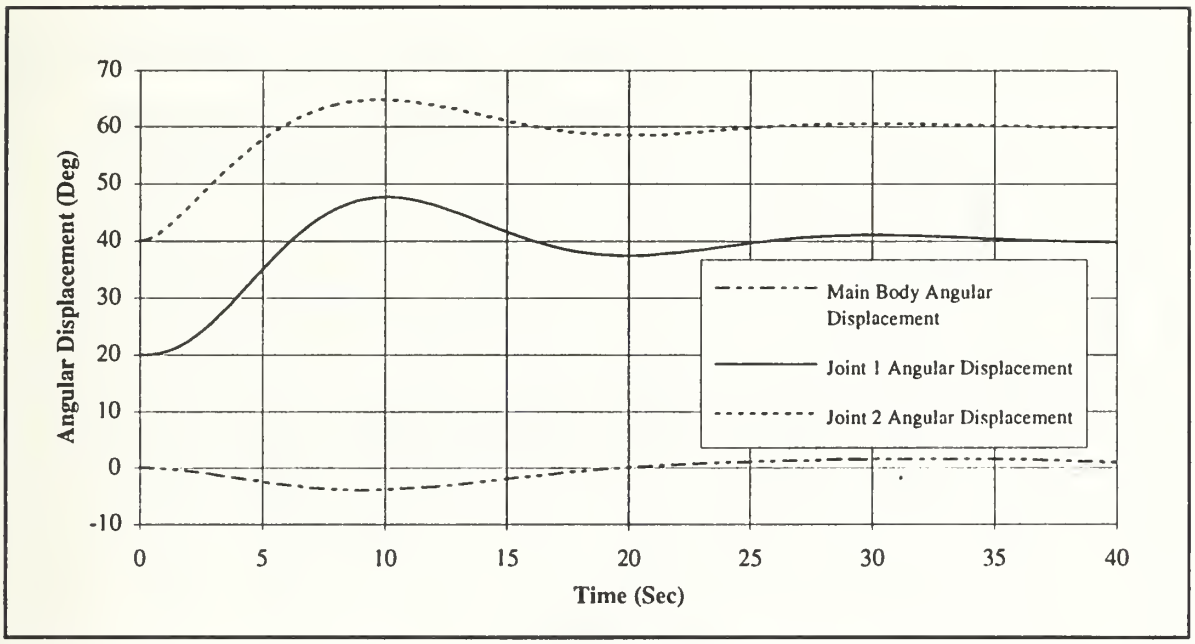

Figure D.1 Linear Constant Gain Feedback Joint Position Time History With G_P=0.1 And G_V=0.2

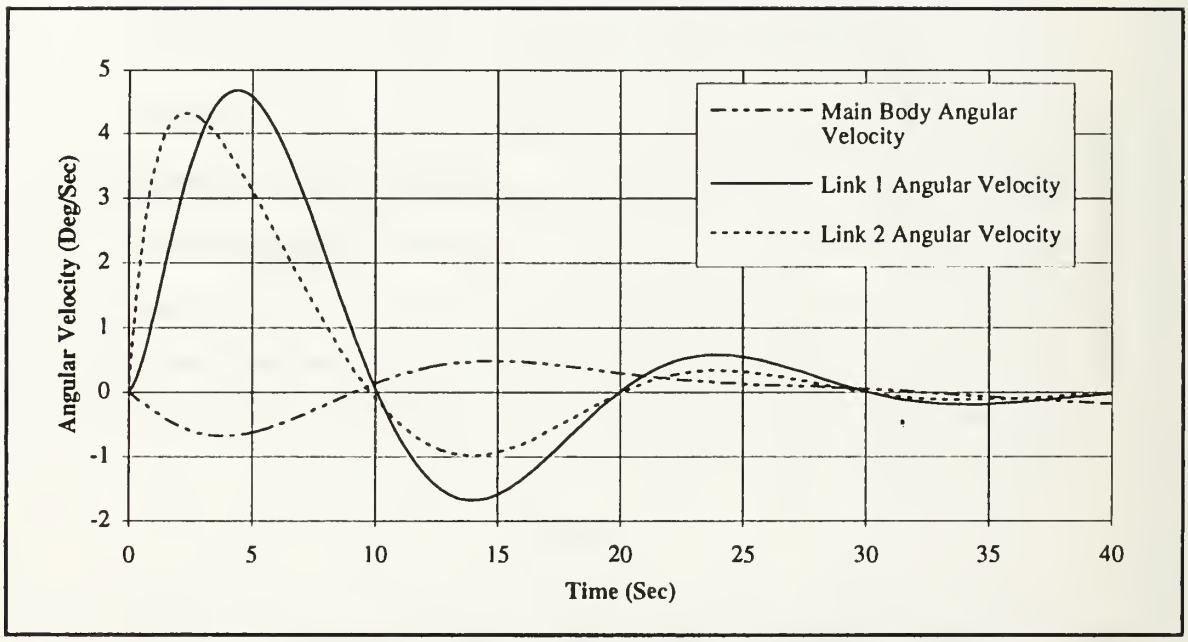

Figure D.2 Linear Constant Gain Feedback Joint Velocity Time History With G_P=0.1 And G_V=0.2

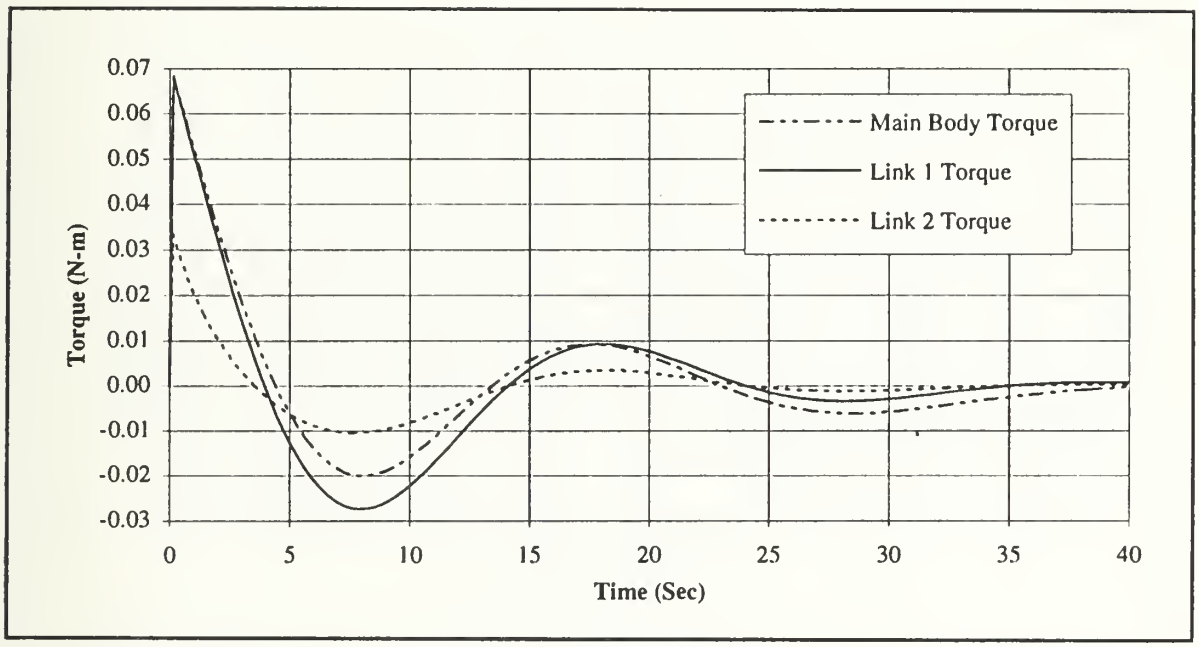

Figure D.3 Linear Constant Gain Feedback Torque Time History With G_P=0.1 And G_V=0.2

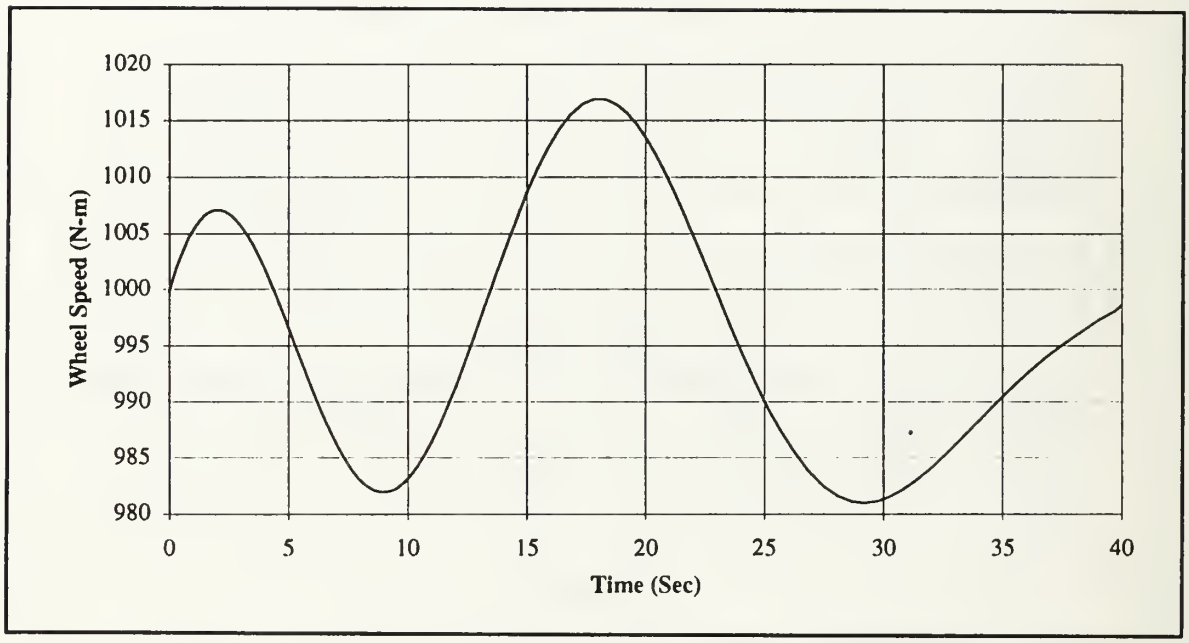

Figure D.4 Linear Constant Gain Feedback Momentum Wheel Speed Time History With G_P=0.1 And G_V=0.2

B. POLYNOMIAL REFERENCE TRACKING CONTROLLER

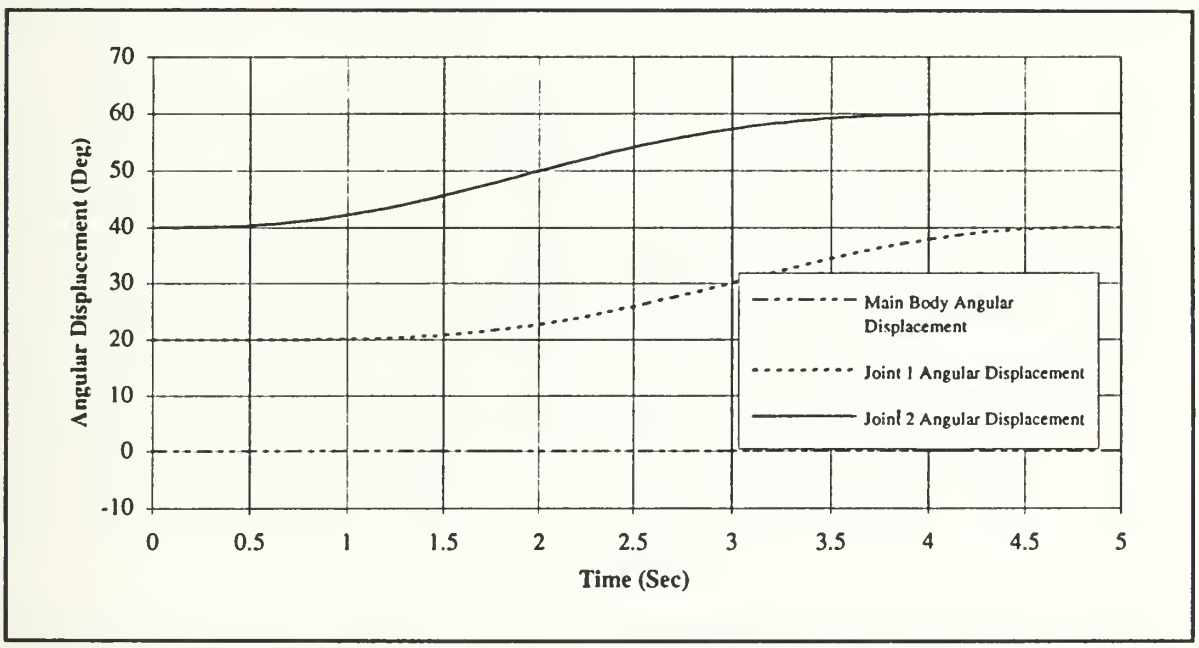

Figure D.5 Polynomial Reference Tracking Controller Joint Position Time History With G_p=1 and G_v=5 And Maneuver Time Of 5 Seconds

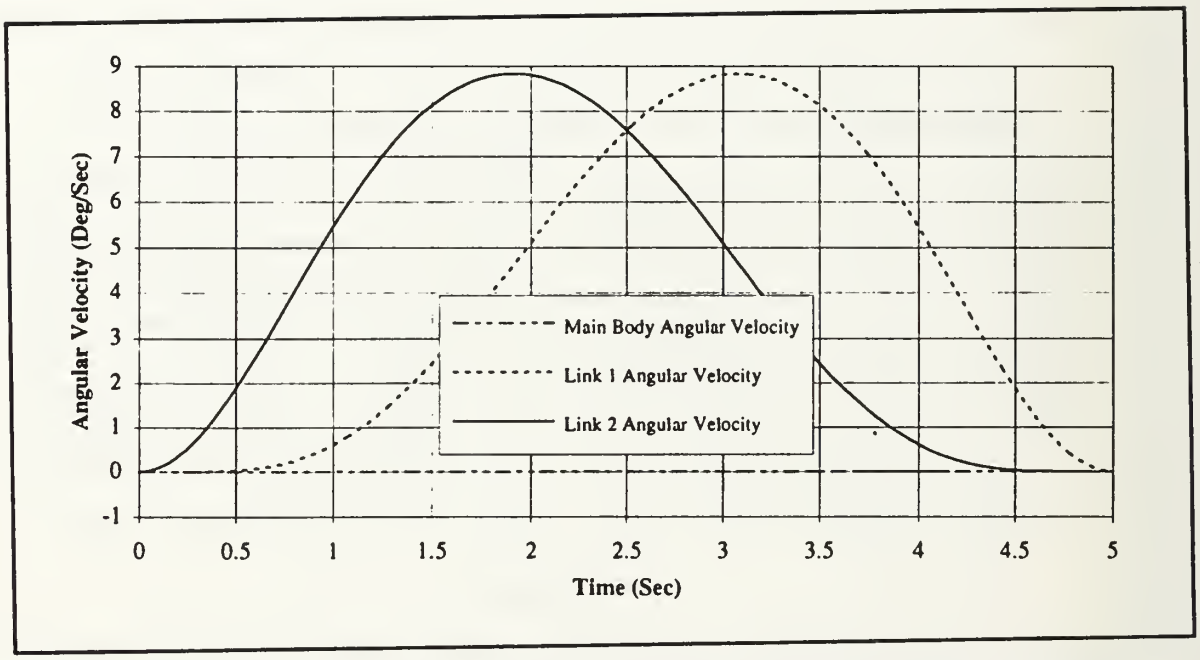

Figure D.6 Polynomial Reference Tracking Controller Joint Velociy Time History With G_P=1 and G_V=5 And Maneuver Time Of 5 Seconds

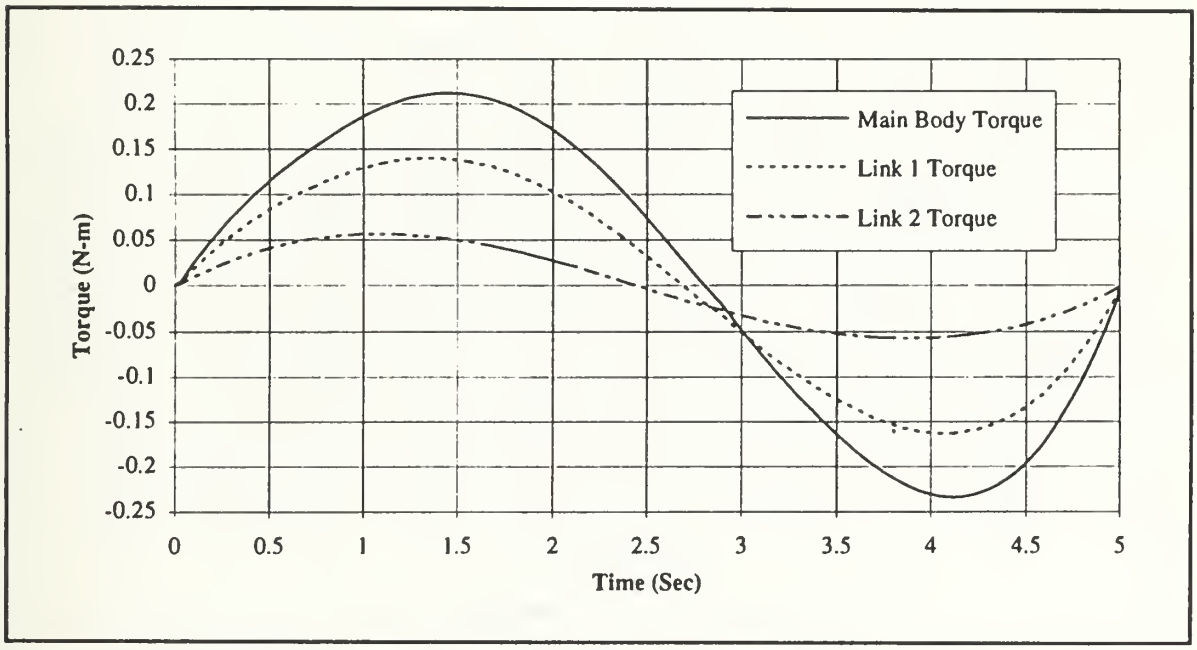

Figure D.7 Polynomial Reference Tracking Controller Torque Time History With G_P=1 and G_V=5 And Maneuver Time Of 5 Seconds

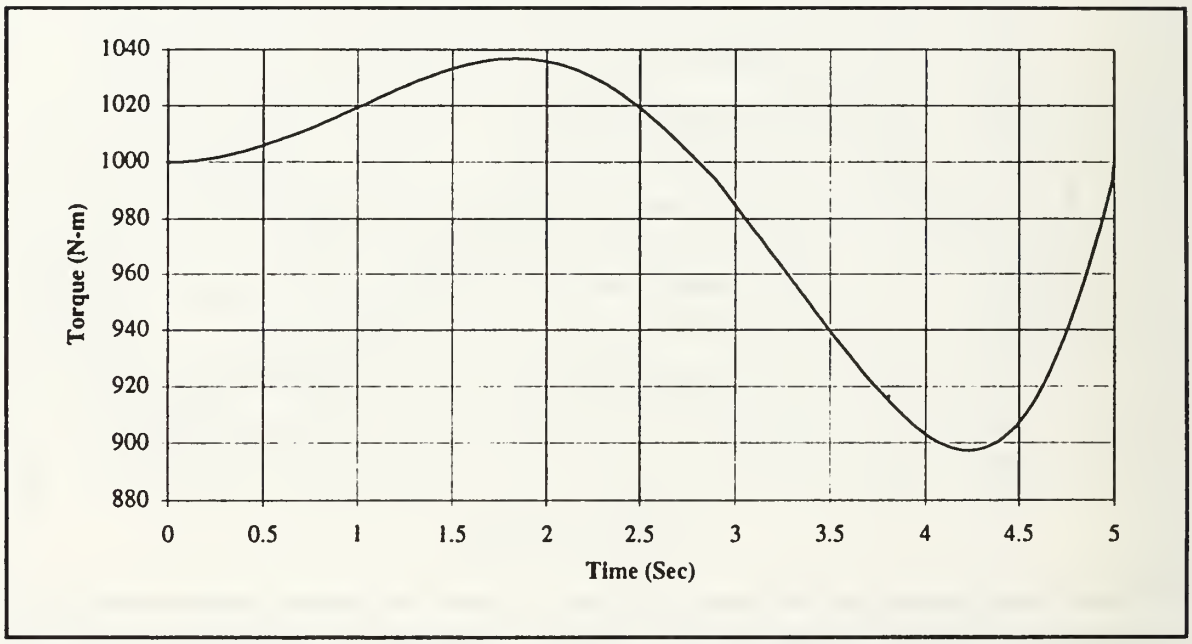

Figure D.8 Polynomial Reference Tracking Controller Momentum Wheel Speed Time History With G_P=1 and G_V=5 And Maneuver Time Of 5 Seconds

C. NEAR-MINIMUM-TIME REFERENCE TRACKING CONTROLLER

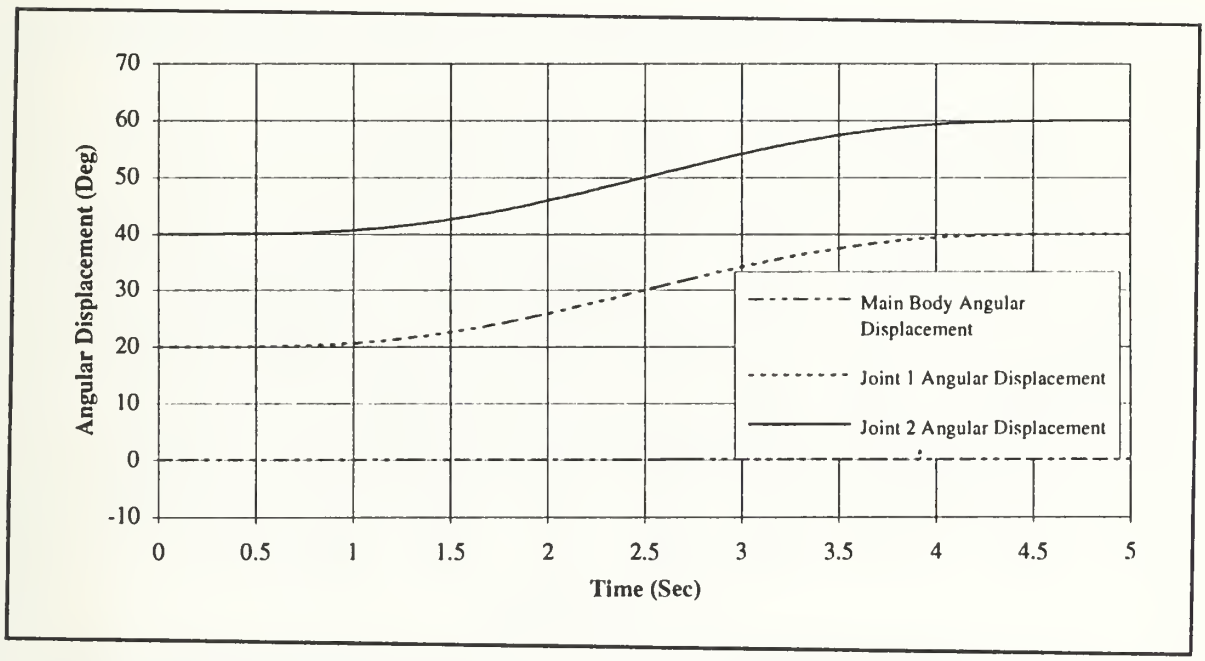

Figure D.9 Near-Minimum Time Tracking Controller Joint Position Time History With G_p=1 , G_v=5, Maneuver Time Of 5 Seconds , And α = 0.25

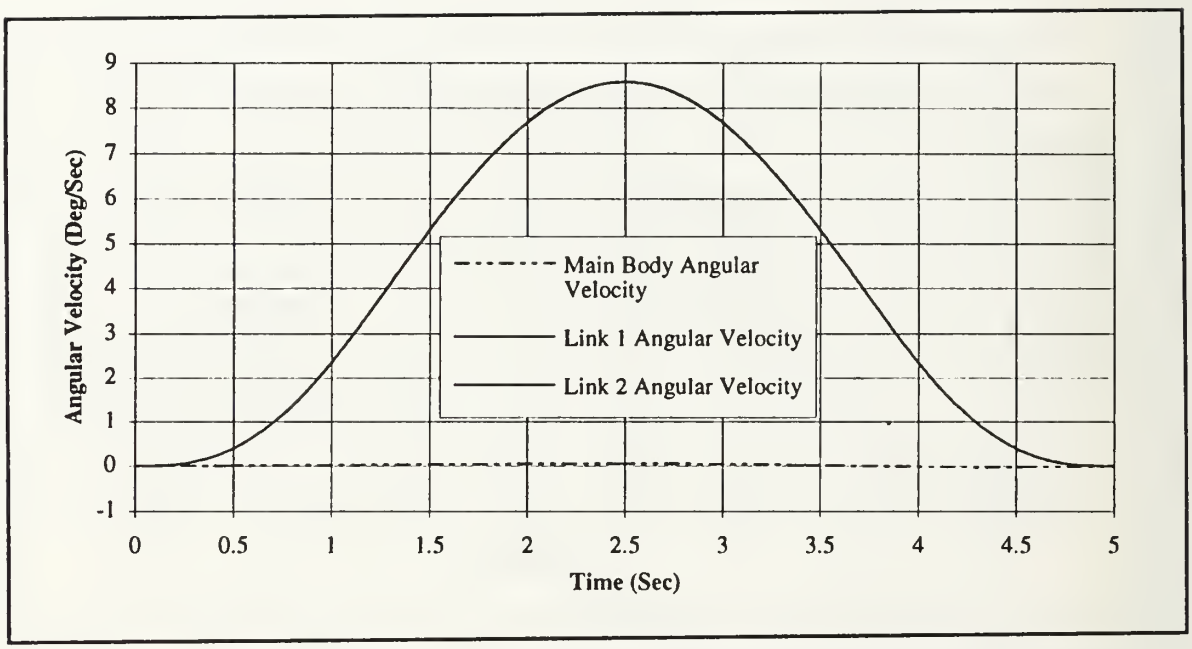

Figure D.10 Near-Minimum Time Tracking Controller Joint Velocity Time History With G_p=1 , G_v=5, Maneuver Time Of 5 Seconds , And α = 0.25

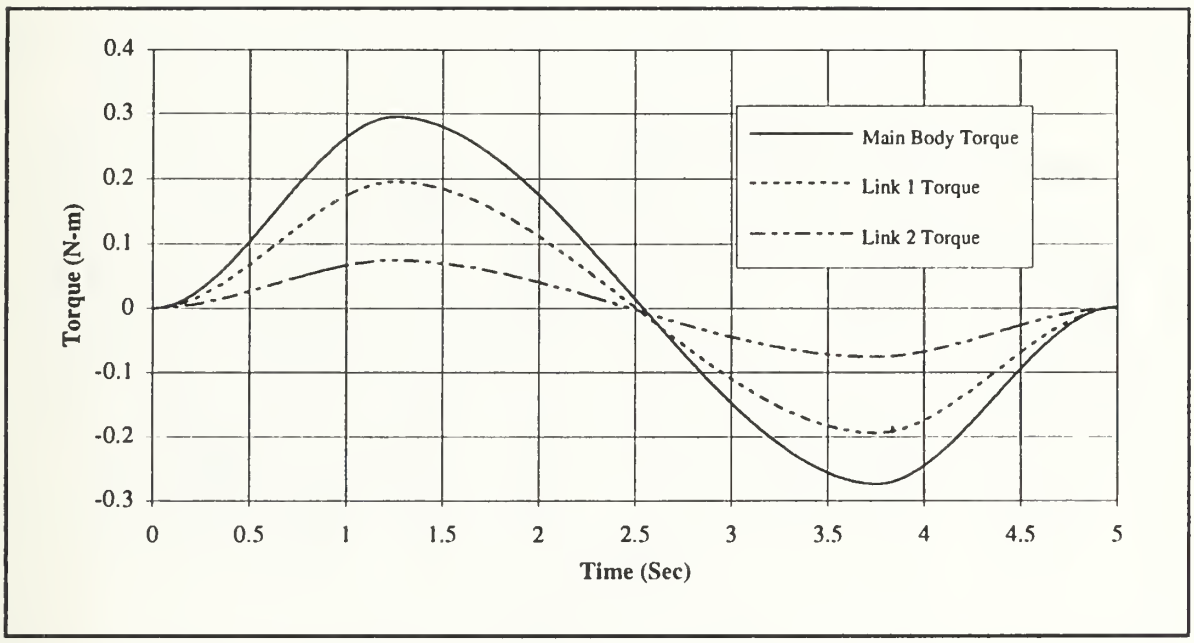

Figure D.11 Near-Minimum Time Tracking Controller Torque Time History With G_P=1 , G_V=5, Maneuver Time Of 5 Seconds , And α = 0.25

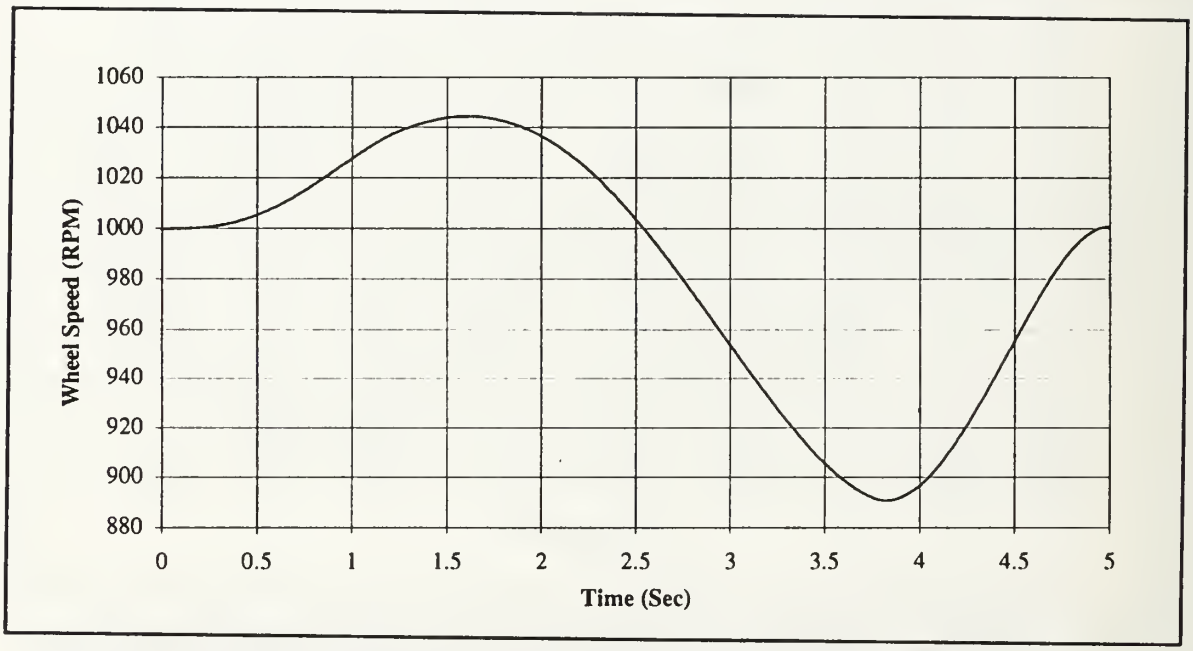

Figure D.12 Near-Minimum Time Tracking Controller Wheel Speed Time History With G_p=1 , G_v=5, Maneuver Time Of 5 Seconds , And α = 0.25

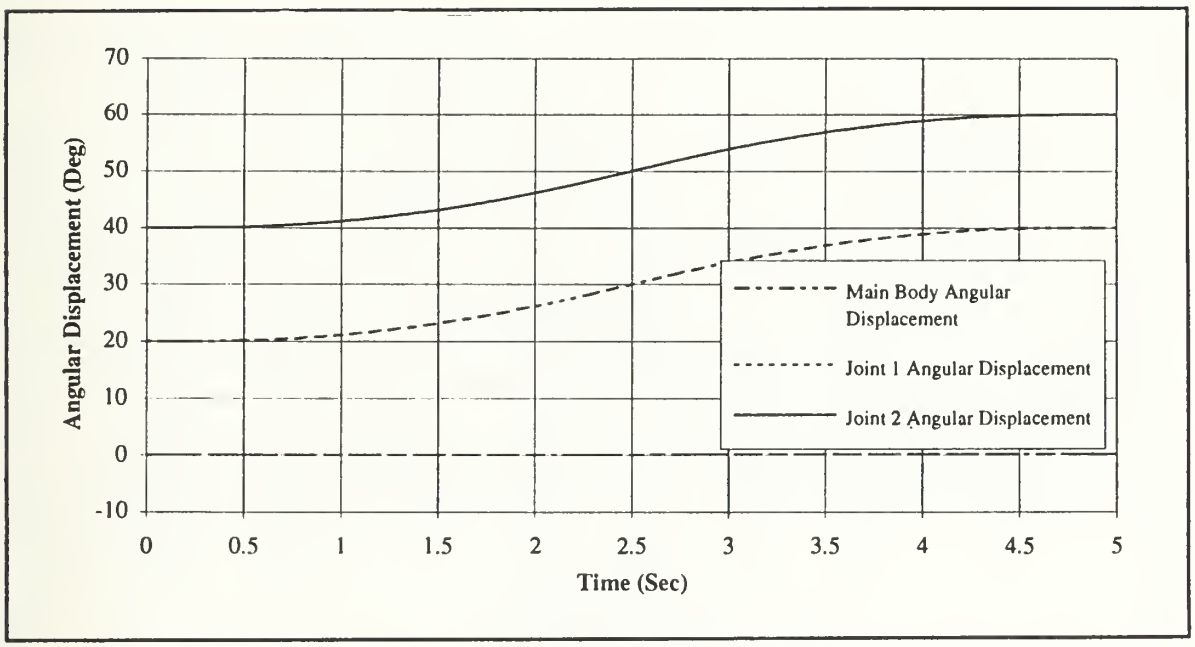

Figure D.13 Near-Minimum Time Tracking Controller Joint Position Time History With G_P=1 , G_V=5, Maneuver Time Of 5 Seconds , And α = 0.1

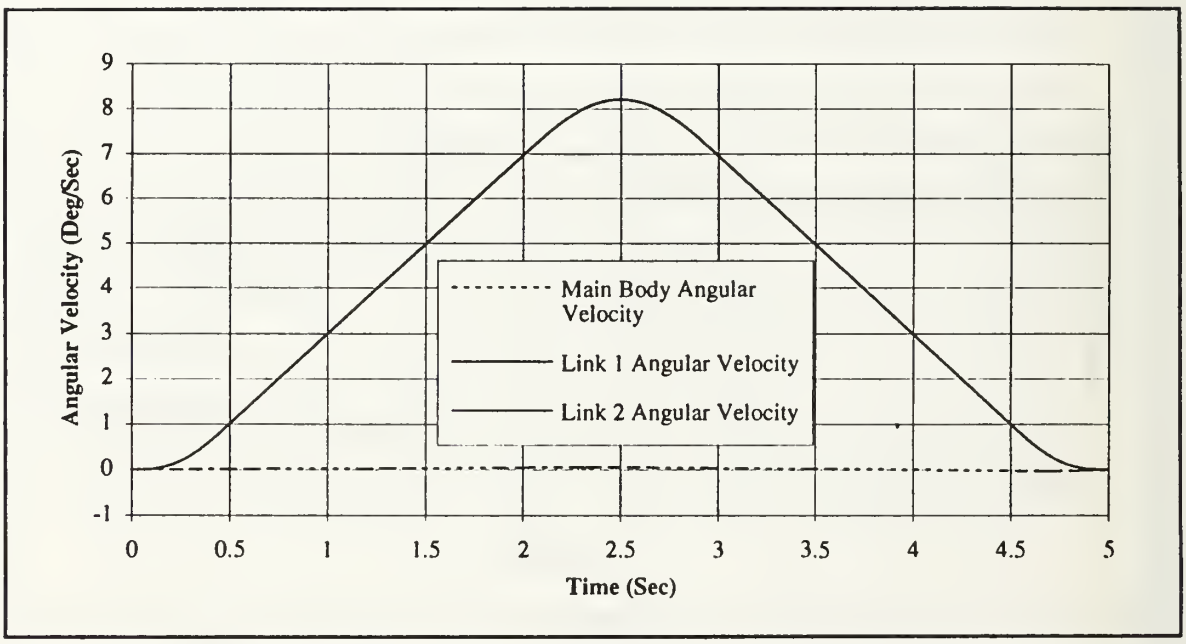

Figure D.14 Near-Minimum Time Tracking Controller Joint Velocity Time History With G_P=1 , G_V=5, Maneuver Time Of 5 Seconds , And α = 0.1

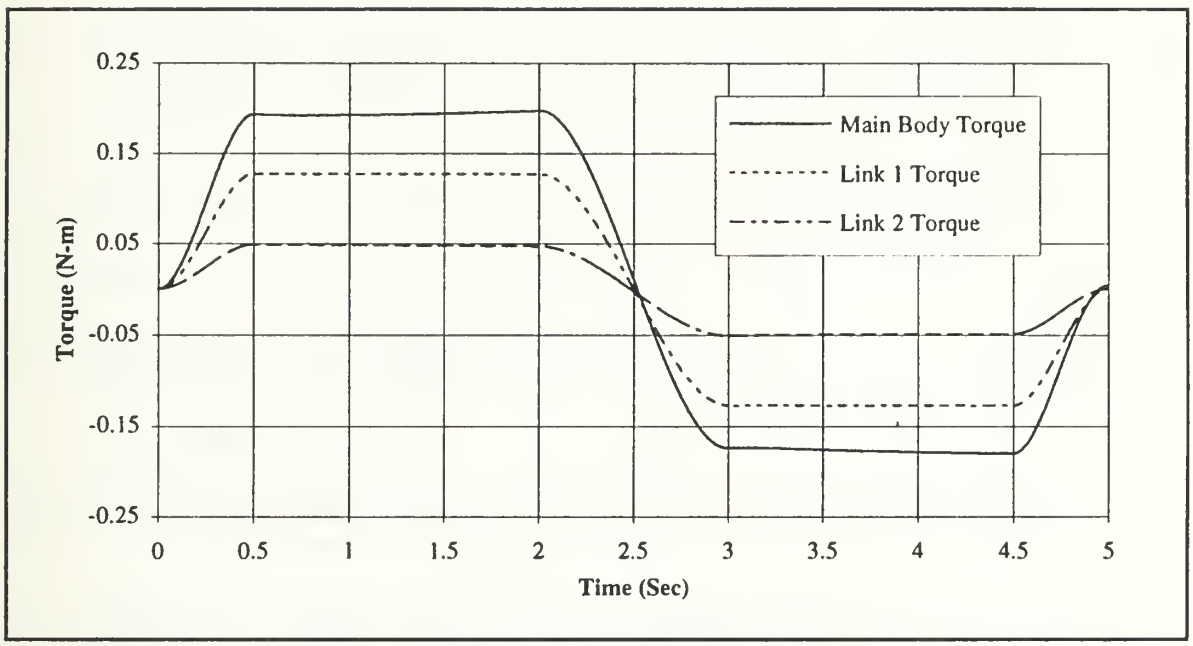

Figure D.15 Near-Minimum Time Tracking Controller Torque Time History With G_P=1 , G_V=5, Maneuver Time Of 5 Seconds , And α = 0.1

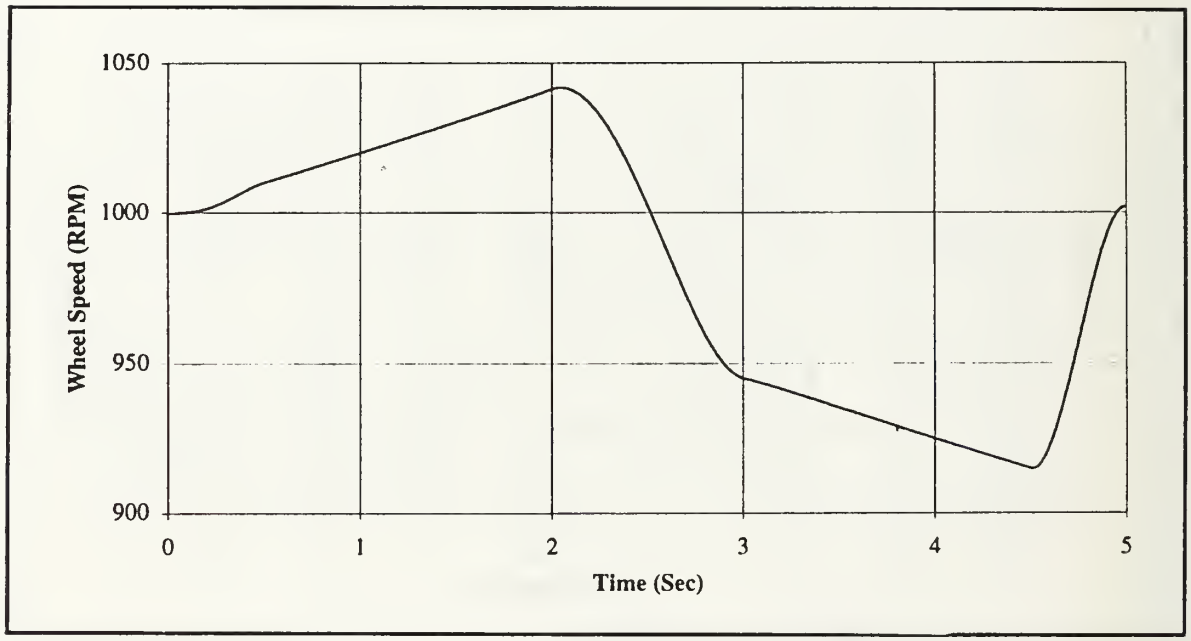

Figure D.16 Near-Minimum Time Tracking Controller Wheel Speed Time History With G_P=1 , G_V=5, Maneuver Time Of 5 Seconds , And α = 0.1

REFERENCES

1. Junkins, John L., Kim, Youdan, *An Introduction To Dynamics And Control Of Flexible Structures,* to appear, American Institute Of Aeronautics and Astronautics Education Series, pp. 73-97, 102-136, 1992.

2. Bang, Hyochoong, *Maneuver And Vibration Control Of Flexible Space Structures By Lyapunov Stability Theory,* Phd Dissertation, Texas A&M University, College Station, Texas, September 1992.

3. Hailey, Jeffrey A., *Experimental Verification of Attitude Control Techniques For Flexible Spacecraft Slew Maneuvers*, Master's Thesis, Naval Postgraduate School, Monterey, California, March 1992.

4. Watkins Jr., R.J., *The Attitude Control Of Flexible Spacecraft,* Master's Thesis, Naval Postgraduate School, Monterey, California, June 1991.

5. Integrated Systems, Inc., *$MATRIX_X$ Core,* 7^{th} ed., January 1990.

6. Kepco, Inc., *Model BOP 20-10M Power Supply Instruction Manual,* Flushing, New York, 1987.

7. Integrated Systems Inc., *AC-100 Users Guide*, V2.4.05, February 1991.

8. Greenwood, Donald T., *Principles Of Dynamics*, 2nd ed., pp. 239-291, Prentice-Hall, New Jersey, 1988.

9. Kalman, R.E., Bertram, J.E., "Control Systems Analysis And Design Via The Second Method Of Lyapunov, Part 1, Continuous Time Systems", *Journal Of Basic Engineering,* pp. 371-393, June 1960.

10. Craig, John, J., *Introduction To Robotics Mechanics And Control, 2^{nd} ed.,* Addision-Wesley Publishing, New York, 1989.

11. Johnson, Eric R., *Servomechanisms,* pp. 209-230, Prentice-Hall, New Jersey, 1963.

12. Lauer, Henri, Lesnick, Robert U., and Matson, Leslie E., *Servomechanism Fundamentals,* 2nd ed., pp. 349-486, McGraw Hill, New York, 1960.

13. Klafter, Richard, D., Chmielewski, Thomas, A., and Negin, Michael, *Robotic Engineering, An Integrated Approach*, Prentice Hall, New Jersey, 1989.

14. Slotine, Jean Jacques E., and Li, Weiping, *Applied Nonlinear Control,* pp. 88-97, 169-228, 266-271, 392-421, Prentice Hall, New Jersey, 1991.

15. Asada, H., and Slotine, J.J.E., *Robot Analysis And Control*, pp. 133-184, John Wiley and Sons, New York, 1986.

16. Nye, Theodore W., LeBlanc, David J., and Cipra, Raymond J., "Design And Modeling Of A Computer Controlled Planar Manipulator", *The Kinematics Of Robot Manipulators,* pp. 191-201, MIT Press, Cambridge, MA, 1987.

INITIAL DISTRIBUTION LIST

		No. Copies
1.	Defense Technical Information Center Cameron Station Alexandria, Virginia 22304-6145	2
2.	Library, Code 52 Naval Postgraduate School Monterey, California 93943-5002	2
3.	Chairman, Code AA Department Of Aeronautics and Astronautics Naval Postgraduate School Monterey, California 93943-5000	1
4.	Chairman, Code SP Department Of Aeronautics and Astronautics Naval Postgraduate School Monterey, California 93943-5000	1
5.	Professor Brij N. Agrawal, Code AA/Ag Department Of Aeronautics and Astronautics Naval Postgraduate School Monterey, California 93943-5000	2
6.	Dr. Hyochoong Bang, Code AA/Bn Department Of Aeronautics and Astronautics Naval Postgraduate School Monterey, California 93943-5000	1
7.	LCDR Dennis Sorensen Naval Air Warfare Center - Weapons Division Point Mugu, CA 93042-5000	1

Thesis
S66596 Sorensen
c.1 Design and control of a space based two link manipulator with Lyapunov based control laws.